SAMPLING INNOVATIONS

THÈSE N° 2369 (2001)

PRÉSENTÉE AU DÉPARTEMENT DE SYSTÈMES DE COMMUNICATION

ÉCOLE POLYTECHNIQUE FÉDÉRALE DE LAUSANNE

POUR L'OBTENTION DU GRADE DE DOCTEUR ÈS SCIENCES

PAR

Pina MARZILIANO

B.Sc. en Mathématiques, M.Sc. Informatiques spécialisée en recherche opérationnelle,
Université de Montréal, Canada
de nationalité canadienne et italienne

acceptée sur proposition du jury:

Prof. M. Vetterli, directeur de thèse
Dr T. Blu, rapporteur
Prof. P. Ferreira, rapporteur
Dr S. Grassi, rapporteur
Prof. M. Unser, rapporteur

Lausanne, EPFL
2002

To my advisor.

–

Acknowledgements

During this journey towards a Ph.D I have met many people I am thankful to.

The first and most important is my great advisor Professor Martin Vetterli. Our weekly eight o'clock Monday morning appointments were very enriching and allowed me to grow not only on a scientific level but also on a personal level. I thank him for his patience, for always encouraging me and believing in me and for giving me all the possible opportunities a Ph.D student can wish for. I thank him from my heart.

I also wish to thank the jury members: Dr. T. Blu, Prof. P. J. S. G. Ferreira, Dr. S. Grassi, Prof. M. Hasler and Prof. M. Unser, for reading and for accepting this work. Your time and efforts have been greatly appreciated.

Thanks to all of my LCAV colleagues, Gianpaolo, Pier Luigi, David, Michael, Jérôme, Claudio, for always being there to answer my sometimes naive questions and for simply making it a fun and friendly working environment. A special thanks to Jocelyne whose friendly ear always managed to keep everything under control during our kindergarten crises.

The lab would not have been the same without Paolo, my first office mate, whose life is a movie or a book that I hope to write one day. His stories and guitar playing in the office not only made the first two years of this journey a one of a kind experience but kept me from jumping out the window (which was on the ground floor anyway).

I am very grateful to all of my friends who were like a second family to me. In particular my three sisters Monique, Maria-Jose, and Gloria and my two big brothers Dani and Mauro whom I could always count on to have a good time, as well as when I would get injured - and there were many such times.

My time here in Lausanne would not have been the same without my special friends Andrea and Francesco who always put up with my crazy ideas and managed to Salsa Merengue with me in the oddest places. I also thank all of my other "LTS" friends.

Last but not least I would like to thank my parents for letting me come to Switzerland. Coming from traditional Italian origins, it is not an easy thing to let your daughter leave the house unwed, and more so the country. I thank my dad for his words: "chi non risica non rosica", my mom for great advice on writing: "just write, don't erase", and my brother Joey whose practical jokes will always keep me on my toes.

Lausanne, April 27, 2001.

Contents

Abstract

Sampling theory has prospered extensively in the last century. The elegant mathematics and the vast number of applications are the reasons for its popularity. The applications involved in this thesis are in signal processing and communications and call out to mathematical notions in Fourier theory, spectral analysis, basic linear algebra, spline and wavelet theory. This thesis is divided in two parts. Chapters 2 and 3 considers uniform sampling of non-bandlimited signals and Chapters 4, 5, and 6 treats different irregular sampling problems.
In the first part we address the problem of sampling signals that are not bandlimited but are characterized as having a finite number of degrees of freedom per unit of time. These signals will be called signals with a finite rate of innovation. We show that these signals can be uniquely represented given a sufficient number of samples obtained using an appropriate sampling kernel. The number of samples must be greater or equal to the degrees of freedom of the signal; in other words, the sampling rate must be greater or equal to the rate of innovation of the signal. In particular, we derive sampling schemes for periodic and finite length streams of Diracs and piecewise polynomial signals using the sinc, the differentiated sinc and the Gaussian kernels. Sampling and reconstruction of piecewise bandlimited signals and filtered piecewise polynomials is also considered. We also derive local reconstruction schemes for infinite length piecewise polynomials with a finite "local" rate of innovation using compact support kernels such as splines. Numerical experiments on all of the reconstruction schemes are shown.
The first topic of the second part of this thesis is the irregular sampling problem of bandlimited signals with unknown sampling instances. The locations of the irregular set of samples are found by treating the problem as a combinatorial optimization problem. Search methods for the locations are described and numerical simulations on a random set and a jittery set of locations are made. The second topic is the periodic nonuniform sampling problem of bandlimited signals. The irregular set of samples involved has a structure which is irregular yet periodic. We develop a fast scheme that reduces the complexity of the problem by exploiting the special pattern of the locations. The motivation for developing a fast scheme originates from the fact that the periodic nonuniform set was also considered in the sampling with unknown locations problem and that a fast search method for the locations was sought. Finally, the last topic is the irregular sampling of signals that are linearly and nonlinearly approximated using Fourier and wavelet bases. We present variants of the Papoulis Gerchberg algorithm which take into account the information given in the approximation of the signal. Numerical experiments are presented in the context of erasure correction.

Résumé

La théorie de l'échantillonage s'est grandement épanouie au courant du dernier siècle. L'élégance des notions mathématiques et les divers domaines où elle peut être appliquée sont les raisons de sa popularité. Les applications envisagées dans cette thèse sont le traitement du signal et les communications. Les outils mathématiques comprennent la théorie de Fourier, l'analyse spectrale, l'algèbre linéaire, la théorie des splines et des ondelettes. La présente thèse est divisée en deux parties. Les chapitres 2 et 3 traitent le problème d'échantillonage régulier pour des signaux à bande non-limitée. Les chapitres 4, 5, et 6 traitent trois problèmes différents de l'échantillonage irrégulier.

Dans la première partie, nous échantillonons des signaux qui ne sont pas à bande limitée mais qui ont la propriété d'avoir un nombre fini de degrés de liberté par unité de temps. Ces signaux seront appelés des signaux à taux d'innovations fini. Nous montrons comment ces signaux peuvent être représentés de façon unique à partir d'un nombre suffisament grand d'échantillons obtenu par un noyau d'échantillonage approprié. Pour cela, le nombre d'échantillons doit être supérieur ou égal au nombre de degrés de liberté du signal; c'est à dire, le taux d'échantillonage doit être supérieur ou égal au taux d'innovation du signal. En particulier nous établissons des schémas d'échantillonage et de reconstruction pour des signaux à taux fini d'innovation tels que le peigne de Diracs et les signaux polynomiaux par morceaux avec des noyaux tels que le sinc, la dérivée du sinc et la Gaussienne. Des signaux composés d'un polynomial par morceaux et d'un signal à bande limitée ainsi que des signaux polynomiaux par morceaux filtrés sont aussi exposés. Nous présentons aussi des schémas de reconstruction locale pour des signaux polynomiaux par morceaux de longueur infinie ayant un taux local d'innovation fini avec des noyaux à support compact tels que les splines. Des résultats numériques sont donnés pour chaque schéma de reconstruction.

Le premier sujet de la deuxième partie de cette thèse est le problème de l'échantillonage irrégulier des signaux à bande limitée où les positions des échantillons ne sont pas connues. Ces positions sont trouvées à l'aide des méthodes utilisées pour des problèmes d'optimisation combinatoire. Des simulations ont été fait pour des ensembles irréguliers dont les positions sont aléatoires et dont les positions ont du "jitter". Le deuxième sujet est un cas particulier du problème d'échantillonage irrégulier des signaux à bande limitée où les positions des échantillons sont irréguliers mais périodiques. Nous développons un schéma qui reduit la complexité du problème en exploitant la structure particulière des positions. Enfin, le dernier sujet est l'échantillonage des approximations linéaires et nonlinéaires d'un signal avec des bases de Fourier et d'ondelettes. Nous présentons des variantes de l'algorithme de Papoulis-Gerchberg qui tien-

nent compte des informations dans les approximations. Des tests numériques ont été effectués dans le cadre de la correction des effacements.

List of Tables

List of Figures

Chapter 1

Introduction

The beauty of sampling lies in the wide spectrum of applications it co-involves in the engineering and the life sciences. For example processing audio signals and digital images, processing information in a communication channel, analyzing and restoring medical images. It also brings to the surface some elegant mathematics such as harmonics analysis, wavelet and spline theory, and approximation theory. An extensive tutorial on sampling and all of its aspects appeared in 1977 by Jerri [40] and a more recent one by Unser [76]. The latest advances in sampling theory and applications can be found in [5] as well as in the Sampling Theory and Applications (SampTA) workshop proceedings.
What is sampling?
Sampling is all about being able to represent a continuous-time signal $x(t), t \in \mathbb{R}$ by a discrete set of values $x[n], n \in \mathbb{Z}$. If the time instances at which these samples are taken are equidistant, for example every T seconds, $x[n] = x(nT)$, then the signal is uniformly sampled. If the time instances are not equidistant, that is, the samples are taken at arbitrary points $t_n \in \mathbb{R}$, $x[n] = x(t_n)$ then this is known as nonuniform or irregular sampling. Examples are illustrated in Figure 1.1.
In both types of sampling the questions of interest are:

- Under what conditions is a signal $x(t)$ perfectly recovered from a set of samples $x[n]$?
- What are the methods of reconstruction?
- Are the numerical reconstruction methods stable?
- What types of sampling kernels are most appropriate for the different types of signals?

In this dissertation, these questions are investigated for different sampling problems. Sections 1.1 and 1.2 give a brief introduction to uniform and irregular sampling. Section 1.3 introduces the notations and definitions that will be used throughout the whole thesis. Section 1.4 gives the outline of the thesis.

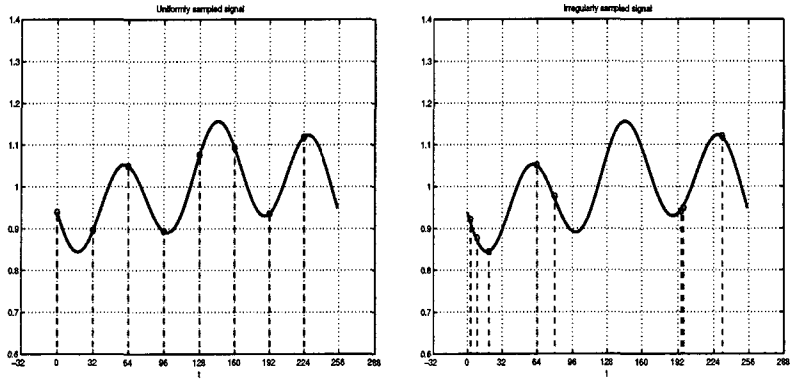

Figure 1.1: (a) Uniformly sampled signal with samples $x[n] = x(nT), n = 0, \ldots, 7, T = 32$. (b) Irregularly sampled signal with samples $x[n] = x(t_n)$, with $t_n \in \{2, 8, 19, 63, 79, 194, 196, 231\}$.

1.1 Uniform sampling

The fundamental result in sampling theory is the well-known theorem by Whittaker [83], Kotel'nikov [43, 44] and Shannon [66] which states: A continuous-time signal $x(t)$ is completely defined by a set of samples $x[n]$ taken at T_s seconds apart, that is, $x[n] = x(nT_s)$, if the sampling frequency $\omega_s = 2\pi/T_s$ radians/second is greater than two times the maximum frequency[1] component ω_m of the signal

$$\omega_s \geq 2\omega_m \quad \text{or} \quad \omega_m \leq \pi/T_s. \tag{1.1}$$

The reconstructed signal $x_r(t)$ is obtained by interpolating the samples $x[n] = x(nT_s)$ with a sinc interpolator

$$x_r(t) = \sum_{n \in \mathbb{Z}} x(nT_s)\,\mathrm{sinc}(t/T_c - n) \tag{1.2}$$

where $\mathrm{sinc}(t) = sin(\pi t)/\pi t$. The interpolating function or the reconstruction filter $h_r(t) = \mathrm{sinc}(t/T_c)$ is an ideal lowpass filter with cutoff frequency $\omega_c = \pi/T_c$, that is, its Fourier transform $H_r(\omega)$ is equal to zero for frequencies outside of the band $[-\omega_c, \omega_c]$. The sampling and reconstruction scheme is illustrated in Figure 1.2. In order to perfectly recover the original signal the cutoff frequency ω_c of the lowpass reconstruction filter $h_r(t)$, must be greater than the maximum frequency, ω_m, and it must be less than the difference between the sampling frequency and the maximum frequency, $\omega_s - \omega_m$, that is,

$$\omega_m < \omega_c < \omega_s - \omega_m. \tag{1.3}$$

Figure 1.3 shows the different steps in the sampling and reconstruction process

[1]The maximum frequency component is the bandlimit of the signal, that is, the Fourier transform of the signal $X(\omega)$ is zero outside the interval $[-\omega_m, \omega_m]$.

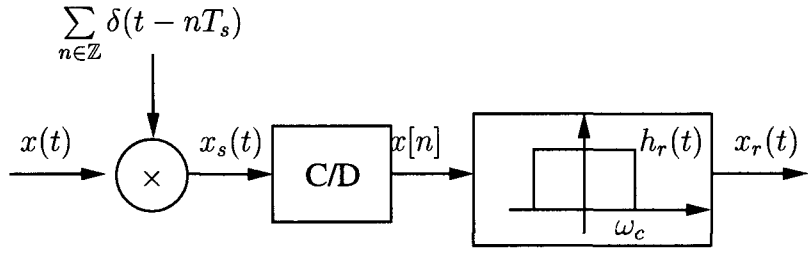

Figure 1.2: Sampling and reconstruction scheme. The continuous-time signal $x(t)$ is multiplied by a stream of Diracs $\sum_{n\in\mathbb{Z}} \delta(t-nT_s)$ leading to the sampled signal $x_s(t) = \sum_{n\in\mathbb{Z}} x(nT_s)\,\delta(t-nT_s)$. The reconstructed signal $x_r(t)$ is obtained by interpolating the samples $x[n] = x(nT_s)$ with the reconstruction filter $h_r(t) = \mathrm{sinc}(t/T_c)$ whose cutoff frequency is $\omega_c = \pi/T_c$.

in the frequency domain.

The sampling theorem relies on the fact that the signal is bandlimited, but what if the signal is not bandlimited? How can the signal be sampled and reconstructed? One way is to make it bandlimited, in other words, we take a lowpass approximation of the signal and then apply the previous sampling and reconstruction scheme, see Figure 1.4.
By filtering the signal with a lowpass filter $\varphi(t) = \mathrm{sinc}(t/T_s)$ whose cutoff frequency is $\omega_c = \pi/T_s$ we obtain a lowpass approximation

$$y(t) = x(t) * \varphi(-t). \tag{1.4}$$

The sample values obtained after sampling the lowpass approximation are given by

$$x[n] =< x(t), \varphi(t-nT_s >= \int_{-\infty}^{\infty} x(t)\,\varphi(t-nT_s)\,dt. \tag{1.5}$$

The question of interest here is how does the reconstruction of the lowpass approximation compare with the original non-bandlimited signal? This is treated in [12]. Take for example a bilevel signal which is commonly found in modulation. The bilevel signal and the reconstructed lowpass approximation are illustrated in Figure 1.5. It is evident that the sampling and reconstruction scheme in Figure 1.4 is far from being satisfactory. Therefore the questions that are pursued in what follows are:

1. How can we perfectly reconstruct non-bandlimited signals from a uniform set of samples $x[n] =< x(t), \varphi(t-nT) >$?

2. For what type of non-bandlimited signals is this possible?

3. What type of sampling kernels $\varphi(t)$ are most appropriate?

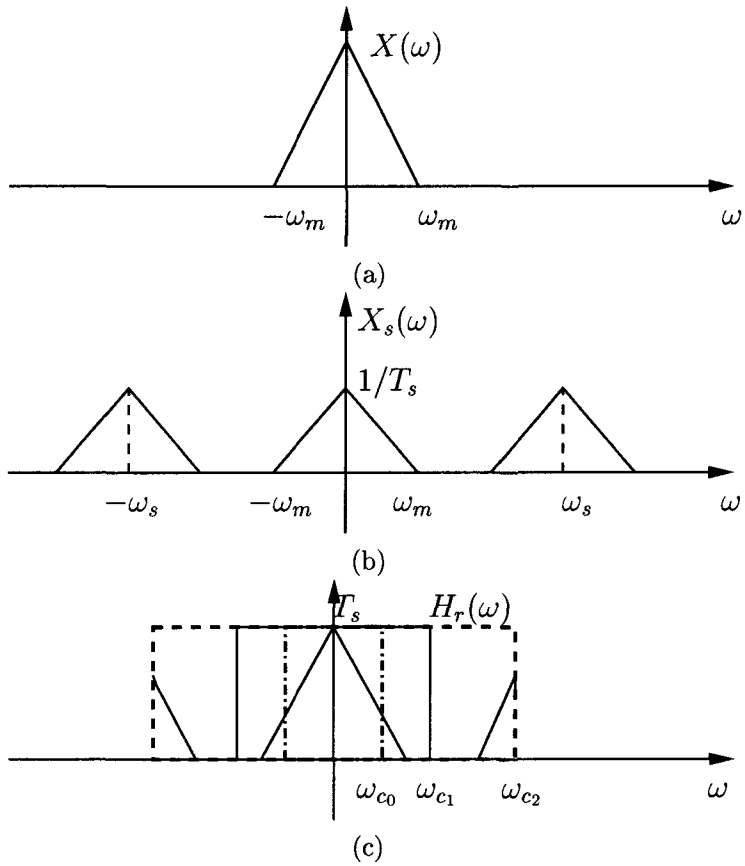

Figure 1.3: Sampling in the frequency domain. (a) Fourier transform of the signal $x(t)$. (b) Fourier transform of sampled signal $x_s(t)$. Original spectrum repeated at every ω_s. (c) Reconstruction filter $H_r(\omega)$ with different cutoff frequencies, $\omega_{c_0} < \omega_{c_1} < \omega_{c_2}$.

Going back to bandlimited signals, these are completely determined by sampling the signal at a rate of 1 sample every T seconds, that is, the signal has $1/T$ degrees of freedom per unit of time. So it is interesting to see if we can sample and reconstruct non-bandlimited signals that are characterized as having a finite number of degrees of freedom per unit of time. These signals are defined as signals with a finite rate of innovation. Formally,

Definition 1.1 *The rate of innovation ρ is the average number of degrees of freedom per unit of time, or, with $C_x(a,b)$ giving the number of degrees of freedom of $x(t)$ over the interval $[a,b]$,*

$$\rho = \lim_{\tau \to \infty} \frac{1}{\tau} C_x(-\frac{\tau}{2}, \frac{\tau}{2}). \tag{1.6}$$

In Chapter 2, periodic signals that have a finite rate of innovation are considered, in particular discrete-time and continuous-time streams of Diracs and piecewise

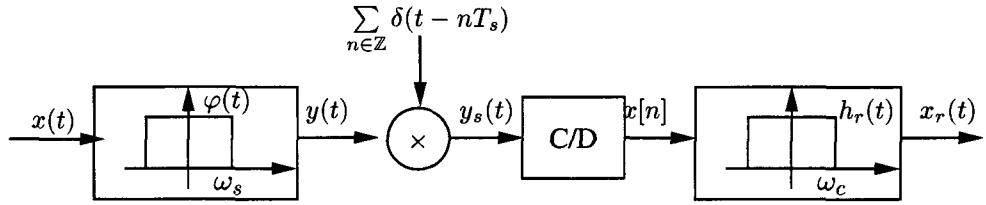

Figure 1.4: Sampling and reconstruction scheme for non bandlimited signals. The continuous-time signal $x(t)$ is first filtered by an ideal lowpass filter followed by the usual sampling/reconstruction scheme.

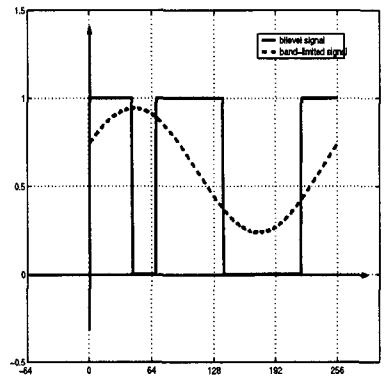

Figure 1.5: Bilevel signal and lowpass approximation.

polynomials. These signals are uniformly sampled using the periodized sinc and differentiated sinc sampling kernels and reconstruction schemes are presented.

In Chapter 3, finite length streams of Diracs are sampled using infinite support sampling kernels such as the sinc and Gaussian kernels. Since these signals are finite they have a finite rate of innovation. The dual problem is also considered, that is, infinite length piecewise polynomial signals are sampled with a compact support sampling kernel, such as spline kernels. Since these signals are infinite, they may be uniformly sampled when they have a finite *local* rate of innovation with respect to a moving window. Formally,

Definition 1.2 *Given a window of size T, the local rate of innovation at time t is*

$$\rho_T(t) = \frac{1}{T} C_x(t - T/2, t + T/2) \tag{1.7}$$

and the maximal local rate $\rho_m(T)$ is defined by

$$\rho_m(T) = \max_{t\in\mathbb{R}} \rho_T(t). \tag{1.8}$$

For example the bilevel signal illustrated in Figure 1.5 is completely determined by the set of transitions in a given window.

1.2 Irregular sampling

Irregular sampling is commonly found in practice since the set of samples are most likely not uniformly spread. A review of the literature on nonuniform sampling theory and applications can be found in [52]. The author also narrates a brief history which dates back the first theoretical works in 1934 by Paley and Wiener, followed by Levinson in 1940, and Duffin and Schaeffer in 1952 [60, 48, 18]. One important theorem which pairs up to the uniform sampling theorem is the Kadec's "One Quarter" theorem [41]. It states that if the irregular set of sampling points $\{t_n\}$ is taken close to the uniform set $\{nT\}$

$$|t_n - nT| \leq D < T/4, \quad n \in \mathbb{Z} \tag{1.9}$$

then we can recover a bandlimited signal from the irregular set of samples using Lagrange's interpolation. An instance of such an irregular set occurs when the sampling device is not precise. For example, instead of taking a sample at every T seconds, it may very well be that this sample corresponds to time $T + \epsilon$. This is called jitter and may be remedied if the jittery locations are known or are modeled correctly. For theoretical work on jittered and random sampling see [2, 11, 7, 46, 42, 49]. If the jitter locations are unknown (which is usually the case in practice) then it is more difficult to recover the signal. Irregular sampling with unknown sampling locations is investigated in Chapter 4. A similar problem has been treated in the context of error correction where the locations of the errors in the received signal are unknown [24, 25].

In certain applications the sampling locations may have a certain pattern. For example suppose one wants to improve the resolution of a digital image by taking multiple shots of the same scene but each differing by a vertical and horizontal shift. If the multiple copies are put on a finer grid according to the shifts then a periodic nonuniform set of samples are obtained and an image with a better resolution can be recovered. In practice the shifts are unknown and this is another example of the irregular sampling with unknown locations problem. In Chapter 5 a fast reconstruction scheme that exploits the nice periodic nonuniform structure of the problem is given. Periodic nonuniform sampling for multiband signals has been studied in [22, 33, 65]. In [27] the problem is considered in terms of an M-channel filter bank and is solved using a projection onto convex sets (POCS) method. In [22] a well-conditioned universal sampling pattern is determined for the reconstruction of multiband signals. An overview on pattern sampling can be found in [64].

In the last decade an important number of publications have been put forth by the Numerical Harmonic Analysis Group (NuHAG) in Vienna and this is a first stop for anyone interested in sampling. Their contribution is not only theoretical but also considerably practical [31, 19, 73]. Gröchenig and Feichtinger have introduced the adaptive weights method which compensates for the irregularities in the irregular sampling set, for example when there are big gaps or bunched samples. Along with Strohmer they developed the ACT or the "Adaptive weights Conjugate gradient Toeplitz" method which is a fast and computationally efficient iterative reconstruction method for one and two dimensional bandlimited signals, [72, 19, 20]. The fast methods rely on the fact that the matrices involved are Toeplitz and this is due to the bandlimited property of the signal. If the signals do not belong to Fourier subspaces but for example to wavelet subspaces as treated in [14, 84, 85] then slower iterative methods

are used. One of the first iterative methods that recover irregularly sampled bandlimited signals is the Papoulis Gerschberg algorithm which is based on the POCS method [67, 86]. The algorithm is described in greater detail in Chapter 6 where we consider recovering irregularly sampled signals that are Fourier-based and wavelet-based approximations.

1.3 Notations and definitions

In this section first the notation and definitions found in the discrete-time world are stated, then in a similar fashion those in the continuous-time world.
In both discrete and continuous-time, matrices will be denoted by bold upper case letters, for example $\mathbf{F}$. A submatrix of $\mathbf{F}$ will be denoted by $\mathbf{F}(\mathcal{N}, \mathcal{M})$ where $\mathcal{N}$ and $\mathcal{M}$ are index sets containing the rows and columns of $\mathbf{F}$, respectively.

1.3.1 Discrete-time

Discrete-time signals and vectors will be denoted by bold lower case letters, $\mathbf{x}$, except for the discrete-time Fourier series coefficients which will be denoted by bold upper case letters $\mathbf{X}$.

- $\mathbf{x} = (x[0], x[1], \ldots, x[N-1])$ is a discrete-time periodic signal $x[n+N] = x[n]$, $x[n] \in \mathbb{C}$.
- N is the period of a discrete-time periodic signal, $N \in \mathbb{N}$.
- $\mathcal{N} = \{0, 1, \ldots, N-1\}$ is the index set of locations of a discrete-time periodic signal.
- $\mathcal{N}_K = \{n_0, n_1, \ldots, n_{K-1}\}$ is an irregular set of locations of a discrete-time periodic signal, $\mathcal{N}_K \subset \mathcal{N}, K < N$ and $K \in \mathbb{N}$.
- $\mathbf{x}(\mathcal{N}_K) = (x[n_0], x[n_1], \ldots, x[n_{K-1}])$ is an irregular set of sample values of a discrete-time periodic signal.
- $\ell^2(\mathbb{Z}) = \{\mathbf{x} : \sum_{n\in\mathbb{Z}} |x[n]|^2 < \infty\}$ is the space of square summable discrete-time signals.

Definition 1.3 *Discrete-time Fourier transform (DTFT) .*
Consider a discrete-time signal $\mathbf{x} \in \ell^2(\mathbb{Z})$. *The discrete-time Fourier transform of* $\mathbf{x}$ *is defined by*

$$X(e^{i\omega}) = \sum_{n\in\mathbb{Z}} x[n]\, e^{-i\omega n}, \quad \omega \in \mathbb{R} \tag{1.10}$$

where $x[n]$ *is synthesized by*

$$x[n] = \frac{1}{2\pi} \int_{-\pi}^{\pi} X(e^{i\omega})\, e^{i\omega n}\, d\omega, \quad n \in \mathbb{Z}. \tag{1.11}$$

Definition 1.4 *Discrete-time Fourier series (DTFS).*
Consider a discrete-time periodic signal $\mathbf{x}$ *with period* N. *The discrete-time Fourier series coefficients of* $\mathbf{x}$ *are defined by*

$$X[m] = \sum_{n=0}^{N-1} x[n]\, e^{-i2\pi nm/N}, \quad m \in \mathcal{N} = \{0, \ldots, N-1\} \tag{1.12}$$

or in matrix/vector form

$$\mathbf{X} = \mathbf{F} \cdot \mathbf{x} \tag{1.13}$$

where $\mathbf{F} = \mathbf{DFT}_N$ *with components* $F_{mn} = W_N^{mn}, m, n \in \mathcal{N}$ *and* $W_N = e^{-i2\pi/N}$. *Alternatively,*

$$x[n] = \frac{1}{N} \sum_{m=0}^{N-1} X[m]\, e^{i2\pi mn/N}, \quad n \in \mathcal{N} \tag{1.14}$$

or in matrix/vector form

$$\mathbf{x} = \mathbf{F}^{-1} \cdot \mathbf{X} \tag{1.15}$$

where $\mathbf{F}^{-1} = \frac{1}{N}\mathbf{F}^*$ *and* * *is the conjugate transpose.*

Definition 1.5 *Discrete-time bandlimited signal (M-BL).*
A discrete-time periodic signal $\mathbf{x}$ *of period* N *is bandlimited to* M *if there are* M *nonzero contiguous and* $N - M$ *zero contiguous DTFS coefficients, that is,*

$$X[m] = \begin{cases} \sum_{n=0}^{N-1} x[n]\, e^{-i2\pi nm/N} & m \in \mathcal{N}_M \\ 0 & m \notin \mathcal{N}_M \end{cases} \tag{1.16}$$

where $\mathcal{N}_M$ *is a contiguous set of* M *indices.*

1.3.2 Continuous-time

Continuous-time signals will be denoted by lower case letters, $x(t)$.

- $x(t)$ is a continuous-time signal, $t \in \mathbb{R}$.
- τ is the period of a continuous-time periodic signal, $x(t+\tau) = x(t), t \in \mathbb{R}$.
- $\mathcal{T}_K = \{t_0, t_1, \ldots, t_{K-1}\} \subset [0, \tau]$ is an irregular set of locations of a continuous-time periodic signal.
- $L^2(\mathbb{R}) = \{x(t) : \int_{t\in\mathbb{R}} |x(t)|^2\, dt < \infty\}$ is the space of square integrable continuous-time signals.

Definition 1.6 *Continuous-time Fourier transform (CTFT).*
Consider a continuous-time signal $x(t) \in L^2(\mathbb{R})$. *The continuous-time Fourier transform of* $x(t)$ *is defined by*

$$X(\omega) = \int_{-\infty}^{\infty} x(t)\, e^{-i\omega t}\, dt, \quad \omega \in \mathbb{R}. \tag{1.17}$$

Alternatively,

$$x(t) = \frac{1}{2\pi} \int_{-\infty}^{\infty} X(\omega)\, e^{i\omega t}\, d\omega, \quad t \in \mathbb{R}. \tag{1.18}$$

Definition 1.7 *Continuous-time Fourier series (CTFS).*
Consider a continuous-time periodic signal $x(t) \in L^2([0,\tau])$. The continuous-time Fourier series coefficients of $x(t)$ are defined by

$$X[m] = \frac{1}{\tau} \int_{0}^{\tau} x(t)\, e^{-i2\pi tm/\tau}\, dt, \quad m \in \mathbb{Z}. \tag{1.19}$$

Alternatively,

$$x(t) = \sum_{m\in\mathbb{Z}} X[m]\, e^{i2\pi tm/\tau}, \quad t \in [0,\tau]. \tag{1.20}$$

Definition 1.8 *Continuous-time bandlimited signal ($\omega_m - BL$).*
A continuous-time signal $x(t)$ is bandlimited to ω_m if the continuous-time Fourier transform is zero outside the band $[-\omega_m, \omega_m]$, that is,

$$X(\omega) = \begin{cases} \int_{-\infty}^{\infty} x(t)\, e^{-i\omega t}\, dt & \omega \in [-\omega_m, \omega_m] \\ 0 & \omega \notin [-\omega_m, \omega_m] \end{cases}. \tag{1.21}$$

1.4 Thesis outline

Following the structure of the Introduction this dissertation is divided in two parts. The first part concerns uniform sampling of a newly defined set of non-bandlimited signals. In Chapter 2 periodic streams of Diracs and piecewise polynomial signals with a finite rate of innovation are sampled using a periodic sinc and a differentiated sinc sampling kernel, respectively. In Chapter 3 finite streams of Diracs are sampled using an infinite length sampling kernel such as the sinc and Gaussian kernels. The dual problem is also investigated. It concerns sampling infinite length bilevel signals with a finite *local* rate of innovation. These are sampled using finite length support kernels such as splines.
The second part addresses three different irregular sampling problems: the irregular sampling problem with unknown sampling locations is introduced in Chapter 4. A particular sampling pattern is considered in Chapter 5 where the irregular set of sampling locations form a periodic nonuniform set. A fast reconstruction scheme is derived by exploiting the special structure of the data set. An application involving superresolution is also given. Finally, Chapter 6 concerns irregular sampling of signals that are Fourier- and wavelet-based linear and nonlinear approximations. The reconstruction methods are variants of the Papoulis Gerchberg algorithm and take into account the information given by the approximations.

Chapter 2

Sampling periodic signals with finite rate of innovation

Sampling theory has been extensively developed for bandlimited signals. In this chapter[1] non-bandlimited signals are investigated in particular periodic signals with a finite rate of innovation. Recall that in Section 1.1 signals with a finite rate of innovation ρ are characterized by having a finite number of degrees of freedom per unit of time. For example take a periodic signal of period N with Diracs at K locations. This signal is not bandlimited and has K degrees of freedom in an interval of length N thus its rate of innovation is $\rho = K/N$.
In Sections 2.1 and 2.2 of this chapter, sampling theorems for discrete-time and continuous-time periodic streams of weighted Diracs and piecewise polynomial signals are derived. Both of these type of signals are not bandlimited and have a finite number of degrees of freedom per period. By taking an appropriate sampling kernel and a sufficiently high sampling rate that captures these degrees of freedom, the signals can be perfectly reconstructed. Section 2.3 derives applications of the above results, in particular to piecewise bandlimited signals, and to filtered piecewise polynomials. In all of the proofs of the aforementioned sampling theorems a method that is commonly used in spectral analysis is employed, namely the "annihilating filter method" [69]. For those unfamiliar with this method it is described in Appendix 2.A.

2.1 Discrete-time periodic signals

The discrete-time periodic signals we consider are streams of weighted Diracs and piecewise polynomials. Through appropriate differentiation, piecewise polynomials can be reduced to streams of Diracs, so we begin with these.

2.1.1 Stream of Diracs

Consider a discrete-time periodic signal, with one period given by

$$\mathbf{x} = (x[0], x[1], \dots, x[N-1])^T \tag{2.1}$$

[1]This chapter includes research conducted jointly with Martin Vetterli and Thierry Blu [82, 81, 80].

and containing K weighted Diracs at locations $\{n_0, n_1, \ldots, n_{K-1}\}$, $n_k \in [0, N-1]$ and $K < \lfloor N/2 \rfloor$,

$$x[n] = \sum_{k=0}^{K-1} c_k \, \delta[n - n_k], \tag{2.2}$$

where $\delta[n]$ is the Kronecker delta and equal to 1 if $n = 0$ and 0 if $n \neq 0$.
Denote by $\mathbf{X} = (X[0], X[1], \ldots, X[N-1])^T$ the discrete-time Fourier series (DTFS) coefficients of $\mathbf{x}$ where

$$X[m] = \sum_{k=0}^{K-1} c_k \, W_N^{n_k m}, \quad m = 0, \ldots, N-1 \tag{2.3}$$

and $W_N = e^{-i2\pi/N}$.
Consider filtering the signal $x[n]$ with a lowpass filter $\tilde{\varphi}[n] = \varphi[-n]$ with bandwidth $[-K, K]$ then the sample values $y_s[l]$ are simply a subsampled version (by M) of the filtered signal $y[n] = x[n] * \tilde{\varphi}[n]$. The DTFS coefficients of $y[n]$ are given by

$$Y[m] = \begin{cases} X[m] & \text{if } m \in [-K, K] \\ 0 & \text{else} \end{cases} \tag{2.4}$$

and those of the subsampled signal $y_s[l] = y[lM]$ are given by the subsampling formula [79]

$$Y_s[m] = \frac{1}{M} \sum_{l=0}^{M-1} Y[(m + lN)/M]. \tag{2.5}$$

With appropriate re-indexing it follows that

$$Y_s[m] = \frac{1}{M} X[m], \quad m \in [-K, K]. \tag{2.6}$$

Figure 2.1 illustrates that we can recover $2K$ spectral values $X[m]$ of the original signal from the subsampled spectra of the lowpass approximation $Y_s[m]$ as long as there is no overlapping in the spectra of the lowpass approximation $Y[m]$ and this occurs only if $N/M \geq 2K$. This leads us to

Proposition 2.1 *Consider a discrete-time periodic signal $x[n]$ of period N containing K weighted Diracs. Let M be an integer divisor of N satisfying $N/M \geq 2K + 1$. Consider the discrete-time periodized sinc sampling kernel $\varphi[n] = \frac{1}{N} \sum_{m=-K}^{K} W_N^{-mn}$, that is, the inverse DTFS of the $Rect_{[-K,K]}$. Then the $N/M \in \mathbb{N}$ samples defined by*

$$y_s[l] = < x[n], \varphi[n - lM] >_{circ}, \quad l = 0, \ldots, N/M - 1 \tag{2.7}$$

are a sufficient representation of the signal.

Proof: We start by showing that the DTFS coefficients $X[m], m \in [-K, K]$ are sufficient to determine the stream of K weighted Diracs . Then we show that the N/M samples $y_s[l]$ are a sufficient representation of $X[m], m \in [-K, K]$.

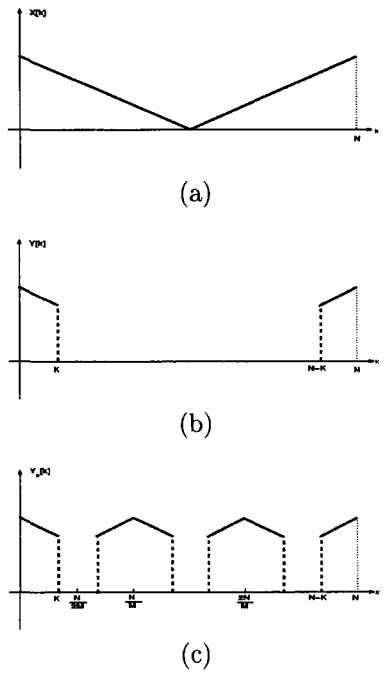

Figure 2.1: (a)DTFS of stream of Diracs, $X[k], k \in [0, N]$; (b) DTFS of lowpass approximation $Y[k] = X[k], k \in [-K, K], 0$ otherwise; (c) DTFS of lowpass approximation subsampled by $M = 3$, $Y_s[k] = 1/MX[k], k \in [-K, K]$.

1. Since $X[m]$ is a linear combination of K complex exponentials, u_k^m, with $u_k = W_N^{n_k}$, the locations n_k of the Diracs can be found using the annihilating filter method described in Appendix 2.A. It suffices to determine the annihilating filter $H(z)$ whose coefficients are $(1, H[1], \ldots, H[K])$ or

$$H(z) = 1 + H[1]\, z^{-1} + H[2]\, z^{-2} + \cdots + H[K]\, z^{-K} \tag{2.8}$$

which factors as

$$H(z) = \prod_{k=0}^{K-1} (1 - z^{-1} W_N^{n_k}) \tag{2.9}$$

and satisfies

$$\sum_{k=0}^{K} H[k]\, X[m-k] = 0, \quad m = 0, \ldots, N-1 \tag{2.10}$$

Since $H[0] = 1$, K equations (2.10) will be sufficient to determine the K unknown filter coefficients $H[k], k = 1, \ldots, K$. Let $m = 1, \ldots, K$ then the system in (2.10) is equivalent to

$$\sum_{k=1}^{K} H[k]\, X[m-k] = -X[m], \quad m = 1, \ldots, K. \tag{2.11}$$

For example take $N = 8$, $K = 3$ and let $m = 1, 2, 3$ then in matrix/vector form the system is

$$\begin{bmatrix} X[0] & X[-1] & X[-2] \\ X[1] & X[0] & X[-1] \\ X[2] & X[1] & X[0] \end{bmatrix} \cdot \begin{pmatrix} H[1] \\ H[2] \\ H[3] \end{pmatrix} = -\begin{pmatrix} X[1] \\ X[2] \\ X[3] \end{pmatrix}. \quad (2.12)$$

Given that there are K sinusoids the matrix in (2.12) is full rank ($= K$) and thus there is a unique solution $H[1], \ldots, H[K]$. The set of locations $\{n_0, n_1, \ldots, n_{K-1}\}$ are given by the the zeros of $H(z)$.
The weights of the Diracs are obtained by solving K equations in (2.3), let $m = 0, \ldots, K-1$, this leads to the following Vandermonde system

$$\begin{bmatrix} 1 & 1 & \ldots & 1 \\ W_N^{n_0} & W_N^{n_1} & \ldots & W_N^{n_{K-1}} \\ \vdots & \vdots & \ldots & \vdots \\ W_N^{n_0(K-1)} & W_N^{n_1(K-1)} & \ldots & W_N^{n_{K-1}(K-1)} \end{bmatrix} \cdot \begin{pmatrix} c_0 \\ c_1 \\ \vdots \\ c_{K-1} \end{pmatrix} = \begin{pmatrix} X[0] \\ X[1] \\ \vdots \\ X[K-1] \end{pmatrix} \quad (2.13)$$

and has a unique solution since the $n_k \neq n_l, \forall k \neq l$.
Therefore, given $2K$ contiguous DTFS coefficients

$$\{X[-K+1], X[-K+2], \ldots, X[0], \ldots, X[K]\}$$

we have found a unique set of locations $\{n_k\}_{k=0}^{K-1}$ and a unique set of weights $\{c_k\}_{k=0}^{K-1}$.

2. We need to show that $2K$ spectral values $X[m], m \in [-K, K]$ can be obtained from the N/M sample values $y_s[l]$ defined in (2.7).
We substitute the discrete-time periodized sinc kernel in the expression of the sample values and we obtain the following:

$$\begin{aligned} y_s[l] &= < x[n], \varphi[n - lM] >_{circ} \quad l = 0, \ldots, N/M - 1 && (2.14) \\ &= \sum_{n=0}^{N-1} x[n]\, \varphi[n - lM] && (2.15) \\ &= \frac{1}{N} \sum_{n=0}^{N-1} x[n] \sum_{m=-K}^{K} W_N^{-m(n-lM)} && (2.16) \\ &= \frac{1}{N} \sum_{n=0}^{N-1} x[n] \sum_{m=-K}^{K} W_N^{-mn}\, W_N^{mlM} && (2.17) \\ &= \frac{1}{N} \sum_{m=-K}^{K} W_{N/M}^{ml} \underbrace{\sum_{n=0}^{N-1} x[n]\, W_N^{-nm}}_{X[-m]} && (2.18) \\ &= \frac{1}{N} \sum_{m=-K}^{K} X[-m]\, W_{N/M}^{ml}. && (2.19) \end{aligned}$$

If we calculate the DTFS coefficients of the sample values $y_s[l]$ we obtain an expression in terms of the DTFS of the signal,

$$Y_s[k] = \sum_{l=0}^{N/M-1} y_s[l]\, W_{N/M}^{lk}, \quad k = 0, \ldots, N/M-1 \tag{2.20}$$

$$= \frac{1}{N} \sum_{l=0}^{N/M-1} \sum_{m=-K}^{K} X[-m]\, W_{N/M}^{ml} W_{N/M}^{lk} \tag{2.21}$$

$$= \frac{1}{N} \sum_{m=-K}^{K} X[-m] \underbrace{\sum_{l=0}^{N/M-1} W_{N/M}^{l(k+m)}}_{= \begin{cases} N/M & \text{if } k+m=0 \\ 0 & \text{otherwise} \end{cases}} \tag{2.22}$$

$$= \frac{1}{M} X[k], \quad k = 0, \ldots, \min\{K, N/M-1\} \tag{2.23}$$

$$\Rightarrow X[k] = M Y_s[k], \quad k = 0, \ldots, K \tag{2.24}$$

by hypothesis, $N/M \geq 2K+1 > K$. Since we are dealing with real signals the DTFS is Hermitian, that is, $X[-k] = X^*[k]$, $k = 0, \ldots, K$, so we have the $2K+1$ spectral values $X[k]$, $k \in [-K, K]$ obtained from the N/M DTFS coefficients of the sample values $y_s[l]$. Therefore we have a sufficient number of spectral values which uniquely define the stream of weighted Diracs.

■

Figure 2.2 illustrates in time and frequency domain the sampling of a discrete-time periodic stream of Diracs with period $N = 256$ and $K = 15$ weighted Diracs. The signal is perfectly reconstructed within machine precision, $MSE = 10^{-11}$.

Note that in the proof of Proposition 2.1 the locations of the Diracs are determined by finding the roots of the annihilating filter $H(z)$. If the locations are bunched up or there are a large number of Diracs then finding the roots of the polynomial is numerically unstable. An alternative method that is commonly used in error correction coding [8] involves extrapolating the $N-K$ spectral values of the signal using K first spectral $X[k], k = 1, \ldots, K$ components and the error locating polynomial which in our case corresponds to the annihilating filter $H[k], k = 1, \ldots, K$,

$$X[k] = -\sum_{l=1}^{K} H[l]\, X[k-l], \quad k = K+1, \ldots, N-K. \tag{2.25}$$

Consider a signal of length $N = 64$ where there are $K = 16$ Diracs in an interval of size $2K$, see Figure 2.3. Figure 2.4 compares the relative reconstruction error between the root finding method and the spectral extrapolation method for different values of K.

2.1.2 Piecewise polynomials of degree R

The previous result on the stream of Diracs is extended to piecewise polynomials. Consider a discrete-time periodic piecewise polynomial of period N with

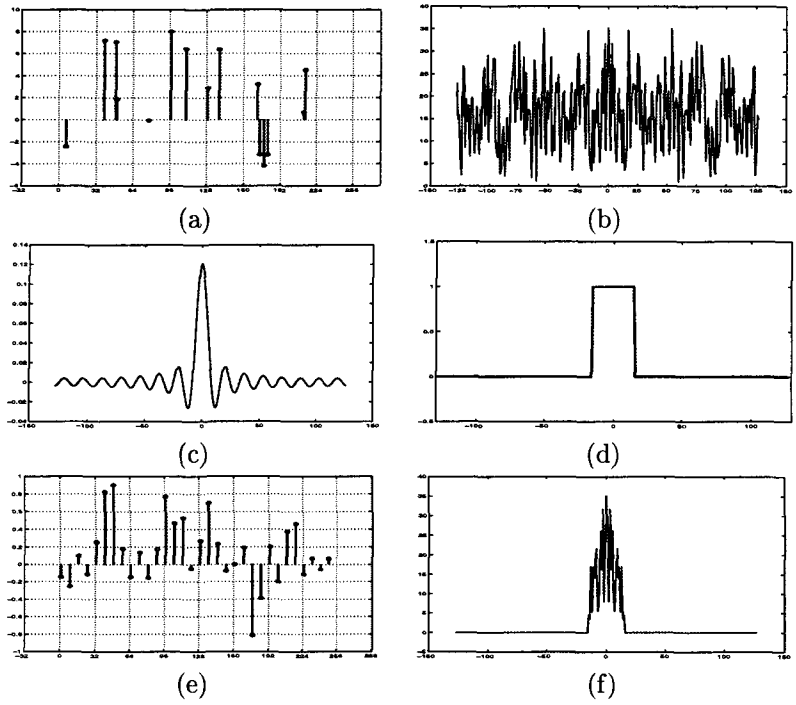

Figure 2.2: (a) Periodic discrete-time signal with $K = 15$ weighted Diracs with period $N = 256$; (b) DTFS $X[m]$; (c) Discrete-time periodized sinc sampling kernel, $\varphi[n]$; (d) DTFS $Rect_{[-K,K]}$, $K = 15$; (e) Sample values $y_s[l] =< x[n], \varphi[n-lM] >$, $l = 0, \ldots, 31$ with $M = 8$; (f) DTFS $\mathbf{Y}_s$.

K polynomial pieces each with maximum degree R and $R+1$ zero moments. Suppose a discrete-time difference operator $d[n] = \delta[n] - \delta[n-1]$ is applied $R+1$ times to the piecewise polynomial signal. The differentiated signal $x^{R+1}[n]$ obtained is a stream of Diracs, that is, in frequency domain

$$X^{(R+1)}[m] = (D[m])^{R+1} X[m], \quad m = 0, \ldots, N-1 \tag{2.26}$$

where $D[m] = 1 - W_N^m$ is the DTFS of the discrete-time difference operator. This results in putting to zero all the polynomial pieces. Assume there are discontinuities between pieces (but no Diracs), then K transitions can lead to at most $K(R+1)$ weighted Diracs and thus the rate of innovation is

$$\rho = 2K(R+1)/N.$$

From Proposition 2.1 we can uniquely recover the $K(R+1)$ Diracs from $2K(R+1)$ DTFS coefficients of the differentiated signal $X^{(R+1)}[k]$. The piecewise polynomial signal is reconstructed by applying the inverse discrete-time difference operator $R+1$ times on the stream of weighted Diracs. Note that the discrete-time difference operator $d[n]$ is a singular operator (since $D[0] = 0$) and so we

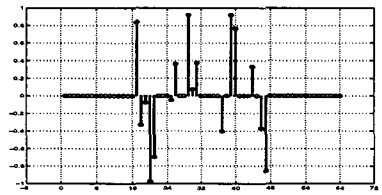

Figure 2.3: Stream of $K = 16$ bunched Diracs with period $N = 64$.

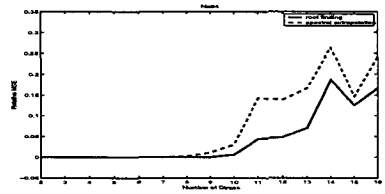

Figure 2.4: Comparison between the root finding method and the spectral extrapolation method on a signal of length $N = 64$, K varying between 2 and 16 on interval $2K$, 100 simulations.

define the inverse discrete-time difference operator as

$$D^{-1}[m] = \begin{cases} 0 & \text{for } m = 0 \\ (1 - W_N^m)^{-1} & \text{for } m = 1, \dots, N-1 \end{cases} . \tag{2.27}$$

Hence instead of using the sinc sampling kernel $\varphi[n]$ we will use the derivative sinc sampling kernel defined by

$$\psi[n] = (\underbrace{d * d * \cdots * d}_{R+1} * \varphi)[n] \tag{2.28}$$

which has at least $R+1$ zeros at the origin $z = 1$. Then the DTFS of $\psi[n]$ is

$$\Psi[m] \;=\; (1 - W_N^m)^{R+1}\, \Phi[m], \quad m = 0, \dots, N-1 \tag{2.29}$$

where $\Phi[m]$ is the $Rect_{[-K(R+1),K(R+1)]}$ function. This brings us to the following theorem.

Theorem 2.1 *Consider a discrete-time periodic piecewise polynomial signal of period N with K pieces of degree R and with $R+1$ zero moments. Let M be an integer and a divisor of N such that $N/M \geq (2K(R+1)+1)$. Take a sampling kernel $\psi[n]$ with DTFS coefficients defined in (2.29). Then we can recover the signal from the $N/M \in \mathbb{N}$ samples*

$$y_s[l] \;=\; < x[n], \psi[n - lM] > \quad l = 0, \dots, N/M - 1. \tag{2.30}$$

Proof: First we show that $2K(R+1)$ DTFS coefficients of the signal, $X[m], m \in [-K(R+1), K(R+1)]$ are sufficient to determine the piecewise polynomial signal, $x[n]$. Then we show that the N/M samples $y_s[l]$ are sufficient to determine the $(2K(R+1)+1)$ values $X[m]$.

1. If we have the DTFS coefficients $X[m], m \in [-K(R+1), K(R+1)]$ then from (2.26) we have the DTFS coefficients of the $(R+1)$th discrete-time differentiated signal, $X^{(R+1)}[m]$. From Proposition 2.1 these are sufficient to reconstruct the stream of $K(R+1)$ Diracs. Thus, the signal is recovered by applying $R+1$ times the inverse discrete-time difference operator, $d^{-1}[n]$, on the stream of Diracs, that is,

$$x[n] = (\underbrace{d^{-1} * d^{-1} * \cdots * d^{-1}}_{R+1} * x^{(R+1)})[n].$$

2. Similar to the second part in the proof of Proposition 2.1 we expand the inner product between the piecewise polynomial signal and the differentiated sinc sampling kernel:

$$\begin{aligned}
y_s[l] &= < x[n], \psi[n - lM] >, \quad l = 0, \ldots, N/M - 1 && (2.31)\\
&= \sum_{n=0}^{N-1} x[n]\, \psi[n - lM] && (2.32)\\
&= \frac{1}{N} \sum_{n=0}^{N-1} x[n] \sum_{m=-K(R+1)}^{K(R+1)} (1 - W_N^m)^{R+1}\, W_N^{-m(n-lM)} && (2.33)\\
&= \frac{1}{N} \sum_{n=0}^{N-1} x[n] \sum_{m=-K(R+1)}^{K(R+1)} (1 - W_N^m)^{R+1}\, W_N^{-mn}\, W_N^{mlM} && (2.34)\\
&= \frac{1}{N} \sum_{m=-K(R+1)}^{K(R+1)} (1 - W_N^m)^{R+1} W_{N/M}^{ml} \underbrace{\sum_{n=0}^{N-1} x[n]\, W_N^{-nm}}_{X[-m]} && (2.35)\\
&= \frac{1}{N} \sum_{m=-K(R+1)}^{K(R+1)} (1 - W_N^m)^{R+1}\, X[-m]\, W_{N/M}^{ml}. && (2.36)
\end{aligned}$$

Taking the DTFS of the sample values $y_s[l]$ we obtain

$$\begin{aligned}
Y_s[k] &= \sum_{l=0}^{N/M-1} y_s[l]\, W_{N/M}^{lk}, \quad k = 0, \ldots, N/M - 1 && (2.37)\\
&= \frac{1}{N} \sum_{l=0}^{N/M-1} \sum_{m=-K(R+1)}^{K(R+1)} (1 - W_N^m)^{R+1}\, X[-m]\, W_{N/M}^{ml} W_{N/M}^{lk} && (2.38)\\
&= \frac{1}{N} \sum_{m=-K(R+1)}^{K(R+1)} (1 - W_N^m)^{R+1}\, X[-m] \underbrace{\sum_{l=0}^{N/M-1} W_{N/M}^{l(k+m)}}_{= \begin{cases} N/M & \text{if } k+m = 0 \\ 0 & \text{otherwise} \end{cases}} && (2.39)\\
&= \frac{1}{M} (1 - W_N^{-k})^{R+1}\, X[k], \quad k = 0, \ldots, \min\{N/M, K(R+1)\} && (2.40)\\
\Rightarrow X[k] &= \begin{cases} M\left[(1 - W_N^{-k})^{R+1}\right]^{-1} Y_s[k] & \text{for } k = 1, \ldots, K(R+1) \\ 0 & \text{for } k = 0 \end{cases} && (2.41)
\end{aligned}$$

Since $N/M \geq (2K(R+1)+1)$ we have a sufficient representation for the spectral values of the signal. This completes the proof.

■

Figure 2.5 illustrates the reconstruction of a discrete-time periodic piecewise linear signal of period $N = 1024$ with $K = 6$ pieces.

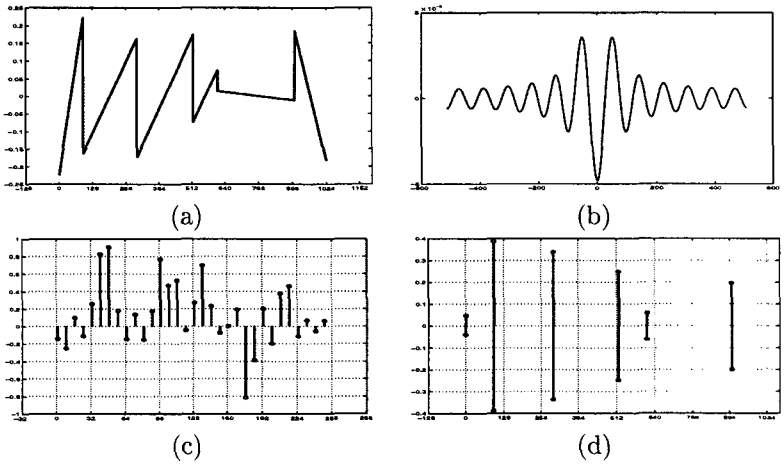

Figure 2.5: (a) Discrete-time periodic piecewise linear ($R = 1$) signal of period $N = 1024$ with $K = 6$ pieces. Note that the vertical lines are not pieces but jumps; (b) Differentiated sinc sampling kernel,$\psi[n] = d[n] * d[n] * \varphi[n]$ with DTFS $D[m] \cdot Rect_{[-K(R+1),K(R+1)]}$ (c) Sample values $y_s[l] =< x[n], \psi[n - lM] >, l = 0, \ldots, 31$ with $M = 32$; (d) Stream of $K(R+1) = 12$ Diracs obtained from $X[m], m \in [-K(R+1), K(R+1)]$.

2.2 Continuous-time periodic signals

We derive now the equivalent results but for continuous-time periodic signals, again building up from a stream of Diracs to piecewise polynomials. We will put in evidence the common points.

2.2.1 Stream of Diracs

Consider a continuous-time periodic signal $x(t)$ of period τ containing K weighted Diracs at locations $\{t_k\}_{k=0}^{K-1}$ with $t_k \in [0, \tau)$, or

$$\begin{aligned} x(t) &= \sum_{n \in \mathbb{N}} c_n \, \delta(t - t_n) \\ &= \sum_{n \in \mathbb{N}} \sum_{k=0}^{K-1} c_k \, \delta(t - (t_k + n\tau)) \end{aligned} \tag{2.42}$$

since $t_{n+K} = t_n + \tau$ and $c_{n+K} = c_n$ for all $n \in \mathbb{N}$.
The continuous-time Fourier series (CTFS) coefficients of $x(t)$ are defined by

$$\begin{aligned} X[m] &= \frac{1}{\tau}\int_0^{\tau} x(t)\, e^{-i2\pi tm/\tau}\, dt, \quad m \in \mathbb{Z} \\ &= \frac{1}{\tau}\sum_{k=0}^{K-1} c_k\, e^{-i2\pi t_k m/\tau}. \end{aligned} \tag{2.43}$$

If the signal $x(t)$ is convolved with a sinc filter of bandwidth $[-K, K]$ then we have a lowpass approximation $y(t)$ given by

$$y(t) = \sum_{m=-K}^{K} X[m]\, e^{i2\pi mt/\tau}. \tag{2.44}$$

Suppose the lowpass approximation $y(t)$ is sampled at multiples of T, we obtain $\tau/T \in \mathbb{N}$ samples defined by

$$y_s[l] = y(lT) = \sum_{m=-K}^{K} X[m]\, e^{i2\pi mlT/\tau}, \quad l = 0, \ldots, \tau/T - 1. \tag{2.45}$$

Similar to the discrete-time case as long as the number of samples is larger than the number of values in the spectral support of the lowpass signal, that is, $\frac{\tau}{T} \geq 2K + 1$, (2.45) can be used to recover $2K + 1$ values of $X[m]$. Thus we can state:

Proposition 2.2 *Consider a continuous-time periodic stream of K weighted Diracs with period τ and a continuous-time periodic sinc sampling kernel $\varphi(t)$ with bandwidth $[-K, K]$. Taking a sampling period T such that $\tau/T \in \mathbb{N}$ and $\tau/T \geq 2K + 1$. Then the samples defined by*

$$y_s[l] = < x(t), \varphi(t - lT) >, \quad l = 0, \ldots, \tau/T - 1 \tag{2.46}$$

are a sufficient representation of $x(t)$.

Proof: Similar to the discrete-time case first we show that $2K + 1$ CTFS coefficients $X[m]$ are sufficient to find the locations and the weights of the Diracs. From (2.43) we have that the CTFS coefficients $X[m]$ are linear combinations of complex exponentials. Thus to find the locations t_k we need to find the annihilating filter $\mathbf{H} = (1, H[1], H[2], \ldots, H[K])$ such that

$$\mathbf{H} *_c \mathbf{X} = 0. \tag{2.47}$$

This is the same Toeplitz system as in (2.10) considered in Sec. 2.1.1 and therefore a solution exists. Factoring the $z-$transform of $\mathbf{H}$, or $H(z) = \sum_{k=0}^{K} H[k]\, z^{-k}$, into

$$H(z) = \prod_{k=0}^{K-1} (1 - z^{-1} u_k), \tag{2.48}$$

we then find the K locations $\{t_0, t_1, \ldots, t_{K-1}\}$ from the zeros of $H(z)$, that is, from

$$u_k = e^{-i2\pi t_k/\tau}. \tag{2.49}$$

Given the locations $\{t_k\}_{k=0}^{K-1}$ and K values $X[m], m = 0, \ldots, K-1$, we find the weights $\{c_k\}_{k=0}^{K-1}$ of the Diracs by solving the Vandermonde system in (2.43). Since the locations t_k are distinct, $t_k \neq t_l, \forall k \neq l$, the Vandermonde system admits a solution.

The second part of the proof consists in showing that the τ/T samples $y_s[l]$ are sufficient to determine the CTFS coefficients $X[m], m \in [-K, K]$. We substitute the continuous-time periodic sinc function $\varphi(t)$ with bandwidth $[-K, K]$ defined by

$$\varphi(t) = \sum_{m=-K}^{K} e^{i2\pi mt}. \tag{2.50}$$

in (2.46) and we obtain

$$\begin{aligned} y_s[l] &= < x(t), \varphi(t - lT) >, \quad l = 0, \ldots, \tau/T - 1 && (2.51)\\ &= \int_0^{\tau} x(t) \sum_{m=-K}^{K} e^{i2\pi m(t-lT)/\tau}\, dt && (2.52)\\ &= \sum_{m=-K}^{K} e^{-i2\pi ml/(\tau/T)} \underbrace{\int_0^{\tau} x(t) e^{i2\pi mt/\tau}\, dt}_{\tau X[-m]} && (2.53)\\ &= \tau \sum_{m=-K}^{K} X[-m]\, e^{-i2\pi mlT/\tau}. && (2.54) \end{aligned}$$

Note that $y_s[l]$ is periodic with period τ/T, thus the DTFS coefficients are $Y_s[k] = TX[k], k = 0, \ldots, \tau/T - 1$. Since $\tau/T \geq 2K + 1$, we have a sufficient number of samples that determine the CTFS $X[m], m \in [-K, K]$. ■

2.2.2 Piecewise polynomials of degree R

Here we consider continuous-time periodic piecewise polynomial signal of period τ, containing K polynomial pieces of maximum degree R and $R-1$ continuous derivatives, C^{R-1}. We differentiate the signal $R+1$ times and we obtain a continuous-time stream of K weighted Diracs, $x^{(R+1)}(t)$. The CTFS of the derivative operator is defined by $D[m] = i2\pi m, m \in \mathbb{Z}$ and therefore the CTFS coefficients of the differentiated signal $x^{(R+1)}(t)$ are equal to

$$X^{(R+1)}[m] = (i2\pi m)^{R+1} X[m], \quad m \in \mathbb{Z}. \tag{2.55}$$

From Proposition 2.2 we can recover the continuous-time periodic stream of K Diracs from the CTFS coefficients, $X^{(R+1)}[m], m \in [-K, K]$. Therefore we can sample the signal with the differentiated sinc sampling kernel whose CTFS coefficients are defined by

$$\Psi[m] = (i2\pi m)^{R+1} \Phi[m], \quad m \in \mathbb{Z} \tag{2.56}$$

where $\Phi[m] = Rect_{[-K,K]}$ is the CTFS of the continuous-time periodized sinc sampling kernel.

Theorem 2.2 *Consider a continuous-time periodic piecewise polynomial signal $x(t)$ with period τ, containing K pieces of maximum degree R, belonging to C^{R-1} and having zero mean. Consider a sampling kernel $\psi(t)$ with its CTFS coefficients defined in (2.56). Let $\tau/T \in \mathbb{N}$ and $\tau/T \geq 2K+1$. Then $x(t)$ can be uniquely recovered from the τ/T samples*

$$y_s[l] = < x(t), \psi(t - lT) >, \quad l = 0, \ldots, \tau/T - 1. \tag{2.57}$$

Proof: Similar to the proof of Theorem 2.1, we first show that CTFS coefficients $X[m], m \in [-K, K]$ are sufficient to determine the piecewise polynomial signal, $x(t)$. Then we show that the τ/T samples $y_s[l]$ are sufficient to determine the values $X[m], m \in [-K, K]$.

1. If we have the CTFS coefficients $X[m], m \in [-K, K]$ then from (2.55) we have the CTFS coefficients of the $(R+1)$th differentiated signal, $X^{(R+1)}[m]$. From Proposition 2.2 these are sufficient to reconstruct the stream of K Diracs. Thus, the signal is recovered by integrating $R+1$ times the stream of Diracs, that is,

$$x(t) = \underbrace{\int \int \cdots \int}_{R+1} x^{(R+1)}(t)\, dt\, dt \cdots dt$$

or in frequency domain from (2.55)

$$\begin{aligned} X[m] &= (D^{-1}[m])^{R+1}\, X^{(R+1)}[m], \quad m \in \mathbb{Z}/\{0\} && (2.58)\\ &= (i2\pi m)^{-(R+1)}\, X^{(R+1)}[m], \quad m \in \mathbb{Z}/\{0\} && (2.59) \end{aligned}$$

with $D^{-1}[m] = 0$ for $m = 0$ and thus

$$x(t) = \sum_{m \in \mathbb{Z}} X[m]\, e^{i2\pi m t/\tau}.$$

2. Similar to the second part in the proof of Proposition 2.2 we expand the inner product between the piecewise polynomial signal and the differentiated sinc sampling kernel defined by $\psi(t) = \sum_{m=-K}^{K} (i2\pi m)^{R+1} e^{i2\pi m t/\tau}$. That is, the sample values are

$$\begin{aligned} y_s[l] &= < x(t), \psi(t - lT) >, \quad l = 0, \ldots, \tau/T - 1 && (2.60)\\ &= \int_0^{\tau} x(t) \sum_{m=-K}^{K} (i2\pi m)^{R+1} e^{i2\pi m(t-lT)/\tau}\, dt && (2.61)\\ &= \sum_{m=-K}^{K} (i2\pi m)^{R+1}\, e^{-i2\pi m l T/\tau} \underbrace{\int_0^{\tau} x(t)\, e^{i2\pi m t/\tau}\, dt}_{\tau X[-m]} && (2.62)\\ &= \tau \sum_{m=-K}^{K} X[-m]\, (i2\pi m)^{R+1}\, e^{-i2\pi m l/(\tau/T)}. && (2.63) \end{aligned}$$

Since $y_s[l]$ is periodic with period τ/T, the DTFS coefficients of $y_s[l]$ are given by

$$Y_s[k] = \sum_{l=0}^{\tau/T-1} y_s[l]\, e^{-i2\pi kl/(\tau/T)} \tag{2.64}$$

$$= \tau \sum_{l=0}^{\tau/T-1} \sum_{m=-K}^{K} X[-m]\,(i2\pi m)^{R+1}\, e^{-i2\pi ml/(\tau/T)}\, e^{-i2\pi kl/(\tau/T)} \tag{2.65}$$

$$= \tau \sum_{m=-K}^{K} X[-m]\,(i2\pi m)^{R+1} \underbrace{\sum_{l=0}^{\tau/T-1} e^{-i2\pi(k+m)l/(\tau/T)}}_{=\begin{cases} \tau/T & \text{if } k+m=0 \\ 0 & \text{otherwise} \end{cases}} \tag{2.66}$$

$$= \frac{\tau^2}{T}\,(-i2\pi k)^{R+1}\, X[k] \tag{2.67}$$

Therefore the CTFS coefficients of the signal are obtained by the DTFS coefficients of the samples values $Y_s[m], m = 0, \ldots, \tau/T-1$ and are defined by

$$X[m] = \begin{cases} TY_s[m]/(\tau^2\,(-i2\pi m)^{R+1}) & \text{for } m = 1, \ldots, \tau/T-1 \\ 0 & \text{for } m = 0 \end{cases}. \tag{2.68}$$

Since $\tau/T \geq 2K+1$ the sample values are a sufficient representation of the spectral values of the signal. This completes the proof.

■

Note that removing the restriction $x(t) \in \mathcal{C}^{R-1}$ leads to the same result as in Theorem. 2.1.

2.3 Applications

The applications we consider involve the discrete-time periodic stream of Diracs and piecewise polynomial signals. It is well known that a bandlimited signal can be perfectly recovered from its samples by sampling it at twice the maximum frequency. But if the bandlimited signal has a jump or a discontinuity then the signal is no longer bandlimited and the usual method is not valid. These are what we call piecewise bandlimited signals. Another type of non-bandlimited signal which we may come across in nature is a signal which is obtained from a system with a certain frequency response. The output of the system is a filtered signal. We will look at filtered stream of Diracs and filtered piecewise polynomials.

2.3.1 Piecewise bandlimited signals

A discrete-time periodic piecewise bandlimited signal is the sum of a bandlimited signal with a stream of Diracs in the simplest case or with a piecewise polynomial signal. An example is illustrated in Figure 2.6(e) and is obviously not bandlimited from Figure 2.6(f). Formally, we have the following

Definition 2.1 *Piecewise bandlimited signals.*
Let $\mathbf{x}_{BL}$ *be a discrete-time periodic* $L-$*bandlimited signal of period* N *with corresponding DTFS coefficients* $\mathbf{X}_{BL}$ *such that* $X_{BL}[m] = 0 \quad \forall m \notin [-L, L]$. *Let* $\mathbf{x}_{PP}$ *be a discrete-time piecewise polynomial signal of period* N *with* K *polynomial pieces each of maximum degree* R *and* $R+1$ *zero moments. Then a piecewise bandlimited signal* $\mathbf{x}$ *is defined by*

$$\mathbf{x} = \mathbf{x}_{BL} + \mathbf{x}_{PP} \tag{2.69}$$

with corresponding DTFS coefficients $\mathbf{X}$ *defined by*

$$X[m] = \begin{cases} X_{BL}[m] + X_{PP}[m] & \text{if } m \in [-L, L] \\ X_{PP}[m] & \text{if } m \notin [-L, L] \end{cases} . \tag{2.70}$$

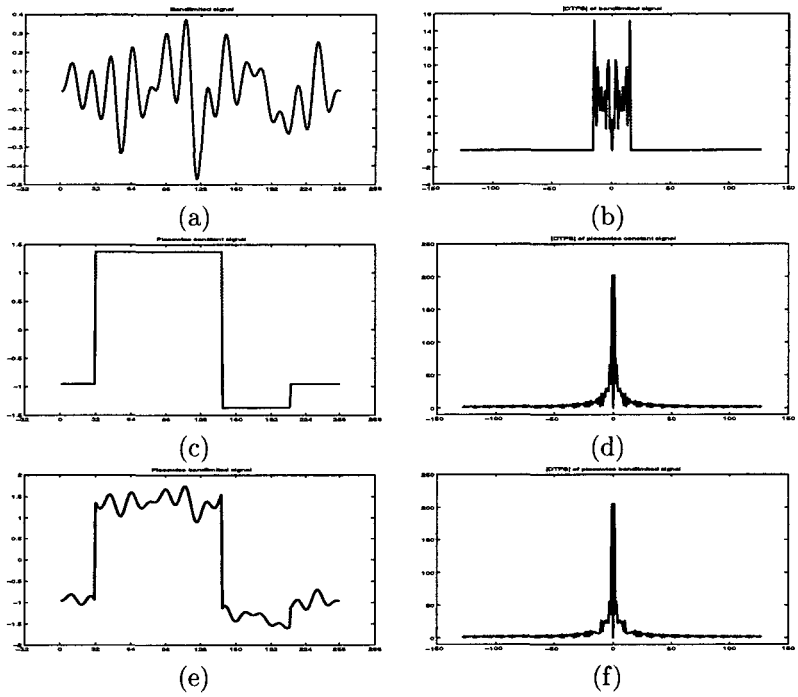

Figure 2.6: (a) Bandlimited signal of length $N = 256$; (b) $|DTFS|$ of Bandlimited signal, $L = 15$; (c) Piecewise constant signal with $K = 3$ pieces; (d) $|DTFS|$ of piecewise constant signal; (e) Bandlimited piecewise constant signal; (f) $|DTFS|$ of bandlimited piecewise constant signal.

First consider a stream of K weighted Diracs, $\mathbf{x}_{PP}$. From Section 2.1.1, we can recover the K weighted Diracs from $2K$ contiguous frequency values $\mathbf{X}_{PP}$. Since the DTFS coefficients of the bandlimited signal, $\mathbf{X}_{BL}$, are equal to zero outside of the band $[-L, L]$, we have that the DTFS coefficients of the signal outside of the band $[-L, L]$ are exactly equal to the DTFS coefficients of the piecewise polynomial, that is, $\mathbf{X}[m] = \mathbf{X}_{PP}[m], \quad \forall |m| > L$. Therefore it is sufficient to take the $2K$ DTFS coefficients of the outside of the band $[-L, L]$,

for instance in $[L+1, L+2K]$. Suppose we have the DTFS of the signal $X[m]$, with $m \in [-(L+2K), L+2K]$ then the DTFS of the bandlimited signal are obtained by subtracting $X_{PP}[m]$ from $X[m]$ for $m \in [-L, L]$.
Recall that the piecewise polynomial has $2K(R+1)$ degrees of freedom and the bandlimited signal has $2L+1$. It follows that we can sample the signal using a discrete-time periodized differentiated sinc sampling kernel bandlimited to $2K(R+1)+L$.

Corollary 2.1 *Consider a piecewise bandlimited signal* $\mathbf{x}$ *as defined in Definition. 2.1. Let* $\psi[n]$ *be the* $(R+1)$*th differentiated sinc sampling kernel with DTFS*

$$\Psi[m] = (D[m])^{R+1}\, Rect_{[-(2K(R+1)+L),2K(R+1)+L]}. \tag{2.71}$$

Let M *be an integer divisor of* N*, and let* $N/M \geq 2(2K(R+1)+L)$ *then the samples*

$$y_s[l] =< x[n], \psi[n-lM] >, \quad l = 0, \ldots, N/M-1 \tag{2.72}$$

are a sufficient representation of $\mathbf{x}$.

Proof: The proof is exactly the same as in Theorem 2.1 until equation (2.40)

$$Y_s[k] = \frac{1}{M}(1-W_N^{-k})^{R+1}\, X[k], k = 0, \ldots, 2K(R+1)+L \tag{2.73}$$

$$= \begin{cases} \frac{1}{M}(1-W_N^{-k})^{R+1}\left(X_{BL}[k]+X_{PP}[k]\right) & \text{if } k = 0, \ldots, L \\ \frac{1}{M}(1-W_N^{-k})^{R+1}\, X_{PP}[k] & \text{if } k = L+1, \ldots, 2K(R+1)+L \end{cases} \tag{2.74}$$

Therefore $2K(R+1)$ values of

$$X_{PP}[k] = \frac{M}{(1-W_N^{-k})^{R+1}}\, Y_s[k], \quad k \in [L+1, 2K(R+1)+L] \tag{2.75}$$

are sufficient to recover the piecewise polynomial $\mathbf{x}_{PP}$. From these we can recover the L spectral components of the bandlimited signal since

$$X_{BL}[k] = \frac{1}{(1-W_N^{-k})^{R+1}}(Y_s[k] - X_{PP}[k]), \quad k = 0, \ldots, L. \tag{2.76}$$

This gives us the the bandlimited signal $\mathbf{x}_{BL}$ and thus the piecewise bandlimited signal as defined in Definition 2.1 is recovered $\mathbf{x} = \mathbf{x}_{BL} + \mathbf{x}_{PP}$. ■

Figure 2.7 illustrates the reconstruction of a bandlimited plus a piecewise constant signal using the following reconstruction scheme:

Algorithm 2.1 *Reconstruction of piecewise bandlimited signals.*
Require: $N, M, N/M \geq 2(2K(R+1)+L)+1$;
Calculate the samples $y_s[l] =< x[n], \psi[n-lM] >, l = 0, \ldots, N/M-1$;
Calculate the DTFS $X[m], m \in [-(2K(R+1)+L), (2K(R+1)+L)]$ *from the DTFS of samples* $y_s[l] \longrightarrow X_{PP}[m] = X[m], m \in [L+1, (2K(R+1)+L)]$;
Solve $\mathbf{h} * X_{PP}[m] = 0, m \in [L+1, (2K(R+1)+L)] \longrightarrow \mathbf{x}_{PP}$;
Calculate $X_{BL}[m] = X[m] - X_{PP}[m], \quad m \in [-L, L] \longrightarrow \mathbf{x}_{BL}$;
The reconstruction is $\mathbf{x} = \mathbf{x}_{BL} + \mathbf{x}_{PP}$.

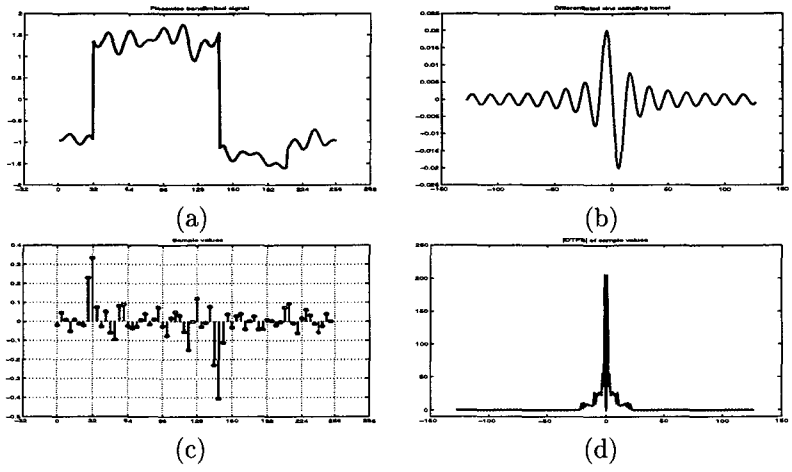

Figure 2.7: (a) Bandlimited piecewise constant signal, $x[n]$, with $K = 3$, $L = 15$,$R = 0$,$N = 256$; (b) Differentiated sinc sampling kernel, $\psi[n] = d[n] * \varphi[n]$, bandlimited to $2K(R+1)+L = 21$; (c) Sample values $y_s[l] =< x[n], \psi[n - lM] >$, $l = 0, \ldots, N/M - 1$, $M = 4$; (d) $|DTFS|$ of sample values; Reconstruction error is 10^{-13}.

2.3.2 Filtered piecewise polynomials

Another application of sampling piecewise polynomial signals consists in sampling their filtered output. Figure 2.8 illustrates that a filtered stream of Diracs is not bandlimited. These signals are formally defined in the following

Definition 2.2 *Filtered piecewise polynomials.*
Let $\mathbf{x}_{PP}$ *be a zero mean discrete-time periodic piecewise polynomial signal of period* N *with* K *pieces of maximum degree* R. *Let* $\mathbf{g}$ *be a filter with DTFS* $\mathbf{G}$. *Then a filtered piecewise polynomial* $\mathbf{x}$ *is defined by*

$$\mathbf{x} = \mathbf{g} * \mathbf{x}_{PP} \tag{2.77}$$

and the corresponding DTFS coefficients $\mathbf{X}$ *are defined by*

$$X[m] = G[m] \cdot X_{PP}[m], \quad m = 0, \ldots, N-1. \tag{2.78}$$

Suppose $\mathbf{x}_{PP}$ is a stream of K Diracs. If the filter has $2K$ contiguous nonzero frequency values $G[m]$ then $2K$ frequency values of the signal $X[m]$ will be enough to determine $2K$ frequency values of the stream of Diracs, since $X_{PP}[m] = X[m]/G[m]$, and from Proposition 2.1 these are sufficient to recover the stream of Diracs .

Corollary 2.2 *Consider a filtered piecewise polynomial signal* $\mathbf{x}$ *as defined in Definition. 2.2 with* $G[m] \neq 0, m \in [-K(R+1), K(R+1)]$. *Consider an* $(R+1)$ *differentiated sinc sampling kernel* $\psi[n]$ *with DTFS*

$$\Psi[m] = (D[m])^{R+1}\, Rect_{[-K(R+1),K(R+1)]}. \tag{2.79}$$

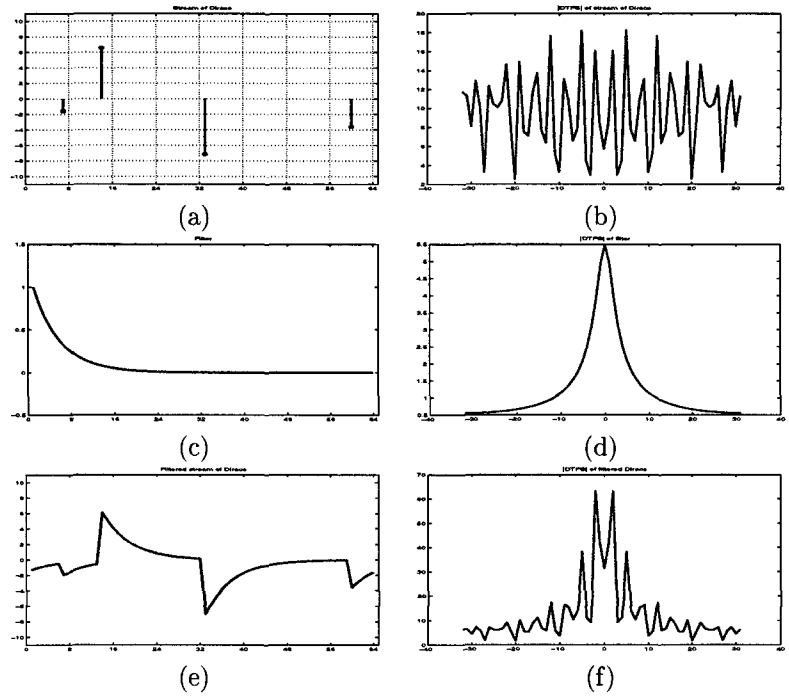

Figure 2.8: (a) Stream of $K = 4$ Diracs with period $N = 64$; (b) $|DTFS|$ of stream of Diracs (c) Known filter $g[n] = \alpha^n, n = 0, \ldots, N-1$, $\alpha = 0.4$; (d) $|DTFS|$ of filter; (e) Filtered stream of Diracs; (f) $|DTFS|$ of filtered stream of Diracs.

Let M be an integer divisor of N such that $N/M \geq 2K(R+1)+1$. Then the filtered piecewise polynomial signal can be recovered from the N/M samples

$$y_s[l] =< x[n], \psi[n - lM] >, \quad l = 0, \ldots, N/M - 1. \tag{2.80}$$

Proof: Similar to the proof of piecewise bandlimited signals, we have that the DTFS coefficients of the samples $y_s[l]$ are equal to

$$\begin{aligned} Y_s[k] &= \frac{1}{M}(1 - W_N^{-k})^{R+1} X[k], \quad k \in [-K(R+1), K(R+1)] \quad (2.81) \\ &= \frac{1}{M}(1 - W_N^{-k})^{R+1} \left(G[k]\, X_{PP}[k]\right). \quad (2.82) \end{aligned}$$

Since $G[k] \neq 0$ for $k \in [-K(R+1), K(R+1)]$ we have $2K(R+1)$ values of the DTFS of the piecewise polynomial

$$X_{PP}[k] = \frac{M}{(1 - W_N^{-k})^{R+1} G[k]} Y_s[k], \quad k \in [-K(R+1), K(R+1)] \tag{2.83}$$

which are sufficient to recover $\mathbf{x}_{PP}$ and which leads to the filtered signal by Definition 2.2. ■

The reconstruction scheme is described in the following algorithm and an example of the reconstruction is illustrated in Figure 2.9.

Algorithm 2.2 ***Require:*** $N, M, N/M \geq 2K(R+1)+1$;
Calculate the samples $y_s[l] =< x[n], \psi[n - lM] >, l = 0, \ldots, N/M - 1$;
Calculate $\mathbf{Y}_s = \mathbf{DFT}_{N/M} \cdot \mathbf{y}_s \longrightarrow X[m], m \in [-K(R+1), K(R+1)]$;
Calculate $X_{PP}[m] = X[m]/G[m], m \in [-K(R+1), K(R+1)]$;
Solve $\mathbf{h} * X_{PP}[m] = 0, m \in [-K(R+1), K(R+1)] \longrightarrow \mathbf{x}_{PP}$;
The reconstruction is $\mathbf{x} = \mathbf{g} * \mathbf{x}_{PP}$.

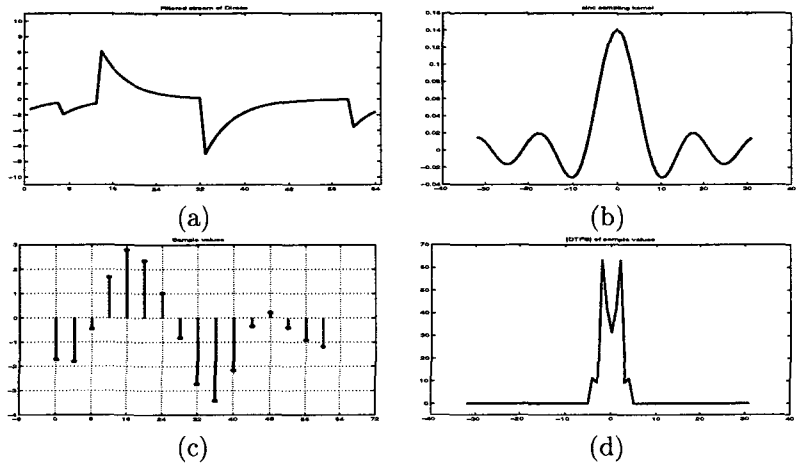

Figure 2.9: (a) Filtered stream of Diracs, $x[n]$, $N = 64$; (b) Sinc sampling kernel $\varphi[n]$ bandlimited to $K = 4$; (c) Sample values $y_s[l] =< x[n], \varphi[n - lM] >, l = 0, \ldots, 15$, $M = 4$; (d) $|DTFS|$ of sample values; Reconstruction error is 10^{-13}.

We have seen that the crux of the proof relies on the fact that the filter is known and is invertible over the number of degrees of freedom of the problem. What if the filter has a finite rate of innovation but is unknown? This is more complex and remains to be investigated.

2.4 Summary

- We derived sampling theorems for periodic signals in particular streams of weighted Diracs and piecewise polynomials. These signals have a finite rate of innovation ρ which is equal to the number of degrees of freedom per period.
- The samples are obtained by taking the inner product of the signal with a shifted version of the periodized sinc kernel or differentiated sinc kernels. The bandwidth of these kernels must be greater or equal to the degrees of freedom of the signal.
- The discrete-time periodic signals are perfectly recovered when the sampling rate $1/M$ is greater or equal to the rate of innovation $\rho = 2K/N$ in the case of streams of weighted Diracs or $\rho = 2K(R+1)/N$ in the case of a piecewise polynomial signal with K pieces and maximum degree R.
- The continuous-time periodic streams of Diracs and piecewise polynomial signals are perfectly recovered when the sampling rate $1/T$ is greater or equal to the rate of innovation $\rho = 2K/\tau$ since we assumed that the piecewise polynomial signal belonged to $\mathcal{C}^{R-1}$.
- The sampling and reconstruction scheme is illustrated in Figure 2.10.

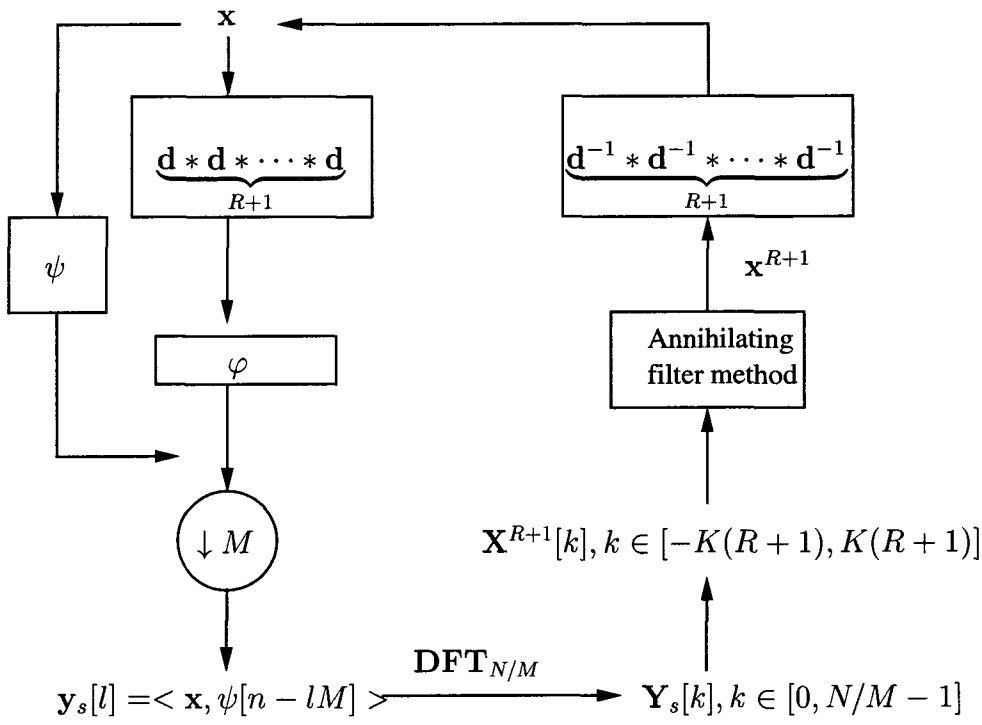

Figure 2.10: Sampling and reconstruction scheme for discrete-time piecewise polynomial signals with K pieces of maximum degree R; N/M is the number of samples; $2K(R+1)+1$ is the bandwidth of the sampling kernel.

Appendix 2.A Annihilating filter method

The problem in spectral line analysis consists in estimating the frequencies of a sinusoidal signal from a set of values. The methods used for estimating such frequencies are known as high-resolution methods, for example MUSIC, ESPRIT and can be found in [69]. We define the following as the annihilating filter method:
Consider a filter $\mathbf{h} = (h_0, h_1, \dots, h_K)$ characterized by its z-transform $H(z) = \sum_{l=0}^{K} h_l\, z^{-l}$.

Definition 2.3 *Annihilating filter.*
A filter h is called an annihilating filter for a signal $s[n]$ if and only if

$$(h * s)[n] = 0, \quad \forall n \in \mathbb{Z}. \tag{2.84}$$

Proposition 2.3 *The filter $H(z) = 1 - u\, z^{-1}$ annihilates the exponential signal $s[n] = u^n$.*

Proof: Let $y = h * s$. Then in $z-$ domain we have $Y(z) = H(z)\, S(z) = S(z) - u\, z^{-1}\, S(z)$ and thus y satisfies the difference equation

$$y[n] = s[n] - u\, s[n-1]. \tag{2.85}$$

Substitute $s[n] = u^n$ in (2.85) we obtain

$$y[n] = u^n - u\, u^{n-1} = 0, \quad \forall n \in \mathbb{Z} \tag{2.86}$$

■

Consider a signal $s[n], n \in \mathbb{Z}$ defined as a finite linear combination of K exponentials u_k^n,

$$s[n] = \sum_{k=0}^{K-1} c_k\, u_k^n \tag{2.87}$$

where c_k are real and u_k are real or complex valued. In the context of spectral line analysis $u_k = e^{i\omega_k}$ where ω_k is the kth frequency component of the signal $s[n]$.

Corollary 2.3 *The filter*

$$H(z) = \prod_{k=0}^{K-1} (1 - u_k\, z^{-1}) \tag{2.88}$$

annihilates the signal $s[n]$ defined in (2.87).

Proof: Let $y = h * s$. Denote the kth annihilating filter by

$$H_k(z) = (1 - u_k\, z^{-1}) \tag{2.89}$$

and let $S_k(z)$ be the z-transform of the kth exponential signal $s_k[n] = u_k^n$. Then we have

$$\begin{aligned} Y(z) &= H(z)\,S(z) && (2.90)\\ &= \prod_{l=0}^{K-1}(1-u_l\,z^{-1})\sum_{k=0}^{K-1} c_k\,S_k(z) && (2.91)\\ &= \sum_{k=0}^{K-1} c_k\Big(\prod_{l=0}^{K-1}(1-u_l\,z^{-1})\,S_k(z)\Big) && (2.92)\\ &= \sum_{k=0}^{K-1} c_k\Big(\prod_{l=0,l\neq k}^{K-1}(1-u_l\,z^{-1})\,\underbrace{(1-u_k\,z^{-1})\,S_k(z)}_{=0}\Big) && (2.93)\\ &= 0 \text{ from Proposition 2.3.} \end{aligned}$$

Therefore to find the values u_k we need to find the filter coefficients h_l in

$$H(z) = \sum_{l=0}^{K} h_l\,z^{-l} \tag{2.94}$$

such that

$$\begin{aligned} \mathbf{h} * \mathbf{s} &= \mathbf{0} && (2.95)\\ \Leftrightarrow \sum_{k=0}^{K} h_k\,s[n-k] &= 0, \quad \forall n. && (2.96) \end{aligned}$$

In matrix/vector form the system in (2.96) is equivalent to

$$\begin{bmatrix} \vdots & \vdots & \cdots & \vdots \\ s[0] & s[-1] & \cdots & s[-K] \\ s[1] & s[0] & \cdots & s[-(K-1)] \\ \vdots & \vdots & \ddots & \\ s[K] & s[K-1] & \cdots & s[0] \\ \vdots & \vdots & \cdots & \vdots \end{bmatrix} \cdot \begin{pmatrix} h_0 \\ h_1 \\ \vdots \\ h_K \end{pmatrix} = 0. \tag{2.97}$$

Suppose a finite number of values $s[n]$ are available. Since there are $K+1$ unknown filter coefficients we need at least $K+1$ equations, and therefore we need at least $2K+1$ values of $s[n]$ to find the filter coefficients.[2] Define $\mathbf{S}$ the appropriate sub-matrix then the system $\mathbf{S}\cdot\mathbf{h} = 0$ will admit a solution when

$$rank(\mathbf{S}) = K. \tag{2.98}$$

In pratice this system is solved using a singular value decomposition where the matrix $\mathbf{S}$ is decomposed into $\mathbf{S} = \mathbf{U}\Sigma\mathbf{V}^*$. We obtain that $\mathbf{h} = \mathbf{V}\cdot\mathbf{e}_{K+1}$ where $\mathbf{e}_{K+1}$ is a vector with 1 on position $K+1$ and 0 elsewhere [36]. The method can be adapted to noise by minimizing $||\mathbf{S}\cdot\mathbf{h}||$ in which case $\mathbf{h}$ is given by the

[2] Actually there are K unknown filter coefficients since $h_0 = 1$ and therefore we will need at least $2K$ values of $s[n]$. The system to solve in this case is known as a Yule-Walker system [30]

eigenvector associated with the smallest eigenvalue of $\mathbf{S}^T\mathbf{S}$.
Once the the filter coefficients are found then the values u_k are simply the roots of the annihilating filter $H(z)$.
To determine the weights c_k it suffices to take K equations in (2.87) and solve the system for c_k. Let $n = 0, \ldots, K-1$ then in matrix vector form we have the following Vandermonde system

$$\begin{bmatrix} 1 & 1 & \ldots & 1 \\ u_0 & u_1 & \ldots & u_{K-1} \\ \vdots & \vdots & \ldots & \vdots \\ u_0^{(K-1)} & u_1^{(K-1)} & \ldots & u_{K-1}^{(K-1)} \end{bmatrix} \cdot \begin{pmatrix} c_0 \\ c_1 \\ \vdots \\ c_{K-1} \end{pmatrix} = \begin{pmatrix} s[0] \\ s[1] \\ \vdots \\ s[K-1] \end{pmatrix} \tag{2.99}$$

and has a unique solution when

$$u_k \neq u_l, \forall k \neq l. \tag{2.100}$$

This concludes the annihilating filter method.

Chapter 3

Sampling signals with finite rate and finite local rate of innovation

In this chapter[1] we go beyond periodicity in terms of the signals and the sampling kernels. Section 3.1 investigates sampling finite length signals with a finite rate of innovation using sampling kernels with infinite support. The signals in question are streams of weighted Diracs sampled with the sinc and the Gaussian kernel. These types of kernels are appealing to mathematicians. It will be shown that if the critical number of samples is taken then a sampling theorem can be derived. Section 3.2 considers the dual problem: infinite length piecewise polynomial signals and compact support sampling kernels. A particular interest is given to bilevel signals with a finite *local* rate of innovation and spline sampling kernels. Given that the signals have a finite local rate of innovation, local reconstruction is possible and schemes are given in Section 3.2.3.

3.1 Finite length signals with finite rate of innovation

A finite length signal with finite rate of innovation ρ clearly has a finite number of degrees of freedom. The question of interest is: Given a sampling kernel with *infinite support*, is there a *finite set of samples* that uniquely specifies the signal? In the following sections we will sample signals with finite number of weighted Diracs with infinite support sampling kernels such as the sinc and Gaussian.

3.1.1 Sinc sampling kernel

Consider a continuous-time signal with a finite number of weighted Diracs

$$x(t) = \sum_{k=0}^{K-1} c_k \, \delta(t - t_k) \tag{3.1}$$

[1]This chapter includes research conducted jointly with Martin Vetterli and Thierry Blu [82, 80].

and an infinite length sinc sampling kernel, see Figure 3.1.

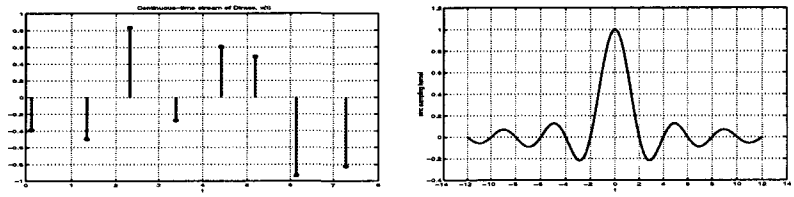

(a) (b)

Figure 3.1: (a) Example of a finite length continuous-time stream of $K = 8$ Diracs randomly spread on an interval $[0, \tau]$ with $\tau = 8$; (b) Sinc sampling kernel, $\text{sinc}(t/T), T = 2$.

The sample values are obtained by filtering the signal with a $\text{sinc}(t/T), t \in \mathbb{R}$, sampling kernel. This is equivalent to taking the inner product between the signal and a shifted version of the sinc

$$y_n =< x(t), \text{sinc}(t/T - n) > \tag{3.2}$$

where $\text{sinc}(t) = \sin(\pi t)/\pi t$. The question that arises is: How many of these samples do we need to recover the signal? The signal has $2K$ degrees of freedom, K from the weights and K from the locations of the Diracs and thus N samples, $N \geq 2K$, will be sufficient to recover the signal. Similar to the previous cases, the reconstruction method will require solving two systems of linear equations: one for the locations of the Diracs and the second for the weights of the Diracs. These systems admit solutions if the following conditions are satisfied:

[C1] $\text{Rank}(\mathbf{V}) = K$ where $v_{nk} = \Delta^K \left((-1)^n n^k y_n \right)$ and $\mathbf{V} \in \mathbb{R}^{(N-K)\times(K+1)}$;

[C2] $\text{Rank}(\mathbf{A}) = K$ where $a_{nk} = \frac{\sin(\pi t_k/T)}{\pi\,(t_k/T - n)}$ and $\mathbf{A} \in \mathbb{R}^{K\times K}$.

Theorem 3.1 *Given a finite stream of K weighted Diracs and a sinc sampling kernel* $\text{sinc}(t/T)$. *If conditions [C1] and [C2] are satisfied then N samples with $N \geq 2K$*

$$y_n \;=\; < x(t), \text{sinc}(t/T - n) > \tag{3.3}$$

are a sufficient representation of the signal.

Proof: Taking the inner products between the signal and shifted versions of the sinc sampling kernel yields a set of N samples

$$\begin{aligned} y_n &= < x(t), \mathrm{sinc}(t/T - n) >, \quad n = 0, \ldots, N-1 && (3.4)\\ &= \int_{-\infty}^{\infty} \sum_{k=0}^{K-1} c_k \, \delta(t - t_k) \, sinc(t/T - n) \, dt && (3.5)\\ &= \sum_{k=0}^{K-1} c_k \, \mathrm{sinc}\left(t_k/T - n\right) && (3.6)\\ &= \sum_{k=0}^{K-1} \frac{c_k \sin\left(\pi t_k/T - \pi n\right)}{\pi\left(t_k/T - n\right)} && (3.7)\\ &= (-1)^n \sum_{k=0}^{K-1} \frac{c_k \sin\left(\pi t_k/T\right)}{\pi\left(t_k/T - n\right)} && (3.8)\\ \Leftrightarrow (-1)^n y_n &= \frac{1}{\pi} \sum_{k=0}^{K-1} c_k \sin\left(\pi t_k/T\right) \cdot \frac{1}{\left(t_k/T - n\right)} && (3.9) \end{aligned}$$

The denominator of the previous expression (3.9) can be rewritten as follows:

$$\frac{1}{\left(t_k/T - n\right)} = \frac{\prod_{l \neq k} \left(t_l/T - n\right)}{\prod_{l=0}^{K-1} \left(t_l/T - n\right)} = \frac{P_k(n)}{P(n)} \qquad (3.10)$$

where $P(u)$ is an interpolation polynomial of degree K with zeros at all values of t_k/T,

$$P(u) = \prod_{l=0}^{K-1} \left(t_l/T - u\right) = \sum_{k=0}^{K} p_k \, u^k \qquad (3.11)$$

and the $P_k(u)$ is a polynomial of degree $K-1$ and has zeros at all locations except at location t_k

$$P_k(u) = \prod_{l \neq k} \left(t_l/T - u\right), \quad k = 0, \ldots, K-1. \qquad (3.12)$$

Therefore if the coefficients of the polynomial $P(u)$ are determined then the locations of the Diracs are simply the K roots of $P(u)$. We can now find an equivalent expression to (3.9) in terms of the interpolating polynomials:

$$(-1)^n P(n) \, y_n = \frac{1}{\pi} \sum_{k=0}^{K-1} c_k \sin\left(\pi t_k/T\right) P_k(n). \qquad (3.13)$$

Note that the right-hand side of (3.13) is a polynomial of degree $K-1$ in the variable n, applying K finite differences makes the left-hand side vanish,[2] that

[2]Note that the K finite difference operator plays the same role as the annihilating filter in the previous chapter.

is,

$$\Delta^K\left((-1)^n P(n)\, y_n\right) = 0, \quad n = K, \ldots, N-1 \tag{3.14}$$

$$\Leftrightarrow \sum_{k=0}^{K} p_k \underbrace{\Delta^K\left((-1)^n n^k\, y_n\right)}_{v_{nk}} = 0 \tag{3.15}$$

$$\Leftrightarrow \mathbf{V}\cdot\mathbf{p} = 0 \tag{3.16}$$

where the matrix $\mathbf{V}$ is an $(N-K)\times(K+1)$ matrix and admits a solution when $N-K \geq K$ and the rank($\mathbf{V}$) is less than $K+1$, that is, condition [C1]. Therefore (3.15) can be used to find the $K+1$ unknowns p_k which lead to the K locations t_k. Once the K locations t_k are determined the weights of the Diracs c_k are found by solving the system in (3.9) for $n = 0, \ldots, K-1$. Since $t_k \neq t_l, \forall k \neq l$, the system admits a solution from condition [C2]. ■

Note that the result does not depend on T. In practice if T is not chosen appropriately then the matrices $\mathbf{V}$ may be ill-conditioned. Figure 3.2(a) illustrates the conditioning of the matrix $\mathbf{V}$ is the least for T close to 0.5 and that the matrix $\mathbf{A}$ is well-conditioned on average.

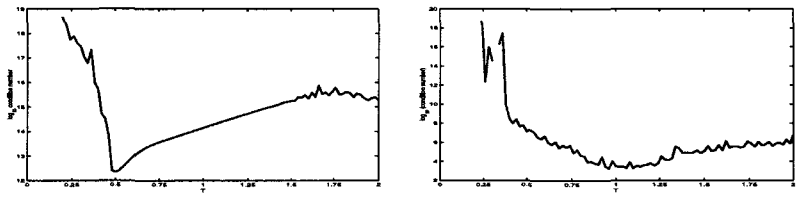

(a) (b)

Figure 3.2: (a) Average condition number of the matrix that leads to the locations of the Diracs, $\mathbf{V}$, versus the sampling interval T, optimal $T \approx 0.5$; (b) Average condition number of the matrix that leads to the weights of the Diracs, $\mathbf{A}$, versus the sampling interval T, optimal $T \approx 1$. Average is taken on 100 signals with 8 Diracs uniformly spread in the interval $[0, 8]$.

By choosing more adequately the interpolating polynomials, for example by taking the Lagrange polynomials, we may reduce the conditioning of the matrix $\mathbf{V}$, but this remains to be investigated. The algorithm is as follows:

Algorithm 3.1 *Finite length stream of Diracs sampled with an infinite sinc sampling kernel*

Given $y_n = < x(t), \mathrm{sinc}(t/T - n) >, \quad n = 0, 1, \ldots, N-1;$
Calculate $v_{nk} = \Delta^K\left((-1)^n n^k\, y_n\right), \quad n = K, \ldots, N-1, \quad k = 0, \ldots, K;$
Solve the linear system $\mathbf{V}\cdot\mathbf{p} = 0 \longrightarrow \{p_0, p_1, \ldots, p_K\};$
Find the K *roots of* $P(u) = \sum_{k=0}^{K} p_k\, u^k \longrightarrow \{t_0/T, t_1/T, \ldots, t_{K-1}/T\};$
Calculate $a_{nk} = \dfrac{\sin\left(\pi t_k/T\right)}{\pi\left(t_k/T - n\right)}, \quad n = 0, 1, \ldots, N-1\ ;$
Calculate $Y_n = (-1)^n P(n)\, y_n, \quad n = 0, 1, \ldots, N-1;$
Solve the linear system $\mathbf{A}\cdot\mathbf{c} = \mathbf{Y} \longrightarrow \{c_0, c_1, \ldots, c_{K-1}\}.$

This method can be extended to piecewise polynomials, similarly to Theorem 2.2. Also, there is an obvious equivalent for discrete-time signals in $\ell^2(\mathbb{Z})$ and discrete-time sinc kernels.

3.1.2 Gaussian sampling kernel

Consider sampling the same signal as in (3.1) but this time with a Gaussian sampling kernel, $\varphi_\sigma(t) = e^{-t^2/2\sigma^2}$, see Figure 3.3.

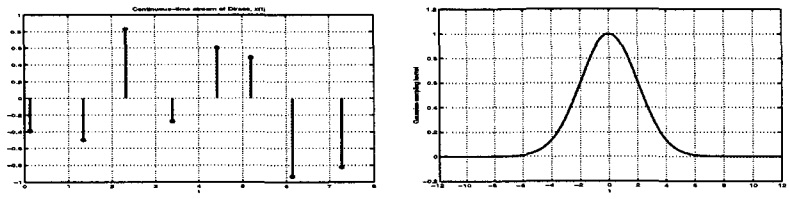

(a) (b)

Figure 3.3: (a) Example of a finite length continuous-time stream of $K = 8$ Diracs randomly spread on an interval $[0, \tau]$ with $\tau = 8$; (b) Gaussian sampling kernel, $\varphi_\sigma(t) = e^{-t^2/2\sigma^2}, \sigma = 2$.

Similar to the sinc sampling kernel, the samples are obtained by filtering the signal with a Gaussian kernel. Since there are $2K$ unknown variables we show next that N samples with $N \geq 2K$ are sufficient to represent the signal.

Theorem 3.2 *Given a finite stream of K weighted Diracs and a Gaussian sampling kernel $\varphi_\sigma(t) = e^{-t^2/2\sigma^2}$. If $N \geq 2K$ then the N sample values*

$$y_n = < x(t), \varphi_\sigma(t/T - n) > \tag{3.17}$$

are sufficient to reconstruct the signal.

Proof: The sample values are given by

$$\begin{aligned} y_n &= < x(t), e^{-(t/T-n)^2/2\sigma^2} >, \quad n = 0, \ldots, N-1 && (3.18)\\ &= \int_{-\infty}^{\infty} \sum_{k=0}^{K-1} c_k \, \delta(t - t_k) \, e^{-(t/T-n)^2/2\sigma^2} \, dt && (3.19)\\ &= \sum_{k=0}^{K-1} c_k \, e^{-(t_k/T-n)^2/2\sigma^2}. && (3.20) \end{aligned}$$

We expand (3.20) and regroup the terms so as to have variables that depend solely on n and solely on k. We obtain

$$y_n = \sum_{k=0}^{K-1} \left(c_k \, e^{-t_k^2/2\sigma^2 T^2} \right) \cdot e^{n t_k/\sigma^2 T} \cdot e^{-n^2/2\sigma^2} \tag{3.21}$$

which is equivalent to

$$Y_n = \sum_{k=0}^{K-1} a_k \, u_k^n \tag{3.22}$$

where we let $Y_n = e^{n^2/2\sigma^2}\, y_n$, $a_k = c_k\, e^{-t_k^2/2\sigma^2 T^2}$ and $u_k = e^{t_k/\sigma^2 T}$. Note that we reduced the expression Y_n to a linear combination of real exponentials. This hints that the annihilating filter method described in the Section 2.1.1 seems appropriate to find the K values u_k. Let $H(z) = h_0 + h_1\, z^{-1} + \cdots + h_K\, z^{-K}$ be an annihilating filter, that is, $\mathbf{h}$ is such that

$$\mathbf{h} * \mathbf{Y} = 0 \tag{3.23}$$

$$\Leftrightarrow \sum_{k=0}^{K} h_k\, Y_{n-k} = 0, \quad n = K, \ldots, N-1. \tag{3.24}$$

Note that this is a Toeplitz system with real exponential components $Y_n = e^{n^2/2\sigma^2}\, y_n$ and therefore a solution exists when the number of equations is greater than the number of unknowns, that is, $N - K \geq K$ and the rank of the system is less than $K+1$ which is the case by hypothesis. Furthermore σ must be carefully chosen otherwise the system is ill-conditioned. If we factor $H(z) = \prod_{k=0}^{K-1} (1 - z^{-1} u_k)$ then we obtain the locations of the Diracs t_k from the roots of the polynomial $H(z)$, that is,

$$t_k = \sigma^2 T \ln u_k. \tag{3.25}$$

Once the values of the Diracs t_k are obtained then we solve for a_k the Vandermonde system in (3.22) for which a solution exists since $u_k \neq u_l, \forall k \neq l$. The weights of the Diracs are simply given by

$$c_k = a_k\, e^{t_k^2/2\sigma^2 T^2}. \tag{3.26}$$

■

The reconstruction scheme is given in the following

Algorithm 3.2 *Finite length stream of Diracs sampled with a Gaussian sampling kernel*

Given $y_n = < x(t), e^{-(t/T-n)^2/2\sigma^2} >, \quad n = 0, \ldots, N-1;$

Calculate $Y_n = e^{n^2/2\sigma^2}, \quad n = 0, \ldots, N-1;$

Solve the linear system $\mathbf{h} * \mathbf{Y} = 0 \longrightarrow \{h_0, h_1, \ldots, h_K\};$

Find the K *roots of* $H(z) = \sum_{k=0}^{K} h_k\, z^k \longrightarrow \{u_0, u_1, \ldots, u_{K-1}\}$

$\longrightarrow t_k = \sigma^2 T \ln u_k;$

Solve the linear system $Y_n = \sum_{k=0}^{K-1} a_k\, u_k^n, \quad n = 0, \ldots, K-1 \longrightarrow \{a_0, a_1, \ldots, a_{K-1}\}$

$\longrightarrow c_k = a_k\, e^{t_k^2/2\sigma^2 T^2}.$

Here unlike in the sinc case, we have an almost local reconstruction because of the exponential decay of the Gaussian sampling kernel which brings us to the next topic.

3.2 Infinite length signals with finite local rate of innovation

In this section we consider the dual problem of Section 3.1, that is, *infinite* length *signals* $x(t), t \in \mathbb{R}^+$ with a finite *local* rate of innovation and sampling

kernels with *compact support.* In particular, the $\beta-$splines of different degree d are considered [75]

$$\varphi_d(t) = (\varphi_{d-1} * \varphi_0)(t), \quad d \in \mathbb{N}^+ \tag{3.27}$$

where $\varphi_0(t)$ is the box spline defined by

$$\varphi_0(t) = \begin{cases} 1 & \text{if } 0 \leq t < 1 \\ 0 & \text{else} \end{cases} . \tag{3.28}$$

We develop local reconstruction algorithms which depend on moving intervals equal to the size of the support of the sampling kernel.[3] The advantage of local reconstruction algorithms is that their complexity does not depend on the length of the signal. We begin by considering bilevel signals, followed by piecewise polynomial signals.

3.2.1 Bilevel signals

Consider an infinite length continuous-time signal $x(t), t \in \mathbb{R}^+$ which takes on two values, 0 and 1, with initial condition $x(t)\big|_{t=0} = 1$ with a finite local rate of innovation, ρ. These are called bilevel signals and are completely represented by their transition values t_k. For example, binary signals such as amplitude or position modulated pulses or PAM, PPM signals [32], see Figure 3.4.

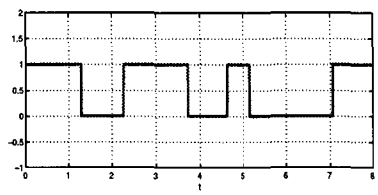

Figure 3.4: Bilevel signal with 6 transitions.

Suppose a bilevel signal is sampled with a box spline $\varphi_0(t/T)$. Then the sample values are given by the inner products between the bilevel signal and the box function,

$$y_n =< x(t), \varphi_0(t/T - n) >= \int_{-\infty}^{\infty} x(t)\, \varphi_0(t/T - n)\, dt. \tag{3.29}$$

It can bee seen in Figure 3.5 that the sample value y_n corresponds to the area occupied by the signal in the interval $[nT, (n+1)T]$. Thus if there is at most one transition per box then we can recover the transition from the sample. This leads us to

Proposition 3.1 *A bilevel signal $x(t), t > 0$, with initial condition $x(t)\big|_{t=0} = 1$, is uniquely determined from the samples $y_n =< x(t), \varphi_0(t/T - n) >$ where $\varphi_0(t)$ is the box spline defined in (3.28) if and only if there is at most one transition t_k in each interval $[nT, (n+1)T]$.*

[3] The size of the support of $\varphi_d(t/T)$ is equal to $(d+1)T$.

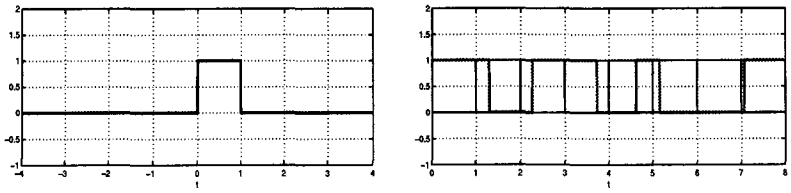

(a) (b)

Figure 3.5: (a) Box spline sampling kernel, $\varphi_0(t)$, $T = 1$. (b) Bilevel signal sampled with the box sampling kernel.

Proof: For simplicity let $T = 1$. Consider an interval $[n, n+1]$ and suppose $x(n) = 1$. First we show sufficiency followed by necessity .

$\Leftarrow$: If there are 0 transitions in the interval $[n, n+1]$ then the area under the bilevel signal, or the sample value, is $y_n = 1$ since we supposed that $x(t)\big|_{t=n} = 1$. If there is one transition in $[n, n+1]$ then the sample value is equal to

$$y_n = < x(t), \varphi_0(t-n) > = \int_{-\infty}^{\infty} x(t)\,\varphi_0(t-n)\,dt \tag{3.30}$$

$$= \int_{n}^{n+1} x(t)\,dt = \int_{n}^{t_k} 1\,dt = t_k - n \tag{3.31}$$

This implies that $t_k = y_n + n$. Similarly if $x(n) = 0$ then we have $t_k = n + 1 - y_n$. Therefore we can uniquely determine the signal in the interval $[n, n+1]$.

$\Rightarrow$: Necessity is shown by counterexample.
Suppose $x(n) = 1$ and there are two transitions t_k, t_{k+1} in the interval $[n, n+1]$ then the sample value is equal to

$$y_n = \int_{n}^{n+1} x(t)\,dt = \int_{n}^{t_k} 1\,dt + \int_{t_{k+1}}^{n+1} 1\,dt \tag{3.32}$$

$$= t_k - n + n + 1 - t_{k+1} = t_k - t_{k+1} + 1. \tag{3.33}$$

That is, there is one equation with two unknowns and therefore insufficient samples to determine both transitions. Thus there must be at most one transition in an interval $[n, n+1]$ to uniquely define the signal.

■

Now consider shifting the bilevel signal by an unknown shift ϵ, see Figure 3.6, then there will be two transitions in the interval $[5, 6]$ and one box function will not be sufficient to recover the transitions. Suppose we double the sampling rate, then the support of the box sampling kernel is doubled and we have two sample values y_n, y_{n+1} covering the interval $[nT, (n+1)T]$ but these values are identical

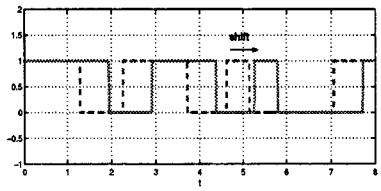

Figure 3.6: Shifted bilevel signal with two transitions in the interval $[5, 6]$.

(see their areas). Therefore increasing the sampling rate is still insufficient. This brings us to consider a sampling kernel not only with a larger support but with added information. For example, the hat spline function $\varphi_1(t/T)$ defined by

$$\varphi_1(t) = \begin{cases} 1 - |t| & \text{if } |t| < 1 \\ 0 & \text{else} \end{cases} \tag{3.34}$$

leads to sample values defined by $y_n =< x(t), \varphi_1(t/T - n) >$ or

$$y_n = \int_{(n-1)T}^{nT} x(t)\big(1 + t/T - n\big)\, dt + \int_{nT}^{(n+1)T} x(t)\big(1 - (t/T - n)\big)\, dt. \tag{3.35}$$

From Figure 3.7 we can see that there are two sample values covering the interval $[nT, (n+1)T]$.

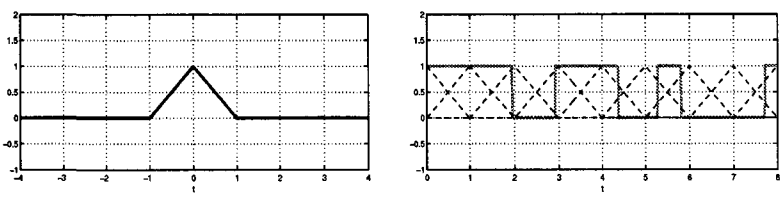

(a) (b)

Figure 3.7: (a) Hat spline sampling kernel,$\varphi(t/T)$, $T = 1$. (b) Bilevel signal with two transitions in an interval $[n, n+1]$ sampled with a hat sampling kernel.

We will show next that we can uniquely determine a bilevel signal with a hat sampling kernel.

Proposition 3.2 *An infinite length bilevel signal $x(t)$, with initial condition $x(0) = 1$ is uniquely determined from the samples defined by*

$$y_n = < x(t), \varphi_1(t/T - n) > \tag{3.36}$$

where $\varphi_1(t)$ is the hat sampling kernel if and only if there are at most two transitions $t_k \neq t_j$ in each interval $[nT, (n+2)T]$.

Proof: Again, for simplicity let $T = 1$ and suppose the signal is known for $t \leq n$ and $x(t)\big|_{t=n} = 1$.
First we show sufficiency by showing the existence and uniqueness of a solution. Then we show necessity by a counterexample.

$\Leftarrow$: Similar to the box sampling kernel the sample values will depend on the configuration of the transitions in the interval $[n, n+2]$. If there are at most 2 transitions in the interval $[n, n+2]$ then the possible configurations are

$$(0,0), (0,1), (0,2), (1,0), (1,1), (2,0)$$

where the first and second component indicate the number of transitions in the intervals $[n, n+1]$, $[n+1, n+2]$ respectively, see Figure 3.8.

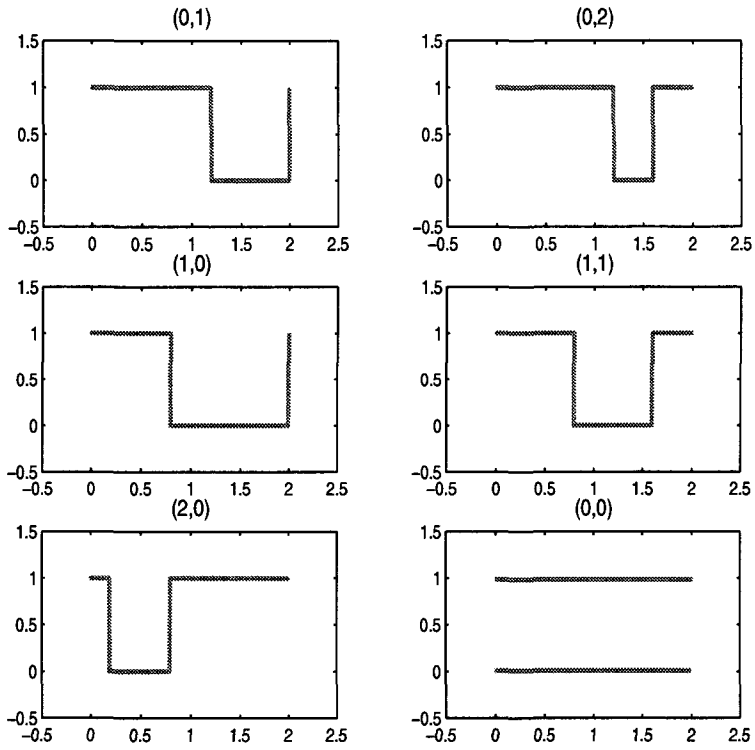

Figure 3.8: Bilevel signal containing at most 2 transitions in the interval $[0, 2]$: All possible configurations.

Furthermore since the hat sampling kernel is of degree one we obtain for

each configuration a quadratic system of equations with variables t_0, t_1.

$$y_n = \int_{n-1}^{n} x(t)\big(1+t-n\big)\,dt + \int_{n}^{n+1} x(t)\big(1-(t-n)\big)\,dt \tag{3.37}$$

$$y_{n+1} = \int_{n}^{n+1} x(t)\big(1+t-(n+1)\big)\,dt + \int_{n+1}^{n+2} x(t)\big(1-(t-(n+1))\big)\,dt. \tag{3.38}$$

First we show that the quadratic system of equations admits a solution and then that it is unique.

(a) Existence.
Take $n = 0$ and so the moving interval is $[0, 2]$.
The configuration $(0, 0)$ will lead to sample values $y_0 = 1$, $y_1 = 1$.
The configuration $(0, 1)$ will lead to sample values

$$y_0 = 1/2 + \int_1^{t_0} (t-1)\,dt = \frac{1}{2}{t_0}^2 + 1 - t_0 \tag{3.39}$$

$$y_1 = 1/2 + \int_1^{t_0} (2-t)\,dt = -\frac{1}{2}{t_0}^2 - 1 + 2t_0 \tag{3.40}$$

$\Rightarrow t_0 = y_0 + y_1 = 1 + \sqrt{-1+2y_0} = 2 - \sqrt{2-2y_1}$.
The configuration $(0, 2)$ will lead to sample values

$$y_0 = \frac{1}{2}{t_0}^2 + 1 - t_0 + t_1 - \frac{1}{2}{t_1}^2 \tag{3.41}$$

$$y_1 = -\frac{1}{2}{t_0}^2 + 1 + 2\,t_0 + \frac{1}{2}{t_1}^2 - 2\,t_1 \tag{3.42}$$

$\Rightarrow t_0 = \frac{(-2-2y_1+y_0^2+2y_0y_1+y_1^2)}{2(-2+y_0+y_1)}, t_1 = \frac{-(10-6y_1-8y_0+y_1^2+y_0^2+2y_0y_1)}{2(-2+y_0+y_1)}$.
The configuration $(1, 0)$ will lead to sample values

$$y_0 = -\frac{1}{2}{t_0}^2 + t_0 \tag{3.43}$$

$$y_1 = \frac{1}{2}{t_0}^2 \tag{3.44}$$

$\Rightarrow t_0 = y_0 + y_1 = 1 - \sqrt{1-2y_0} = \sqrt{2y_1}$.
The configuration $(1, 1)$ will lead to sample values

$$y_0 = -\frac{1}{2}{t_0}^2 + t_0 - \frac{1}{2}{t_1}^2 + t_1 \tag{3.45}$$

$$y_1 = \frac{1}{2}{t_0}^2 + 2 + \frac{1}{2}{t_1}^2 - 2\,t_1 \tag{3.46}$$

$\Rightarrow t_0 = \frac{y_0+y_1+\sqrt{-y_1^2-2y_0y_1+4y_1-y_0^2}}{2}, t_1 = \frac{-y_1-y_0+4+\sqrt{-y_1^2-2y_0y_1+4y_1-y_0^2}}{2}$
The configuration $(2, 0)$ will lead to sample values

$$y_0 = -\frac{1}{2}{t_0}^2 + 1 + t_0 + \frac{1}{2}{t_1}^2 - t_1 \tag{3.47}$$

$$y_1 = \frac{1}{2}{t_0}^2 + 1 - \frac{1}{2}{t_1}^2 \tag{3.48}$$

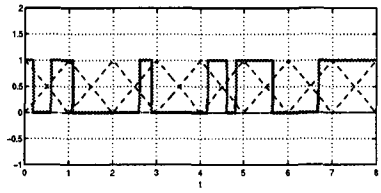

Figure 3.9: Bilevel signal containing three transitions in an interval $[4,5]$, sampled with the hat sampling kernel $\varphi_1(t)$.

$$\Rightarrow t_0 = \frac{2-2y_1+y_1^2+2y_0y_1+y_0^2-4y_0}{2(-2+y_1+y_0)}, t_1 = -\frac{6-4y_0-6y_1+y_1^2+2y_0y_1+y_0^2}{2(-2+y_1+y_0)}.$$

(b) Uniqueness.
If $y_n = 1$ and $y_{n+1} = 1$ then this implies configuration $(0,0)$.
If $y_n = 1$ and $1/2 \leq y_{n+1} \leq 1$ then the possible configurations are $(0,1),(0,2)$. By hypothesis, there are at most two transitions in the interval $[n+1, n+3]$ therefore if $y_{n+2} \leq 1/2$ then the configuration in the interval $[n, n+2]$ is $(0,1)$ otherwise if $y_{n+2} \geq 1/2$ then the configuration is $(0,2)$.
If $1/2 \leq y_n \leq 1$ and $1/2 \leq y_{n+1} \leq 1$ then this implies configuration $(2,0)$.
If $1/2 \leq y_n \leq 1$ and $0 \leq y_{n+1} \leq 1/2$ then this implies configuration $(1,0)$.

$\Rightarrow$: Necessity is shown by counterexample.
Consider a bilevel signal with three transitions in the interval $[0,2]$ but with all three in the interval $[0,1]$, see Fig. 3.9. Then the sample values in this case are are equal to

$$y_0 = 1/2 + \int_0^{t_0} (1-t)\,dt + \int_{t_1}^{t_2} (1-t)\,dt \tag{3.49}$$

$$= 1/2 + t_0 - t_1 + t_2 - t_0^2/2 + t_1^2/2 - t_2^2/2 \tag{3.50}$$

$$y_1 = \int_0^{t_0} t\,dt + \int_{t_1}^{t_2} t\,dt \tag{3.51}$$

$$= t_0^2/2 - t_1^2/2 + t_2^2/2. \tag{3.52}$$

There is no unique solution for this quadratic system of equations. Therefore there must be at most 2 transitions in an interval $[0,2]$.

■

Once again if there is an unknown shift in the bilevel signal then there may be three transitions in an interval $[nT,(n+2)T]$ and so we increase the number of samples by sampling with $\varphi_1(t/(T/2))$. The pseudo-code for sampling bilevel signals using the box and hat functions are given in full detail in Section 3.2.3. When going to higher order splines, necessity carries over. Sufficiency is more tedious since we must solve a system of higher order polynomial equations.

3.2.2 Piecewise polynomials

Similar to bilevel signals we consider sampling piecewise polynomials with the box sampling kernel. Consider an infinite length piecewise polynomial signal $x(t)$ where each piece is a polynomial of degree R and defined on an interval $[t_{k-1}, t_k]$, that is,

$$x(t) = \begin{cases} x_0(t) = \sum_{m=0}^{R} c_{0m}\, t^m & t \in [0, t_0] \\ x_1(t) = \sum_{m=0}^{R} c_{1m}\, t^m & t \in [t_0, t_1] \\ \vdots & \\ x_K(t) = \sum_{m=0}^{R} c_{Km}\, t^m & t \in [t_{K-1}, t_K] \\ \vdots & \end{cases} . \tag{3.53}$$

Each polynomial piece $x_k(t)$ contains $R+1$ unknown coefficients c_{km}. The transition value t_k is easily obtained once the pieces $x_{k-1}(t)$ and $x_k(t)$ are determined, thus there are $2(R+1)+1$ degrees of freedom. If there is one transition in an interval of length T the maximal local rate of innovation is $\rho_m(T) = (2(R+1)+1)/T$. Therefore in order to recover the polynomial pieces and the transition we need to have at least $2(R+1)+1$ samples per interval T. This is achieved by sampling with the following box sampling kernel $\varphi_0(t/\frac{T}{2(R+1)+1})$. For example if $x(t)$ is a piecewise linear signal with 2 pieces, as illustrated in Figure 3.10, then to recover the signal it is sufficient to take 5 samples: two before the transition, two after the transition and one sample covering the transition.

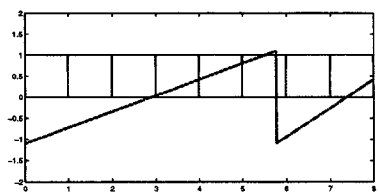

Figure 3.10: Piecewise linear signal sampled with a box sampling kernel.

We can generalize by noting that the Rth derivative of a piecewise polynomial of degree R is a piecewise constant signal. The pseudo-code for sampling piecewise constant signals with the box sampling kernel is found in Section 3.2.3 .

3.2.3 Local reconstruction algorithms

The following algorithms have been implemented in Maple^{TM}. In all of the algorithms k is the index of a transition value and n is the index of the current interval $[n, n+1]$. We suppose that $x(t) = 1, \forall t \leq 0$.

Bilevel signals

Suppose N sample values $y_n =< x(t), \varphi_0(t-n) >$ are available.

Algorithm 3.3 *Bilevel signal with box sampling kernel.*

Require: $k \leftarrow 0$, $n \leftarrow 0$
  while $n \leq N-1$ ***do***
    if $y_n = 1$ ***then***
      $x(t) = 1 \quad \forall t \in [n, n+1]$.
    end if
    if $y_n = 0$ ***then***
      $x(t) = 0 \quad \forall t \in [n, n+1]$.
    end if
    if $0 < y_n < 1$ ***then***
      if $x(n^+) = 1$ ***then***
        $t_k \leftarrow y_n + n$
      else
        $t_k \leftarrow n + 1 - y_n$
      end if
      $k \leftarrow k + 1$
    end if
    $n \leftarrow n + 1$
  end while

Next we give the pseudo-code for bilevel signals sampled with a hat sampling kernel. Suppose N sample values $y_n =< x(t), \varphi_1(t-n) >$ are available. The variable tncode is a set whose last component indicates the number of transitions in the interval $[n-1, n]$.

Algorithm 3.4 *Bilevel signal with hat sampling kernel.*

Require: $tncode \leftarrow \emptyset$, $k \leftarrow 0$, $n \leftarrow -1$
  while $n \leq N-1$ ***do***
    if $y_n = 1$ ***then***
      $tncode \leftarrow 0$
      $x(t) = 1 \qquad \forall t \in [n-1, n+1]$
    end if
    if $y_n = 0$ ***then***
      $tncode \leftarrow 0$
      $x(t) = 0 \qquad \forall t \in [n-1, n+1]$
    end if
    if $0 < y_n < 1$ ***then***
      if 0 *transitions in the interval* $[n-1, n]$ ***then***
        if $y_n = 0.5$ ***then***
          $t_k \leftarrow n$
          $tncode \leftarrow 0$
        else
          $sol =$ *solve for configuration* $(1, 0) \in [n, n+2]$
          if $sol \neq \emptyset$ ***then***
            $tncode \leftarrow 1, 0$
            if $x(n^+) = 1$ ***then***
              $t_k \leftarrow n + 1 - \sqrt{2 - 2\,y_n}$

else
$t_k \leftarrow n + 1 - \sqrt{2}\sqrt{y_n}$
end if
$n \leftarrow n + 2$
$k \leftarrow k + 1$
solfound $\leftarrow$ *True*
else
sol = *solve for configuration* $(1,1) \in [n, n+2]$
if *sol* $\neq \emptyset$ **then**
tncode $\leftarrow 1,1$
if $x(n^+) = 1$ **then**
$t_k \leftarrow n + 1 - \sqrt{2 - 2\,y_n}$
$t_{k+1} \leftarrow n + 2 - \sqrt{-3 + 2\,y_{n+1} + 2\sqrt{2 - 2\,y_n} + 2\,y_n}$
else
$t_k \leftarrow n + 1 - \sqrt{2}\sqrt{y_n}$,
$t_{k+1} \leftarrow n + 2 - \sqrt{1 + 2\sqrt{2}\sqrt{y_n} - 2\,y_{n+1} - 2\,y_n}$
end if
$n \leftarrow n + 2$
$k \leftarrow k + 2$
solfound $\leftarrow$ *True*
else
solfound $\leftarrow$ *False*
end if
end if
end if
if *not solfound* **then**
sol = *solve for configuration* $(2,0) \in [n, n+2]$
if *sol* $\neq \emptyset$ **then**
tncode $\leftarrow 2,0$
if $x(n^+) = 1$ **then**
$t_k \leftarrow \frac{1}{2}\,\frac{2-2\,y_{n+1}-4\,y_n+2\,y_{n+1}\,y_n+y_n^2+y_{n+1}^2-4\,n+2\,y_n\,n+2\,y_{n+1}\,n}{-2+y_{n+1}+y_n}$
$t_{k+1} \leftarrow -\frac{1}{2}\,\frac{6-6\,y_{n+1}+4\,n-4\,y_n-2\,y_n\,n+y_n^2+2\,y_{n+1}\,y_n-2\,y_{n+1}\,n+y_{n+1}^2}{-2+y_{n+1}+y_n}$
else
$t_k \leftarrow -\frac{1}{2}\,\frac{-2\,y_{n+1}-2\,y_n\,n+y_n^2+2\,y_{n+1}\,y_n-2\,y_{n+1}\,n+y_{n+1}^2}{y_n+y_{n+1}}$
$t_{k+1} \leftarrow \frac{1}{2}\,\frac{2\,y_{n+1}+2\,y_n\,n+y_n^2+2\,y_{n+1}\,y_n+2\,y_{n+1}\,n+y_{n+1}^2}{y_n+y_{n+1}}$
end if
$n \leftarrow n + 2$
$k \leftarrow k + 2$
end if
end if
else if 1 *transition in the interval* $[n-1, n]$ **then**
sol = *solve for configuration* $(1,0) \in [n-1, n+1]$ *given* $t_{k-1} \in [n-1, n]$
if *sol* $\neq \emptyset$ **then**
tncode $\leftarrow 0$
$n \leftarrow n + 1$
else
sol = *solve for configuration* $(1,1) \in [n-1, n+1]$ *given* $t_{k-1} \in$

```
        [n − 1, n]
        if sol ≠ ∅ then
          tncode ← 1
          if x((n − 1)^+) = 1 then
            t_k ← n + √(2 − 2y_{n+1})
          else
            t_k ← n + √2 √(y_{n+1})
          end if
          n ← n + 1
          k ← k + 1
        end if
      end if
    else
      { 2 transitions in the interval [n − 1, n]}
      tncode ← 0
    end if
  end if
end while
```

Piecewise constant signal

We consider sampling a piecewise constant signal with the box sampling kernel. doubling the sampling rate is sufficient to recover the signal, thus we suppose $2N$ sample values y_n are available.

Algorithm 3.5 *Piecewise constant signal with box sampling kernel.*

```
Require: , k ← 0,n ← 0 y_n, n = 0 . . . 2N − 1
  while n ≤ 2N − 2 do
    if |y_{n+1} − y_n| = 0 then
      n = n + 1
    else
      c_k = y_{n−1}
      c_{k+1} = y_{n+1}
      t_k = (y_n + n c_k − (n+1) c_{k+1}) / (c_k − c_{k+1})
      n ← n + 2
      k ← k + 1
    end if
  end while
```

3.3 Summary

- A finite length stream of K Diracs can be recovered from N samples y_n obtained as the inner product between the signal and shifted versions of the sinc and Gaussian sampling kernel, when $N \geq 2K$.
- For both, sinc and Guassian, sampling kernels two systems of equations must be solved: the first system is to find the locations of the Diracs and the second is to find the weights of the Diracs.
- When sampling a randomly spaced stream of Diracs with the *sinc* kernel the system leading to the transitions may be ill-conditioned if the sampling interval T is not chosen appropriately. It is illustrated that at critical sampling, that is, when we have $N = 2K$ sample values, the optimal sampling interval obtained for these type of signals is $T = 0.5$.
- When sampling a randomly spread stream of Diracs with the *Gaussian* kernel the conditioning of both systems depends also on the value of the variance σ^2 in the Gaussian kernel.
- In the same fashion as in Chapter 2, the sampling schemes using the sinc and the Gaussian kernels can be generalized to both continuous-time and discrete-time piecewise polynomial signals.
- Infinite length signals were sampled using a compact support sampling kernel.
- Bilevel signals can be recovered using a *Box* sampling kernel $\varphi_0(t/T)$ if and only if there is at most one transition in each interval $[n, (n+1)T]$.
- Bilevel signals can be recovered using a *Hat* sampling kernel $\varphi_1(t/T)$ if and only if there is at most two transitions in each interval $[n, (n+2)T]$.
- In general, to recover the infinite length piecewise polynomials with K pieces of of maximum degree R using a box sampling kernel, the sampling rate must be greater than the maximum local rate of innovation

$$\rho_m(T) = (2(R+1)+1)/T.$$

- Sampling and reconstruction algorithms were given for each problem in their respective sections.

Chapter 4

Irregular sampling with unknown locations

Irregular sampling addresses the problem of recovering a signal $x(t)$ from a set of samples $x[n] = x(t_n)$ whose times instances $\{t_n\}$ form an irregular set. Irregular sampling of bandlimited signals has been extensively studied in the past and fast iterative reconstruction methods do exist [67, 20]. Most of the reconstruction methods require as input the following parameters: the bandlimit, the sample values, the sampling instances or locations.

In this chapter[1] we consider irregular sampling of bandlimited signals with **unknown** sampling locations. This problem arises in practice when a sampling device is not accurate. The samples obtained are not uniform but, most importantly their time instances contain jitter, that is, their locations are unknown. A similar problem is treated in the context of error correction when the locations of the errors in the received signal are unknown [24]. The irregular sampling problem with unknown bandlimit has also been investigated in [74].
A solution for the irregular sampling with unknown locations ($ISUL$) problem for discrete-time band-limited signals is defined geometrically and algebraically in Section 4.1. Four solving methods for the $ISUL$ problem are proposed in Section 4.2. In Section 4.3 numerical experiments are made on a random and on a jittered sampling set of locations.

4.1 Problem description

Consider a discrete-time periodic signal $\mathbf{x} = (x[0], x[1], \ldots, x[N-1])$ bandlimited to M, that is, the DTFS coefficients $\mathbf{X}$ are such that $X[m] = 0 \, \forall m \notin \mathcal{N}_M$ where $\mathcal{N}_M = \{0, 1, \ldots, M-1\}$, $M < N$. Note that these signals are complex. Real signals are obtained by taking a Hermitian spectrum. A real bandlimited signal with $N = 32$ and $M = 5$ is illustrated in Figure 4.1.

The irregular sampling with unknown locations ($ISUL$) problem consists in recovering a discrete-time periodic $M-$bandlimited signal $\mathbf{x}$ from a set of sample

[1] This chapter includes research conducted jointly with Martin Vetterli [54, 56].

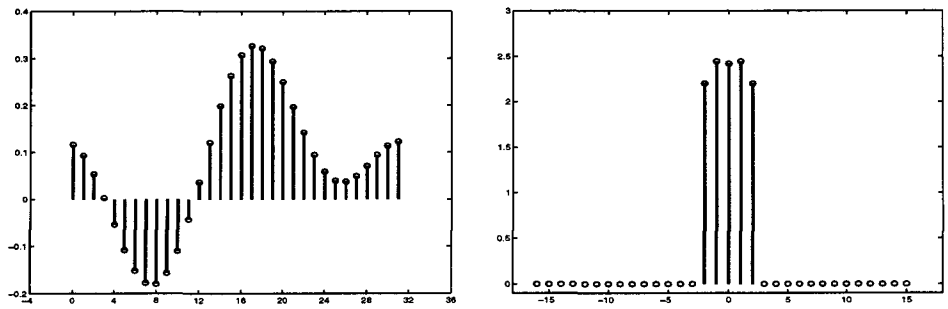

(a) (b)

Figure 4.1: (a) Discrete-time periodic signal, $N = 32$ bandlimited to $M = 5$; (b) Discrete-time Fourier series coefficients.

values

$$\mathbf{s} = \mathbf{x}(\mathcal{N}_K) = (x[n_0], x[n_1], \ldots, x[n_{K-1}]) \tag{4.1}$$

whose locations $\mathcal{N}_K = \{n_0, n_1, \ldots, n_{K-1}\}$ are **unknown**. Pictorially the problem is illustrated in Figure 4.2.

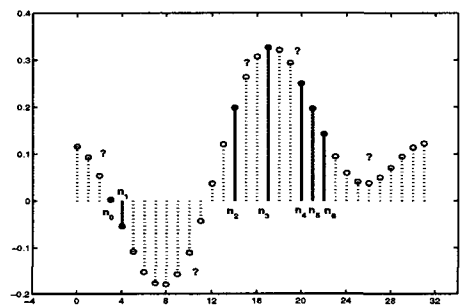

Figure 4.2: Irregularly sampled periodic discrete-time signal of length $N = 32$ with $K = 7$ unknown sampling locations.

4.1.1 Subspace approach

The first question that needs to be answered is: What subspace does the signal belong to? Note that

$$\mathbf{x} = \mathbf{F}^{-1} \cdot \mathbf{X} \tag{4.2}$$

where $\mathbf{F} = \mathbf{DFT}_N$ is the discrete-time Fourier transform matrix. The signal in question is bandlimited to M so from the synthesis formula in Definition 1.4 the signal values are

$$x[n] = \frac{1}{N} \sum_{m=0}^{M-1} X[m]\, e^{i2\pi mn/N}, \quad n \in \mathcal{N} = \{0, 1, \ldots, N-1\} \tag{4.3}$$

or in matrix/vector form,

$$\begin{pmatrix} x[0] \\ x[1] \\ \vdots \\ x[N-1] \end{pmatrix} = \frac{1}{N} \begin{bmatrix} 1 & 1 & \dots & 1 \\ 1 & W_N^{-1} & \dots & W_N^{-(M-1)} \\ \vdots & \vdots & \dots & \vdots \\ 1 & W_N^{-(N-1)} & \dots & W_N^{-(N-1)(M-1)} \end{bmatrix} \cdot \begin{pmatrix} X[0] \\ X[1] \\ \vdots \\ X[M-1] \end{pmatrix} \tag{4.4}$$

where $W_N = e^{-i2\pi/N}$. Equation (4.4) can be rewritten in shorter form as

$$\mathbf{x}(\mathcal{N}) = \frac{1}{N}\mathbf{F}^*(\mathcal{N}, \mathcal{N}_M) \cdot \mathbf{X}(\mathcal{N}_M) \tag{4.5}$$

where $\mathcal{N}_M = \{0, 1, \dots, M-1\}, M < N$. It is clear that the signal belongs to the subspace spanned by the M first column vectors of the matrix $\mathbf{F}^*$. This signal subspace is denoted by

$$\mathcal{S}(\mathcal{N}, \mathcal{N}_M) = span\{\mathbf{F}^*(\mathcal{N}, m)\}_{m \in \mathcal{N}_M}. \tag{4.6}$$

Consider an irregular set of locations $\mathcal{N}_K = \{n_k\}_{k=0}^{K-1}$ associated to the sample values $\mathbf{s}$, that is, $\mathbf{s} = \mathbf{x}(\mathcal{N}_K)$, then

$$\mathbf{s} = \frac{1}{N}\mathbf{F}^*(\mathcal{N}_K, \mathcal{N}_M) \cdot \mathbf{X}(\mathcal{N}_M) \tag{4.7}$$

and consequently the irregular set of sample values

$$\mathbf{s} \in \mathcal{S}(\mathcal{N}_K, \mathcal{N}_M). \tag{4.8}$$

The subspace $\mathcal{S}(\mathcal{N}_K, \mathcal{N}_M)$ can also be seen as a projection of $\mathcal{S}(\mathcal{N}, \mathcal{N}_M)$ onto the subspace spanned by the canonical base vectors associated to the irregular set of locations $\mathcal{N}_K$, that is, $span\{\mathbf{e}_{n_0}, \mathbf{e}_{n_1}, \dots, \mathbf{e}_{n_{K-1}}\}$. Thus follows the definition of a solution to the $ISUL$ problem:

Definition 4.1 *Consider a discrete-time periodic signal* $\mathbf{x}$ *with period* N *and bandlimited to* M. *Let* $\mathbf{s} = (x[n_0], x[n_1], \dots, x[n_{K-1}])$ *be a set of* K *sample values of* $\mathbf{x}$. *If*

$$\mathbf{s} \in \mathcal{S}(\mathcal{N}_K, \mathcal{N}_M) \tag{4.9}$$

then $\mathcal{N}_K = \{n_k\}_{k=0}^{K-1}$ *is the set of locations corresponding to the sample values* $\mathbf{s}$.

Figure 4.3 illustrates when a set of locations is and is not a solution to the $ISUL$ problem.
The respective subspaces have been identified so it is now appropriate to find the solution algebraically; this is the topic of the next section.

4.1.2 Algebraic approach

The ultimate goal is to determine the whole signal $\mathbf{x}(\mathcal{N})$ from the samples $\mathbf{s}$. Note that if the DTFS coefficients $X[m], m \in \mathcal{N}_M$ are known then the signal $\mathbf{x}$

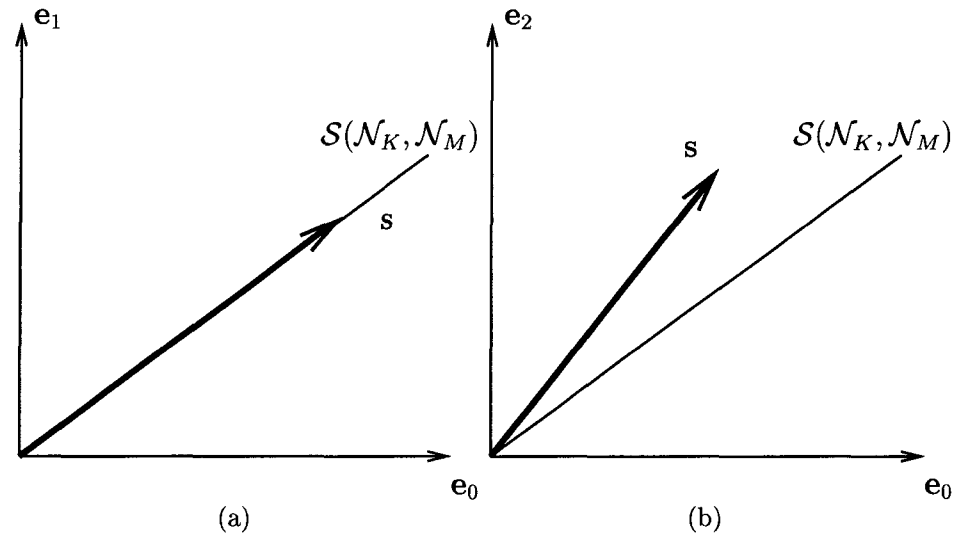

Figure 4.3: (a) $\mathcal{N}_K^{(1)} = \{0, 1\}$ is a solution;(b) $\mathcal{N}_K^{(2)} = \{0, 2\}$ is not a solution.

is determined by (4.4). The *ISUL* problem is difficult to solve because it is a nonlinear system composed of K equations of the form

$$s[k] = X[0] + X[1]\, W^{-n_k} + \ldots + X[M-1]\, W^{-n_k(M-1)}, \quad k = 0, \ldots, K-1 \tag{4.10}$$

and $M + K$ unknown variables $\{X[m]\}_{m \in \mathcal{N}_M}$ and $\{n_k\}_{k=0}^{K-1}$. Table 4.1 summarizes the known and unknown variables.

known	unknown
$\mathbf{s} = (x[n_0], x[n_1], \ldots, x[n_{K-1}])$	$\mathbf{X}(\mathcal{N}_M) = (X[0], X[1], \ldots, X[M-1])$
$\mathcal{N}_M = \{0, 1, \ldots, M-1\}$	$\mathcal{N}_K = \{n_0, n_1, \ldots, n_{K-1}\}$

Table 4.1: Known and unknown information, $M \leq K < N$.

On the other hand, if the location set $\mathcal{N}_K$ is known then the values $X[m], m \in \mathcal{N}_M$, can be determined by solving the system of K equations and M unknowns defined in (4.7). It is supposed that the number of sample values is at least equal to or greater than the bandlimit, that is, $K \geq M$, otherwise the system is underdetermined. A least squares solution to the system in (4.7) is obtained

using the generalized inverse[2] of $\mathbf{F}^*(\mathcal{N}_K,\mathcal{N}_M)$, that is,

$$\begin{aligned} \mathbf{s} &= \frac{1}{N}\mathbf{F}^*(\mathcal{N}_K,\mathcal{N}_M)\cdot\mathbf{X}(\mathcal{N}_M) \\ \Leftrightarrow \mathbf{F}(\mathcal{N}_K,\mathcal{N}_M)\cdot\mathbf{s} &= \frac{1}{N}\mathbf{F}(\mathcal{N}_K,\mathcal{N}_M)\cdot\mathbf{F}^*(\mathcal{N}_K,\mathcal{N}_M)\cdot\mathbf{X}(\mathcal{N}_M) \\ \Rightarrow \mathbf{X}(\mathcal{N}_M) &= N\left[\mathbf{F}(\mathcal{N}_K,\mathcal{N}_M)\cdot\mathbf{F}^*(\mathcal{N}_K,\mathcal{N}_M)\right]^{-1}\cdot\mathbf{F}(\mathcal{N}_K,\mathcal{N}_M)\cdot\mathbf{s}. \end{aligned} \tag{4.11}$$

Note that the expression for the DTFS of the signal $\mathbf{X}(\mathcal{N}_M)$ in (4.11) depends on the unknown location set $\mathcal{N}_K$. If the location set is the correct one then $\mathbf{x}(\mathcal{N})$ is given by

$$\mathbf{x}(\mathcal{N}) = \mathbf{F}^*(\mathcal{N},\mathcal{N}_M)\cdot\left[\mathbf{F}(\mathcal{N}_K,\mathcal{N}_M)\cdot\mathbf{F}^*(\mathcal{N}_K,\mathcal{N}_M)\right]^{-1}\cdot\mathbf{F}(\mathcal{N}_K,\mathcal{N}_M)\cdot\mathbf{s}.$$

How can one verify algebraically that a given set of locations $\tilde{\mathcal{N}}_K = \{\tilde{n}_k\}_{k=0}^{K-1}$ is a solution to the *ISUL* problem? One way is to compare the corresponding sample values, $\mathbf{x}(\tilde{\mathcal{N}}_K)$, with the observed sample values $\mathbf{s}$, that is, we verify if

$$\mathbf{x}(\tilde{\mathcal{N}}_K) = \mathbf{s} \tag{4.12}$$

or equivalently if

$$\left(\mathbf{F}^*(\mathcal{N}_K,\mathcal{N}_M)\cdot\left[\mathbf{F}(\mathcal{N}_K,\mathcal{N}_M)\cdot\mathbf{F}^*(\mathcal{N}_K,\mathcal{N}_M)\right]^{-1}\cdot\mathbf{F}(\mathcal{N}_K,\mathcal{N}_M) - \mathbf{I}\right)\cdot\mathbf{s} = 0. \tag{4.13}$$

Before presenting the numerical solving methods it is interesting to study the different types of solutions.

4.1.3 Classification of the solution

In this section the uniqueness and multiplicity conditions of the solutions to the *ISUL* problem are identified. Intuitively, if the intersection of the subspaces associated to two sets of locations, $\mathcal{N}_K^{(1)}$ and $\mathcal{N}_K^{(2)}$, is empty except for $\mathbf{s} = 0$ then there is a unique set of locations that correspond to the sample values $\mathbf{s}$. Thus,

Theorem 4.1 *If* $\mathcal{S}(\mathcal{N}_K^{(1)},\mathcal{N}_M)\cap\mathcal{S}(\mathcal{N}_K^{(2)},\mathcal{N}_M) = \emptyset$ *then* $\mathcal{N}_K^{(1)} = \mathcal{N}_K^{(2)}$.

Proof: Consider two distinct sets of locations $\mathcal{N}_K^{(1)}$ and $\mathcal{N}_K^{(2)}$. The difference between the reconstructed signals associated to these sets of locations is given by

$$\begin{aligned} &\left[\left(\mathbf{F}^*(\mathcal{N}_K^{(1)},\mathcal{N}_M)\cdot\left[\mathbf{F}(\mathcal{N}_K^{(1)},\mathcal{N}_M)\cdot\mathbf{F}^*(\mathcal{N}_K^{(1)}\mathcal{N}_M)\right]^{-1}\cdot\mathbf{F}(\mathcal{N}_K^{(1)},\mathcal{N}_M) - \mathbf{I}\right)\right. \\ &\left.-\left(\mathbf{F}^*(\mathcal{N}_K^{(2)},\mathcal{N}_M)\cdot\left[\mathbf{F}(\mathcal{N}_K^{(2)},\mathcal{N}_M)\cdot\mathbf{F}^*(\mathcal{N}_K^{(2)},\mathcal{N}_M)\right]^{-1}\cdot\mathbf{F}(\mathcal{N}_K^{(2)},\mathcal{N}_M) - \mathbf{I}\right)\right]\cdot\mathbf{s} = 0. \end{aligned} \tag{4.14}$$

[2] If $K = M$ then the generalized inverse is the inverse of the matrix. The existence of the generalized inverse or the inverse is assured due to the Vandermonde structure of $\mathbf{F}^*(\mathcal{N}_K,\mathcal{N}_M)$.

If there are no common elements in the two subspaces then the system in (4.14) is satisfied only if $\mathcal{N}_K^{(1)} = \mathcal{N}_K^{(2)}$ since $\mathbf{s} \neq 0$. ■

Similarly if the intersection of two subspaces generated by different sets of locations is not empty then there are multiple solutions to the $ISUL$ problem as illustrated in Figure 4.4.

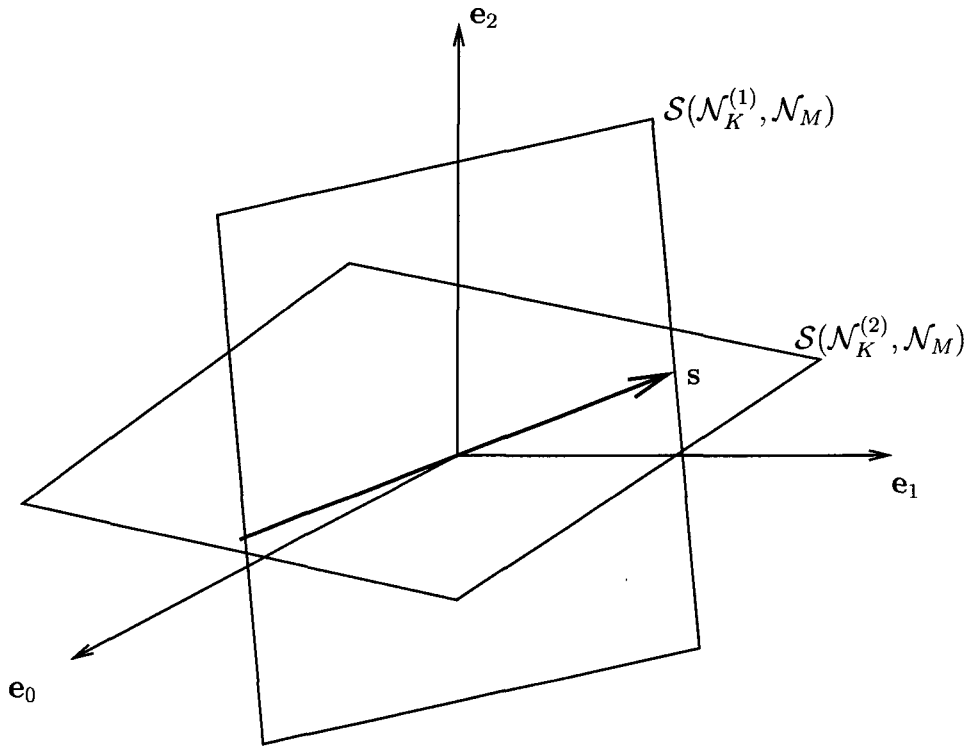

Figure 4.4: Example of multiple solutions: $\mathcal{N}_K^{(1)} = \{0,1\}$, $\mathcal{N}_K^{(2)} = \{0,2\}$. If the sample values s belong to the intersection of the two spans then there is no way to differentiate the two sets.

Corollary 4.1 *If* $\mathcal{N}_K^{(1)} \neq \mathcal{N}_K^{(2)}$ *and* $\mathbf{s} \in \mathcal{S}(\mathcal{N}_K^{(1)}, \mathcal{N}_M) \cap \mathcal{S}(\mathcal{N}_K^{(2)}, \mathcal{N}_M) \neq \emptyset$ *then* $\mathcal{N}_K^{(1)}, \mathcal{N}_K^{(2)}$ *are both solutions to the* $ISUL$ *problem.*

Proof: If the rank of the matrix on the left of s in (4.14) is greater than K then the system may admit one or more solutions and therefore $\mathcal{N}_K^{(1)}, \mathcal{N}_K^{(2)}$ are both solutions to the $ISUL$ problem. ■

Example 4.1 *Consider a discrete-time signal* $\mathbf{x} = (a, b, a, a, c, a, a, d)^T$ *and the irregular set of sample values* $\mathbf{s} = (a, b, a, c, a)^T$, *that is,* $N = 8, K = 5$. *Then the possible sets of locations are* $\mathcal{N}_K^{(1)} = \{0,1,2,4,5\}, \mathcal{N}_K^{(2)} = \{0,1,2,4,6\}, \mathcal{N}_K^{(3)} = \{0,1,3,4,5\}, \mathcal{N}_K^{(4)} = \{0,1,3,4,6\}$.

Furthermore, due to the shift property of the discrete-time Fourier transform matrix $\mathbf{DFT}_N$, if a set of locations is a solution to the $ISUL$ problem then any set of locations which is a shift of that set is also a solution.

Theorem 4.2 *If* $\mathcal{N}_K = \{n_k\}_{k=0}^{K-1}$ *is a solution to the* $ISUL$ *problem then* $\mathcal{N}_K + r = \{n_k + r\}_{k=0}^{K-1}$ *with* $r \in \{1, \ldots, N - n_K\}$ *is also a solution to the* $ISUL$ *problem.*

Proof: Suppose $\mathcal{N}_K$ is a solution to the $ISUL$ problem. Note that,

$$\begin{aligned} \mathcal{S}(\mathcal{N}_K + r, \mathcal{N}_M) &= span\{\mathbf{F}^*(\mathcal{N}_K + r, m)\}_{m \in \mathcal{N}_M} \\ &= span\{W_N^{-r}\mathbf{F}^*(\mathcal{N}_K, m)\}_{m \in \mathcal{N}_M} \\ &= span\{\mathbf{F}^*(\mathcal{N}_K, m)\}_{m \in \mathcal{N}_M} \\ &= \mathcal{S}(\mathcal{N}_K, \mathcal{N}_M). \end{aligned}$$

From Definition 4.1, $\mathcal{N}_K + r$ is also a solution to the $ISUL$ problem. ■

4.2 Numerical solving methods

The $ISUL$ problem is solved numerically in two steps: first the set of locations corresponding to the given sample values need to be found and then the signal is reconstructed. Define the mean squared error between the sample values $\mathbf{s}$ and those associated to a given set of locations $\mathcal{N}_K$ by

$$E(\mathcal{N}_K) = \left\| \left(\mathbf{F}(\mathcal{N}_K, \mathcal{N}_M) \cdot \left[\mathbf{F}(\mathcal{N}_K, \mathcal{N}_M) \cdot \mathbf{F}^*(\mathcal{N}_K, \mathcal{N}_M) \right]^{-1} \cdot \mathbf{F}(\mathcal{N}_K, \mathcal{N}_M) - \mathbf{I} \right) \cdot \mathbf{s} \right\|. \tag{4.15}$$

The first step is accomplished by verifying if $E(\mathcal{N}_K)$ is null. To evaluate $E(\mathcal{N}_K)$ is computationally expensive for large values of K and M and therefore it is important to exploit the structure of the matrices involved in the calculation. First it must be noted that $\mathbf{F}^*(\mathcal{N}_K, \mathcal{N}_M)$ is a Vandermonde matrix and the product $\mathbf{F}(\mathcal{N}_K, \mathcal{N}_M) \cdot \mathbf{F}^*(\mathcal{N}_K, \mathcal{N}_M)$, as well as its inverse $\left(\mathbf{F}(\mathcal{N}_K, \mathcal{N}_M) \cdot \mathbf{F}^*(\mathcal{N}_K, \mathcal{N}_M)\right)^{-1}$, is a Toeplitz matrix. Therefore it is sufficient to calculate the first row and first column of $\mathbf{F}(\mathcal{N}_K, \mathcal{N}_M) \cdot \mathbf{F}^*(\mathcal{N}_K, \mathcal{N}_M)$, that is, $K\,M$ operations. Consequently, by fast Toeplitz methods it can be inverted in $K\,M \log M$ operations [20].

4.2.1 Exhaustive search

An elementary way to solve the $ISUL$ problem is using an exhaustive search approach. This method consists in verifying if $E(\mathcal{N}_K) = 0$ for all $\binom{N}{K}$ sets of locations. From Theorem 4.2 since some sets of locations are just shifts of each other, these sets are put in one class. The representative of each class satisfying $E(\mathcal{N}_K) = 0$ is a solution of the $ISUL$ problem. Clearly, this method can only be used for small size problems because of the combinatorial explosion. Figure 4.5 shows the behavior of the cost function $E(\mathcal{N}_K)$ for the $ISUL$ problem with parameters $N = 16, K = 8, M = 4$.

4.2.2 Random search method

The random search method is an iterative descent algorithm. Given is an initial set of locations, $\mathcal{N}_K^{(0)}$. While the solution is not found, that is, $E(\mathcal{N}_K^{(0)}) > 0$, a component k of the location set is perturbed by λ following a probability distribution, $\mathcal{P}(\cdot)$. If the cost value of the perturbed set decreases then the

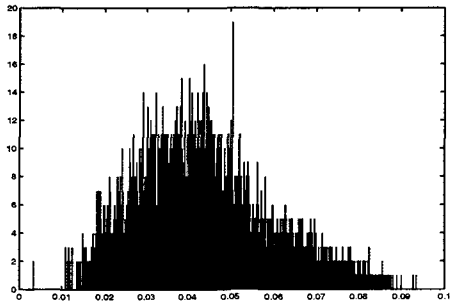

Figure 4.5: Distribution of the cost function $E(\mathcal{N}_K)$ $(N = 16, K = 8, M = 4)$ over all possible location sets, $\binom{N}{K} = 12870$.

latter becomes the new initial set and the same component is perturbed. If the cost value increases then the next component of the initial set is perturbed. The algorithm comes to halt when there is no change in the cost value from one perturbation to the other, this is a local minimum, or when the cost value is $E(\mathcal{N}_K^{(0)}) = 0$, this is a global minimum. The random search method is described in pseudo-code in Algorithm 4.1.

Algorithm 4.1 Random search method

$\mathcal{N}_K^{(0)} = \{n_0^{(0)}, n_1^{(0)}, \ldots, n_{K-1}^{(0)}\}, \epsilon = 10^{-8}, k = 0.$
while $k \leq K-1$ *and* $E(\mathcal{N}_K^{(0)}) > 0$ ***do***
  $\mathcal{N}_K^{(1)} \longleftarrow \mathcal{N}_K^{(0)}$ *and* $n_k^{(1)} = n_k^{(0)} + \lambda$, $\lambda \sim \mathcal{P}(\cdot)$.
  if $E(\mathcal{N}_K^{(1)}) < \epsilon$ ***then***
    $\mathcal{N}_K \longleftarrow \mathcal{N}_K^{(1)}$ *is a global minimum.*
  else
    if $|E(\mathcal{N}_K^{(1)}) - E(\mathcal{N}_K^{(0)})| < \epsilon$ ***then***
      $\mathcal{N}_K \longleftarrow \mathcal{N}_K^{(1)}$ *is a local minimum.*
    else
      if $E(\mathcal{N}_K^{(1)}) < E(\mathcal{N}_K^{(0)})$ ***then***
        $\mathcal{N}_K^{(0)} \longleftarrow \mathcal{N}_K^{(1)}$. *Goto perturbation step.*
      else
        $k = k + 1$. *Goto next component .*
      end if
    end if
  end if
end while

Practicalities

The initial set as well as the distribution of the perturbations is chosen adequately to the application. More on this is found in Section 4.3.

4.2.3 Cyclic coordinate method

The cyclic coordinate method [3] is similar to the gradient descent in that it descends in the best direction except that it does not require any derivative information. It differs from the Random search method in that the perturbation value λ is not a random variable but belongs to a deterministic set Λ which is chosen appropriately. Also there are at most K perturbations in this algorithm as opposed to the RS method in which for a given component there can be more than one perturbation. The cyclic coordinate method is described in pseudo-code in Algorithm 4.2.

Algorithm 4.2 Cyclic coordinate method

$\mathcal{N}_K^{(0)} = \{n_0^{(0)}, n_1^{(0)}, \ldots, n_{K-1}^{(0)}\}$.
$k = 0$.
while $k \leq K-1$ *and* $E(\mathcal{N}_K^{(0)}) > 0$ ***do***
  $\mathcal{N}_K^{(1)} \longleftarrow \mathcal{N}_K^{(0)}$ *and* $n_k^{(1)} = n_k^{(0)} + \lambda_k$ *where* $\lambda_k = arg\min_{\lambda \in \Lambda}\{E(\mathcal{N}_K^{(0)} + \lambda \mathbf{d}_k)\}$.
  if $E(\mathcal{N}_K^{(1)}) < \epsilon$ ***then***
    $\mathcal{N}_K \longleftarrow \mathcal{N}_K^{(1)}$ *is a global minimum.*
  else
    if $|E(\mathcal{N}_K^{(1)}) - E(\mathcal{N}_K^{(0)})| < \epsilon$ ***then***
      $\mathcal{N}_K \longleftarrow \mathcal{N}_K^{(1)}$ *is a local minimum.*
    else
      if $E(\mathcal{N}_K^{(1)}) < E(\mathcal{N}_K^{(0)})$ ***then***
        $\mathcal{N}_K^{(0)} \longleftarrow \mathcal{N}_K^{(1)}$.
      else
        $\mathcal{N}_K^{(0)} \longleftarrow \mathcal{N}_K^{(0)}$.
      end if
      $k = k + 1$.
    end if
  end if
end while

Both the random search method and the cyclic coordinate methods do not guarantee a global minimum. When stuck in a local minimum, a random set of locations is generated and the methods are repeated. The tested algorithm comes to a halt when a global minimum is attained or an upper bound on the number of local minima is exceeded.

4.2.4 Tabu search method

The Tabu search method is used to avoid getting stuck in local minimum. Two key elements are that: it constrains the search by classifying certain perturbations as forbidden or tabu, and it contains a memory function which keeps a list of perturbations that lead to local minima [29].

4.3 Experiments

Here the methods described in Section 4.2 are tested on two types of irregular sets: the first is a random set of locations and the second is a jittered set of

locations. A third set- periodic nonuniform set- was also tested but this will be discussed in detail in the next chapter.

4.3.1 Unknown random sampling set of locations

In this experiment a discrete-time signal with period $N = 32$ is considered with $K = 8$ random samples and band-limited to $M = 2$. In Figure 4.6(a) the convergence of the CC and RS methods are compared. The conclusion is that the CC method converges faster. This is due to the deterministic nature of the algorithm. The number of iterations required to find a global minimum varies from one simulation to another as illustrated in Figure 4.6(b). The maximum number of local minima was restricted to 30. Finally in Figure 4.7 it is shown

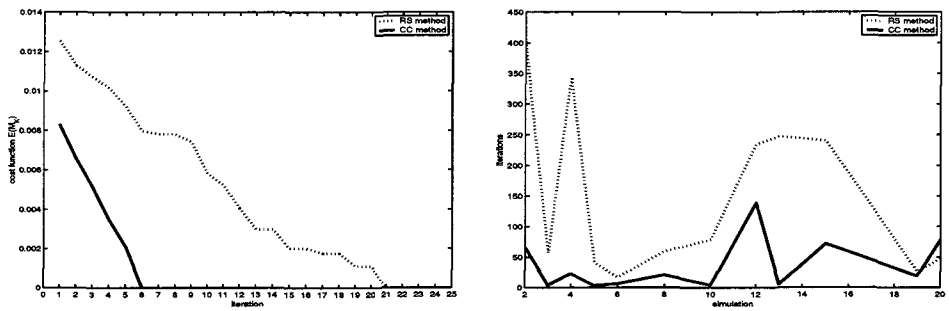

(a) (b)

Figure 4.6: (a) Convergence VS iterations of the Cyclic Coordinate and Random Search methods;(b) Total number of iterations to find the global minimum. Maximum number of local minima is 30.

that the probability of finding a global minimum depends on the smoothness of the signal, that is, the smaller the band-limit M as compared to K the more likely it is to find the right set of locations.

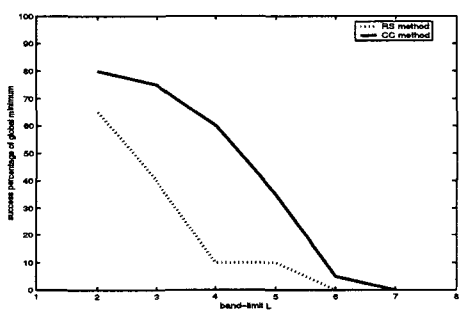

Figure 4.7: Success percentage of finding global minimum using the CC and RS methods for random sampling set VS the bandlimit M. Average of 20 simulations on 20 different signals.

4.3.2 Unknown jittered set of locations

In this experiment samples are taken around multiples of a sampling interval T, which forms an irregular set of locations $\mathcal{N}_K = \{kT + \epsilon_k\}_{k=0}^{K-1}$ where ϵ is the jitter. The assumed jitter follows a binomial distribution centered at $\epsilon = 0$ with parameters $(2, p)$ where p is the probability of no jitter and $\epsilon \in \{-1, 0, 1\}$. Figure 4.8 illustrates an example when $N = 32, K = 8, T = 4, p = 0.5$. The RS and CC methods are applied on the jittered data with p varying from 0.01 to 0.3. Figure 4.9 compares the two methods and illustrates that the percentage of finding a global minimum using the CC method is on average 83%.

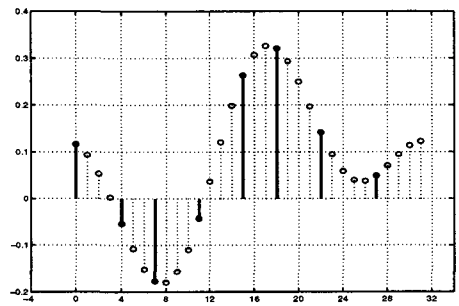

Figure 4.8: Discrete-time signal of length $N = 32$ with a jittered set of unknown locations of size $K = 8$.

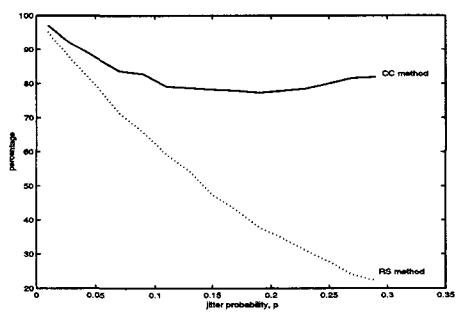

Figure 4.9: Success percentage of finding global minimum using CC and RS methods for sampling with jitter in locations where the jitter follows a binomial probability distribution with parameters $(2, p)$ centered at $\epsilon = 0$. Average of 100 simulations on 50 different signals with parameters $N = 16, K = 4, M = 2$.

4.4 Summary

- The irregular sampling problem with unknown locations was described and a solution was derived algebraically and using a subspace approach.
- There is a unique set of locations $\mathcal{N}_K$ when the irregular set of sample values is spanned by a unique set of vectors $\mathbf{F}(\mathcal{N}_K, m), m \in \mathcal{N}_M$
- There are multiple solutions $\mathcal{N}_K^{(1)}, \mathcal{N}_K^{(2)}$ when the irregular set of sample values belongs to the intersection of the two subspaces

$$\mathcal{S}(\mathcal{N}_K^{(1)}, \mathcal{N}_M) \cap \mathcal{S}(\mathcal{N}_K^{(2)}, \mathcal{N}_M) \neq \emptyset.$$

  This is the case when the locations are just shifts of each other.
- The problem was set up as a mixed, real and integer, combinatorial optimization problem.
- Four solving methods were proposed. The first is an exhaustive search method which tests all the possible sets of locations. Two other methods are the random search and cyclic coordinate. These are descent algorithms in which a solution set is obtained by perturbing a location in a deterministic or probabilistic manner. These methods are heuristic and therefore do not guarantee a global minimum. The Tabu search method is proposed to help avoiding local minima.
- Two experiments were also described. The first consisted in finding a random irregular set of locations. In the second one, the irregular set is composed of a uniform set with a given jitter.
- The cyclic coordinate method showed to be more successful than the random search method in finding the sets of locations .

Chapter 5

Periodic Nonuniform Sampling

Periodic nonuniform sampling addresses the problem of sampling a signal with a certain periodic sampling pattern. Consider for instance a few uniform sets where each set differs by a shift. The agglomerated set is nonuniform but in a periodic fashion. For example, if we take many pictures of the same scene then we obtain multiple overlapping pictures which differ by a vertical and horizontal shift. This problem is a particular case of the irregular sampling problem and so it is important to exploit the special structure of the data.
Section 5.1 of this chapter[1] gives a formal definition of the periodic nonuniform sampling problem for discrete-time bandlimited signals. Section 5.2 shows how the problem can be simplified by exploiting the periodic structure of the samples and a fast direct reconstruction scheme is derived via an example. The motivation in developing a fast reconstruction scheme is to speed up the search methods described in Chapter 4 when the shifts in the superimposed uniform sets are unknown. Finally Section 5.3 describes an application involving super-resolution.

5.1 Problem definition

We begin by specifying the problem. How is a discrete-time periodic $M-$bandlimited signal, $\mathbf{x} = (x[0], x[1], \ldots, x[N-1])$, **efficiently** reconstructed from a periodic nonuniform set of samples $\mathbf{x}(\mathcal{N}_K)$? A formal definition of the periodic nonuniform set follows.

Definition 5.1 *Periodic nonuniform set.*
A periodic nonuniform set of locations $\mathcal{N}_K$ of length K is the union of C uniform sets $\mathcal{N}_{K_i}$,

$$\mathcal{N}_K = \bigcup_{i=1}^{C} \mathcal{N}_{K_i}. \tag{5.1}$$

The variables involved in the problem are the following:

[1]This chapter includes research conducted jointly with Martin Vetterli [55, 56].

- $N \in \mathbb{N}$ is the length of the signal;
- $T \in \mathbb{N}$ is the discrete-time uniform sampling interval;
- $C \in \mathbb{N}$ is the number of uniform sets;
- $K_i = N/T \in \mathbb{N}$ is the size of one uniform set of locations, $i = 1, \ldots, C$;
- $\mathcal{N}_{K_i} = \{kT + s_i\}_{k=0,\ldots,K_i-1}$ is the ith uniform set of locations;
- $s_i \in [0, T-1]$ is the ith shift from the uniform set $\{kT\}$;
- $K = CK_i$ is the size of the periodic nonuniform set;
- $M = RK_i$ is the bandlimit of the signal, $1 \leq R \leq C$.

An example of a periodic nonuniformly sampled signal is illustrated in Figure 5.1. The length of the signal is $N = 32$ and the uniform sampling interval is $T = 8$. Therefore there are $K_i = N/T = 4$ values in each of the $C = 3$ uniform sets: $\mathcal{N}_{K_1} = \{3, 11, 19, 27\}, \mathcal{N}_{K_2} = \{4, 12, 20, 28\}, \mathcal{N}_{K_3} = \{6, 14, 22, 30\}$ where the shifts are $s_1 = 3, s_2 = 4, s_3 = 6$. Thus the periodic nonuniform set is $\mathcal{N}_K = \{3, 4, 6, 11, 12, 14, 19, 20, 22, 27, 28, 30\}$.

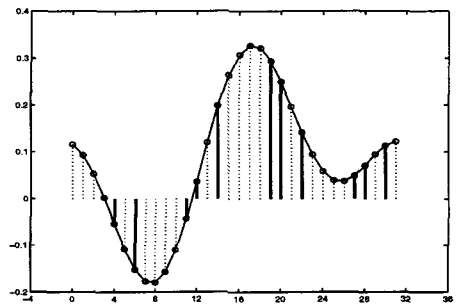

Figure 5.1: Periodic nonuniformly sampled signal.

5.1.1 Direct solving method

The periodic nonuniform sampling problem is a special case of the irregular sampling problem. In terms of the notation in Section 4.1.1 the $M-$bandlimited signal can be recovered by solving for $\mathbf{X}(\mathcal{N}_M)$ in the system of equations

$$\frac{1}{N}\mathbf{F}^*(\mathcal{N}_K, \mathcal{N}_M) \cdot \mathbf{X}(\mathcal{N}_M) = \mathbf{x}(\mathcal{N}_K) \tag{5.2}$$

where $\mathbf{F} = \mathbf{DFT}_N$, $\mathcal{N}_K$ is the periodic nonuniform set and $\mathcal{N}_M = \{0, \ldots, M-1\}$ and then substituting $\mathbf{X}(\mathcal{N}_M)$ in

$$\mathbf{x}(\mathcal{N}) = \frac{1}{N}\mathbf{F}^*(\mathcal{N}, \mathcal{N}_M) \cdot \mathbf{X}(\mathcal{N}_M). \tag{5.3}$$

The matrix $\mathbf{F}^*(\mathcal{N}_K, \mathcal{N}_M)$ is a Vandermonde matrix which assures the existence of a solution. As in Section 4.1.2 a solution, in the least squares sense, is

obtained using the generalized inverse. Some of the iterative methods mentioned in Section 1.2 can also be applied but these do not take into account the periodic structure of the samples.

5.1.2 Computational complexity

The calculation of the generalized inverse of $\mathbf{F}^*(\mathcal{N}_K, \mathcal{N}_M)$ requires matrix multiplication and inversion and is costly for large values of K and M. The number of operations are found on the left hand side of Table 5.1, more on this later.

5.2 Fast reconstruction scheme

In this section the goal is to exploit the periodic nonuniform sampling pattern so as to reduce the dimension of the problem and speed up the direct method.

5.2.1 Derivation of fast scheme via an example

Consider a discrete-time signal $\mathbf{x}$ of length $N = 8$, bandlimited to $M = 4$,

$$\mathbf{x}(\mathcal{N}) = \frac{1}{N}\mathbf{F}^*(\mathcal{N}, \mathcal{N}_M) \cdot \mathbf{X}(\mathcal{N}_M) \tag{5.4}$$

$$\begin{pmatrix} x[0] \\ x[1] \\ x[2] \\ x[3] \\ x[4] \\ x[5] \\ x[6] \\ x[7] \end{pmatrix} = \frac{1}{8} \begin{bmatrix} 1 & 1 & 1 & 1 \\ 1 & W_8^{-1} & W_8^{-2} & W_8^{-3} \\ 1 & W_8^{-2} & W_8^{-4} & W_8^{-6} \\ 1 & W_8^{-3} & W_8^{-6} & W_8^{-1} \\ 1 & W_8^{-4} & 1 & W_8^{-4} \\ 1 & W_8^{-5} & W_8^{-2} & W_8^{-7} \\ 1 & W_8^{-6} & W_8^{-4} & W_8^{-2} \\ 1 & W_8^{-7} & W_8^{-6} & W_8^{-5} \end{bmatrix} \cdot \begin{pmatrix} X[0] \\ X[1] \\ X[2] \\ X[3] \end{pmatrix} \tag{5.5}$$

where $W_8 = e^{-i2\pi/8}$. The minimal number of samples to recover the signal $\mathbf{x}$ is equal to $M = 4$. Consider a discrete-time uniform sampling interval $T = 4$ then the number of samples in the uniform set is $K_i = N/T = 2$ which is less than $M = 4$ and is insufficient to reconstruct the signal. Taking two uniform sets would do the trick. For illustration purposes take $C = 3$ uniform sets of samples, for example, at locations $\mathcal{N}_{K_1} = \{0, 4\}$, $\mathcal{N}_{K_2} = \{1, 5\}$ and $\mathcal{N}_{K_3} = \{2, 6\}$ then the periodic nonuniform set of locations is $\mathcal{N}_K = \bigcup_{i=1}^{3} \mathcal{N}_{K_i} = \{0, 1, 2, 4, 5, 6\}$. The problem is reformulated by partitioning the system in (5.5) according to the three uniform sets $N_{K_i}, (i = 1, 2, 3)$,

$$\begin{pmatrix} x[0] \\ x[4] \\ x[1] \\ x[5] \\ x[2] \\ x[6] \end{pmatrix} = \frac{1}{8} \begin{bmatrix} 1 & 1 & 1 & 1 \\ 1 & W_8^{-4} & 1 & W_8^{-4} \\ 1 & W_8^{-1} & W_8^{-2} & W_8^{-3} \\ 1 & W_8^{-5} & W_8^{-2} & W_8^{-7} \\ 1 & W_8^{-2} & W_8^{-4} & W_8^{-6} \\ 1 & W_8^{-6} & W_8^{-4} & W_8^{-2} \end{bmatrix} \cdot \begin{pmatrix} X[0] \\ X[1] \\ X[2] \\ X[3] \end{pmatrix} \tag{5.6}$$

The crux of the fast reconstruction scheme lies in the fact that the matrix in (5.6) can be broken up as the product of the following two matrices

$$\begin{bmatrix} \begin{bmatrix} 1 & 1 \\ 1 & W_8^{-4} \end{bmatrix} & \begin{matrix} 1 & 1 \\ 1 & W_8^{-4} \end{matrix} & \mathbf{O}_2 & \mathbf{O}_2 & \mathbf{O}_2 & \mathbf{O}_2 \\ \mathbf{O}_2 & \mathbf{O}_2 & \begin{matrix} 1 & 1 \\ 1 & W_8^{-4} \end{matrix} & \begin{matrix} 1 & 1 \\ 1 & W_8^{-4} \end{matrix} & \mathbf{O}_2 & \mathbf{O}_2 \\ \mathbf{O}_2 & \mathbf{O}_2 & \mathbf{O}_2 & \mathbf{O}_2 & \begin{matrix} 1 & 1 \\ 1 & W_8^{-4} \end{matrix} & \begin{matrix} 1 & 1 \\ 1 & W_8^{-4} \end{matrix} \end{bmatrix} \cdot \begin{bmatrix} \begin{bmatrix} 1 & 0 \\ 0 & 1 \end{bmatrix} & \mathbf{O}_2 \\ \mathbf{O}_2 & \begin{bmatrix} 1 & 0 \\ 0 & 1 \end{bmatrix} \\ \begin{bmatrix} 1 & 0 \\ 0 & W_8^{-1} \end{bmatrix} & \mathbf{O}_2 \\ \mathbf{O}_2 & \begin{bmatrix} W_8^{-2} & 0 \\ 0 & W_8^{-3} \end{bmatrix} \\ \begin{bmatrix} 1 & 0 \\ 0 & W_8^{-2} \end{bmatrix} & \mathbf{O}_2 \\ \mathbf{O}_2 & \begin{bmatrix} W_8^{-4} & 0 \\ 0 & W_8^{-6} \end{bmatrix} \end{bmatrix} \tag{5.7}$$

where $\mathbf{O}_2$ is a 2×2 zero matrix. Note that the matrix $\begin{bmatrix} 1 & 1 \\ 1 & W_8^{-4} \end{bmatrix}$ is equal to $\begin{bmatrix} 1 & 1 \\ 1 & W_2^{-1} \end{bmatrix} = \mathbf{DFT}_2^* = 2 \cdot \mathbf{DFT}_2^{-1}$. Therefore by multiplying (5.6) on each side by the following diagonal block matrix,

$$\frac{1}{2} \begin{bmatrix} \mathbf{DFT}_2 & \mathbf{O}_2 & \mathbf{O}_2 \\ \mathbf{O}_2 & \mathbf{DFT}_2 & \mathbf{O}_2 \\ \mathbf{O}_2 & \mathbf{O}_2 & \mathbf{DFT}_2 \end{bmatrix} \tag{5.8}$$

the following partitioned system is obtained

$$\frac{8}{2} \begin{pmatrix} \mathbf{DFT}_2 \begin{pmatrix} x[0] \\ x[4] \end{pmatrix} \\ \mathbf{DFT}_2 \begin{pmatrix} x[1] \\ x[5] \end{pmatrix} \\ \mathbf{DFT}_2 \begin{pmatrix} x[2] \\ x[6] \end{pmatrix} \end{pmatrix} = \begin{bmatrix} \begin{bmatrix} 1 & 0 \\ 0 & 1 \end{bmatrix} & \begin{bmatrix} 1 & 0 \\ 0 & 1 \end{bmatrix} \\ \begin{bmatrix} 1 & 0 \\ 0 & W_8^{-1} \end{bmatrix} & \begin{bmatrix} W_8^{-2} & 0 \\ 0 & W_8^{-3} \end{bmatrix} \\ \begin{bmatrix} 1 & 0 \\ 0 & W_8^{-2} \end{bmatrix} & \begin{bmatrix} W_8^{-4} & 0 \\ 0 & W_8^{-6} \end{bmatrix} \end{bmatrix} \cdot \begin{pmatrix} X[0] \\ X[1] \\ X[2] \\ X[3] \end{pmatrix}. \tag{5.9}$$

Each block of the partitioned matrix in (5.9) is a diagonal matrix whose values are given by the rows associated to $x[0], x[1], x[2]$ and columns $\{0,1\}$,$\{2,3\}$ of the matrix in (5.6). The fact that the blocks are diagonal matrices hints that the number of operations to calculate the generalized inverse of the partitioned system will be less than the unstructured one.

5.2.2 Generalized fast scheme

The key step in the example of Section 5.2.1 which reduces the problem is the multiplication of (5.6) by the diagonal block $\mathbf{DFT}_2$ matrix in (5.8). This is

generalized by the following

$$\frac{N}{K_1}\begin{pmatrix} \mathbf{DFT}_{K_1}\mathbf{x}(\mathcal{N}_{K_1}) \\ \mathbf{DFT}_{K_2}\mathbf{x}(\mathcal{N}_{K_2}) \\ \vdots \\ \mathbf{DFT}_{K_C}\mathbf{x}(\mathcal{N}_{K_C}) \end{pmatrix} = \begin{bmatrix} \mathbf{D}_{11} & \mathbf{D}_{12} & \dots & \mathbf{D}_{1R} \\ \mathbf{D}_{21} & \mathbf{D}_{22} & \dots & \mathbf{D}_{2R} \\ \vdots & \vdots & \dots & \vdots \\ \mathbf{D}_{C1} & \mathbf{D}_{C2} & \dots & \mathbf{D}_{CR} \end{bmatrix} \cdot \begin{pmatrix} X[0] \\ X[1] \\ \vdots \\ X[M-1] \end{pmatrix}$$

$$\mathbf{y} = \mathbf{D} \cdot \mathbf{X}(\mathcal{N}_M) \tag{5.10}$$

where $\mathbf{D}_{ij}$ are diagonal matrices defined by

$$\mathbf{D}_{ij} = diag(\{W_N^{-s_i l}\}_{l \in \{(j-1)K_i, \dots, jK_i - 1\}}), \quad i = 1, \dots, C, j = 1, \dots, R. \tag{5.11}$$

As described in Section 5.1.1 a solution in the least squares sense is obtained by means of the generalized inverse of the partitioned matrix $\mathbf{D}$ in (5.10), that is,

$$\mathbf{X}(\mathcal{N}_M) = (\mathbf{D}^*\mathbf{D})^{-1}\mathbf{D}^*\mathbf{y} \tag{5.12}$$

where $\mathbf{y} = [\mathbf{DFT}(\mathbf{x}(\mathcal{N}_{K_1}), \dots, \mathbf{DFT}(\mathbf{x}(\mathcal{N}_{K_C})]^T$ and $(\mathbf{D}^*\mathbf{D})^{-1}\mathbf{D}^*$ is also a partitioned matrix whose blocks are diagonal matrices. The fast reconstruction scheme is illustrated in Figure 5.2.

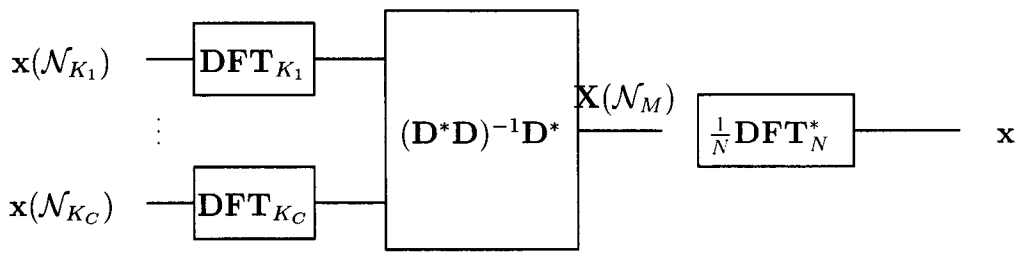

Figure 5.2: Fast reconstruction scheme for periodic nonuniform sampling

5.2.3 Computational complexity

Here, the complexity of the fast reconstruction scheme is compared with the direct unstructured one. The inverse of a partitioned matrix is obtained from (5.14) in the Appendix 5.A where $\mathbf{A} = \mathbf{D}^*\mathbf{D}$. Note that $\mathbf{A}$ is a partitioned $R \times R$ matrix where each block $\mathbf{A}_{mn}$ is a $K_i \times K_i$ diagonal matrix. Define $op_{\mathbf{A}}(R)$ as the number of operations required to invert $\mathbf{A}$. Suppose that R is a power of 2 and use a divide and conquer approach to determine $\mathbf{A}^{-1} = (\mathbf{D}^*\mathbf{D})^{-1}$ (that is, let $\alpha = \{1, \dots, R/2\}$). The result is the following recurrence equation

$$\begin{aligned} op_{\mathbf{A}}(R) &= 10 op_{\mathbf{A}}(R/2) + 12(R/2)^3 K_i + 4(R/2)^2 K_i \\ op_{\mathbf{A}}(1) &= K_i \end{aligned}$$

and we conclude that $op_{\mathbf{A}}(R) \in O(R^{log_2 10} K_i)$. Table 5.1 summarizes the number of operations required for each scheme. The two schemes are compared in Figure 5.3 where $K = CK_i$ and $M = RK_i$ in Table 5.1 and the parameters C and R are constant and K_i varies.

Complexity			
Direct scheme		Fast scheme	
$\mathbf{F^*F}$	M^2K	$\mathbf{D^*D}$	R^2CK_i
$(\mathbf{F^*F})^{-1}$	M^3	$(\mathbf{D^*D})^{-1}$	$R^{log_2 10}K_i$
$\mathbf{F^*} \cdot \mathbf{x}(\mathcal{N}_K)$	MK	$\mathbf{D^*y}$	$RCK_i logK_i$

Table 5.1: Summary of complexity $O(operations)$ for direct and fast scheme.

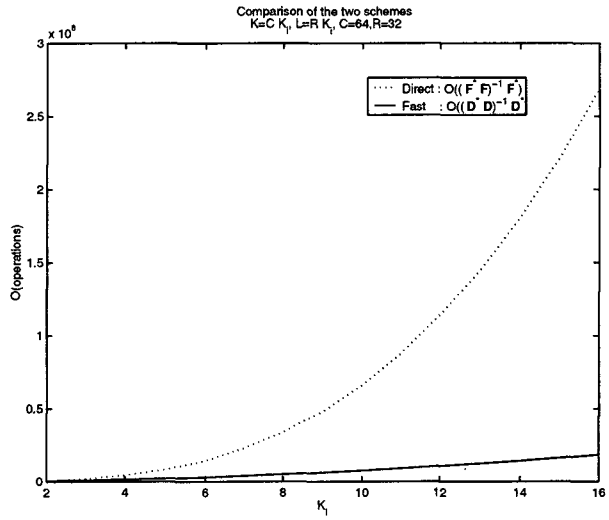

Figure 5.3: Comparison of the unstructured direct method and the fast structured scheme.

5.3 Application: super-resolution

The motivation for developing a fast reconstruction scheme is due to an application of the irregular sampling with unknown locations problem described in Chapter 4 . Suppose one wants to improve the resolution of an image. By taking multiple copies of the image where each copy differs by a shift and then placing the data on a finer grid one obtains a periodic nonuniform set of samples from which a better resolved image can be recovered. Usually these shifts are unknown and need to be determined. By applying the fast reconstruction scheme these shifts are found in a more efficient way.

5.3.1 Synthetic data

An exhaustive method is used to find the shifts. Thanks to the fast scheme the number of possible locations is reduced to $\binom{T}{C}$ which is much less than $\binom{N}{K}$. To extend the 1-D to the 2-D case we suppose that the spectrum is such that the first M columns of the 2-D **DFT** are nonzero and the last $N - M$ columns are zero. Furthermore we suppose there are no vertical shifts. Hence only the

shifts on one row of the image need to be found since it is supposed that they are the same for the other rows. Figure 5.4 shows 3 images of "Lena" of size 256×32. Each of the three images were taken from a 256×256 image and differ by a horizontal shift. The discrete uniform sampling period is $T = 8$ and so the shifts must be between 0 and 7. Using the exhaustive method instead of verifying $\binom{256}{3\times 32}$ locations, the shifts are determined by verifying $\binom{T}{C} = \binom{8}{3}$ locations. Once the shifts are found each set of data is placed on a finer grid of size 256×256 and the better resolved image is recovered. The periodic nonuniform sampled image and the reconstruction are shown in Figure 5.5.

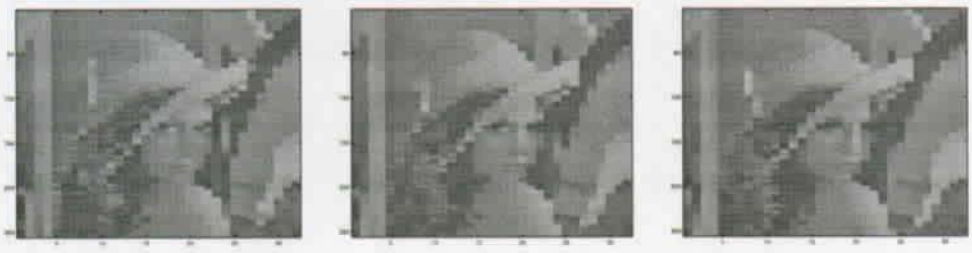

(a) (b) (c)

Figure 5.4: Three copies ($C = 3$) of Lena with low resolution. Each image is of size $N \times K_0$,with $N = 256, K_0 = 32$.

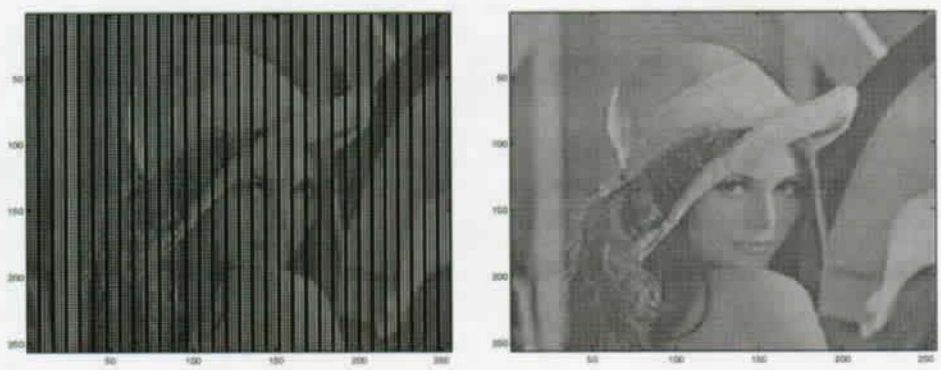

(a) (b)

Figure 5.5: (a) Periodic non-uniform sampling set obtained from three copies of Lena put on a finer grid ($N \times K_0 \cdot T, N = 256, K_0 = 32, T = 8$) according to the shifts found by the exhaustive method, $\mathcal{N}_{K_i} = \{kT + s_i\}_{k=0}^{K_0-1}, i = 1, 2, 3, s_1 = 1, s_2 = 3, s_3 = 5$; (b) Reconstruction of Lena.

5.4 Summary

- The periodic nonuniform sampling problem for discrete-time bandlimited signals has been described.
- A fast reconstruction scheme was derived via an example and its complexity was compared to the unstructured scheme.
- By exploiting the structure of the data the complexity of the problem is reduced.
- An application involving super-resolution of images has also been illustrated.

Appendix 5.A Partitioned matrices

Suppose $\mathbf{A}$ is an $R \times R$ partitioned matrix,

$$\mathbf{A} = \begin{bmatrix} \mathbf{A}_{11} & \mathbf{A}_{12} & \dots & \mathbf{A}_{1R} \\ \mathbf{A}_{21} & \mathbf{A}_{22} & \dots & \mathbf{A}_{2R} \\ \vdots & \vdots & \dots & \vdots \\ \mathbf{A}_{R1} & \mathbf{A}_{R2} & \dots & \mathbf{A}_{RR} \end{bmatrix} \tag{5.13}$$

where $\mathbf{A}_{mn}$ are square matrices. The inverse $\mathbf{B} = \mathbf{A}^{-1}$ of a partitioned matrix is given by [36]

$$\begin{aligned} \mathbf{B}(\alpha,\alpha) &= \left[\mathbf{A}(\alpha,\alpha) - \mathbf{A}(\alpha,\alpha')\mathbf{A}(\alpha',\alpha')^{-1}\mathbf{A}(\alpha',\alpha)\right]^{-1} \\ \mathbf{B}(\alpha,\alpha') &= \mathbf{A}(\alpha,\alpha)^{-1}\mathbf{A}(\alpha,\alpha') \\ &\quad \cdot \left[\mathbf{A}(\alpha',\alpha)\mathbf{A}(\alpha,\alpha)^{-1}\mathbf{A}(\alpha,\alpha')\mathbf{A}(\alpha',\alpha')\right]^{-1} \end{aligned} \tag{5.14}$$

where α is a subset of $\{1,\dots,R\}$ and α' is the complement index set of α. Note that if $R = 4$ and $\alpha = \{1,2\}$, $\alpha' = \{3,4\}$ then

$$\mathbf{A}(\alpha,\alpha) = \begin{bmatrix} \mathbf{A}_{11} & \mathbf{A}_{12} \\ \mathbf{A}_{21} & \mathbf{A}_{22} \end{bmatrix} \text{ and } \mathbf{A}(\alpha,\alpha') = \begin{bmatrix} \mathbf{A}_{13} & \mathbf{A}_{14} \\ \mathbf{A}_{23} & \mathbf{A}_{24} \end{bmatrix}.$$

Chapter 6

Irregular sampling in approximation subspaces

In a communication channel data may be lost or corrupted: the receiving end obtains only an incomplete set of data packets and recovering the lost or corrupted packets can be cast as an irregular sampling problem. Under what conditions can the packets/signal be recovered with minimum error? These conditions depend on the signal subspace.
In this chapter[1] the signals of interest are linearly and nonlinearly approximated signals using Fourier and wavelet bases. In Section 6.1 signal approximation is reviewed and an iterative algorithm for recovering these signals is described, namely the Papoulis Gerchberg (PG) algorithm. A signal that is nonlinearly approximated regardless of the expansion basis results in a smaller approximation error than a linearly approximated one. This is the motivation for developing the PG algorithm in nonlinear approximation subspaces. We study the different cases and present PG variants in Fourier and wavelet subspaces in Section 6.2. In Section 6.3 some numerical experiments are made on a 1D signal and a 2D signal in the context of erasure correction.

6.1 Preliminaries

In this section first we recall some basic notions on signal approximation, followed by the Papoulis Gerchberg algorithm.

6.1.1 Signal approximation

The goal in signal approximation is to determine the basis which will best approximate a given signal. Consider for instance a discrete-time periodic signal $\mathbf{x} \in \ell^2(\mathcal{N})$, with $\mathcal{N} = \{0, \ldots, N-1\}$, and suppose the set $\{\mathbf{g}_m\}_{m \in \mathcal{N}}$ is an orthogonal basis for $\ell^2(\mathcal{N})$, then the signal can be expressed as linear combination of the basis vectors, that is,

$$\mathbf{x} = \sum_{m \in \mathcal{N}} < \mathbf{x}, \mathbf{g}_m > \mathbf{g}_m. \tag{6.1}$$

[1] This chapter includes research conducted jointly with Martin Vetterli [53].

Furthermore the signal $\mathbf{x}$ can be approximated by a linear combination of an arbitrary set of M basis vectors with $M < N$. The basis vectors may be a fixed set in the case of linear approximation or a signal-dependent set in the case of nonlinear approximation.

Linear approximation

A linear approximation $\tilde{\mathbf{x}}_L$ of a signal $\mathbf{x}$ is a projection of $\mathbf{x}$ onto a subspace spanned by M **fixed** basis vectors. For example the M first, then

$$\tilde{\mathbf{x}}_L = \sum_{m \in \mathcal{N}_M} < \mathbf{x}, \mathbf{g}_m > \mathbf{g}_m. \tag{6.2}$$

where $\mathcal{N}_M = \{0, \ldots, M-1\}$. The linear approximation error is

$$\tilde{e}_L = \|\mathbf{x} - \tilde{\mathbf{x}}_L\|^2 = \sum_{m \in \mathcal{N} \setminus \mathcal{N}_M} | < \mathbf{x}, \mathbf{g}_m > |^2. \tag{6.3}$$

Note that the basis set is fixed to $\{\mathbf{g}_m\}_{m \in \mathcal{N}_M}$ for all signals.

Nonlinear approximation

A nonlinear approximation $\tilde{\mathbf{x}}_{NL}$ of a signal $\mathbf{x}$ is a projection of $\mathbf{x}$ onto a subspace spanned by M basis vectors which are not fixed but depend on the signal. The M basis vectors are chosen such that the approximation error is minimized. These correspond to the basis vectors to which are associated the M largest expansion coefficients $| < \mathbf{x}, \mathbf{g}_m > |$. Define the associating index set by

$$\mathcal{N}_M(\mathbf{x}) = \{m_i \in \mathcal{N}, i = 0, \ldots, M-1 : | < \mathbf{x}, \mathbf{g}_{m_0} > | \geq \cdots \geq | < \mathbf{x}, \mathbf{g}_{m_{M-1}} > |\}. \tag{6.4}$$

Clearly $\mathcal{N}_M(\mathbf{x})$ depends on the signal. The nonlinear approximation of $\mathbf{x}$ is given by

$$\tilde{\mathbf{x}}_{NL} = \sum_{m \in \mathcal{N}_M(\mathbf{x})} < \mathbf{x}, \mathbf{g}_m > \mathbf{g}_m \tag{6.5}$$

with approximation error

$$\tilde{e}_{NL} = \|\mathbf{x} - \tilde{\mathbf{x}}_{NL}\|^2 = \sum_{m \in \mathcal{N} \setminus \mathcal{N}_M(\mathbf{x})} | < \mathbf{x}, \mathbf{g}_m > |^2. \tag{6.6}$$

Since the nonlinear approximation of a signal is defined by taking the basis vectors which will minimize the approximation error, it is evident that the nonlinear approximation of a signal is always better than its linear approximation since the respective errors satisfy

$$\tilde{e}_{NL} \leq \tilde{e}_L. \tag{6.7}$$

6.1.2 Papoulis Gerchberg algorithm

The PG algorithm is a special case of the projection onto convex sets method [67] in that the convex sets are linear. It assumes that the signal belongs to two convex sets with non empty intersection and involves two projections. At the initialization step the algorithm puts the value zero on the locations where the samples are unknown. Projection 1 then projects this signal into the bandlimited subspace. Projection 2 substitutes the zeros with the sample values obtained from Projection 1 and so forth, see Figure 6.1.

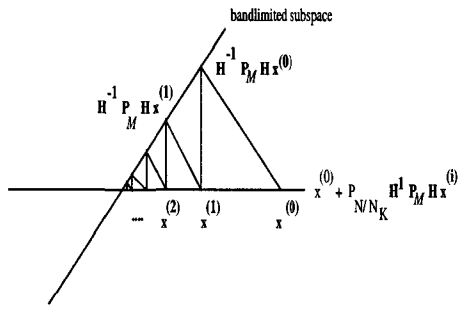

Figure 6.1: PG algorithm for M-BL signals. The first projection is onto a bandlimited subspace and the second projection is onto the space of unknown samples, $\mathbf{H} = \mathbf{DFT}$.

The algorithm is as follows:

Algorithm 6.1 *PG algorithm for M-BL discrete-time periodic signal* $\mathbf{x}$.

$$\mathbf{x}^{(0)} = \mathcal{P}_{\mathcal{N}_K}\mathbf{x}$$
$$\mathbf{x}^{(i+1)} = \mathbf{x}^{(0)} + \underbrace{\mathcal{P}_{\mathcal{N}\setminus\mathcal{N}_K}}_{Proj_2}\underbrace{\mathbf{DFT}_N^{-1}\mathcal{P}_{\mathcal{N}_M}\mathbf{DFT}_N}_{Proj_1}\mathbf{x}^{(i)}$$

where

- $\mathcal{N} = \{0, 1, \ldots, N-1\}$;
- $\mathcal{N}_K = \{n_0, n_1, \ldots, n_{K-1}\}$;
- $\mathcal{N}_M = \{0, 1, \ldots, M-1\}$;
- $\mathcal{P}_{\mathcal{N}_K}\mathbf{x} = \begin{cases} x[n] & \text{if } n \in \mathcal{N}_K \\ 0 & \text{if } n \in \mathcal{N}\setminus\mathcal{N}_K \end{cases}$ is a projection operator which puts to 0 all the values not belonging to the irregular set;
- $\mathbf{DFT}^{-1}\mathcal{P}_{\mathcal{N}_M} \cdot \mathbf{DFT} \cdot \mathbf{x}$ is the projection of $\mathbf{x}$ onto the M-BL subspace.

We can modify the Papoulis Gerchberg algorithm by projecting the irregularly sampled signal into the associating subspace. These variants are presented at the end of Section 6.2.

6.2 Reconstruction of approximated signals

One of the goals in approximation theory is to find the basis that will give the best approximation of a given signal. In this section we investigate irregular sampling of four types of approximated signals and present the Papoulis Gerchberg variants. In particular, we consider

- signals that are linearly approximated using a Fourier basis;
- signals that are nonlinearly approximated using a Fourier basis;
- signals that are linearly approximated using a wavelet basis;
- signals that are nonlinearly approximated using a wavelet basis.

The general superiority of the nonlinear approximation suggests extending the Papoulis Gerchberg algorithm described for $M-$bandlimited signals in Section 6.1.2 to nonlinearly approximated signals. We seek conditions for which reconstruction in these "approximation" subspaces is feasible. Throughout this section a toy example on a signal of length $N = 8$ is used to illustrate these conditions.

6.2.1 Fourier basis

Consider a discrete-time periodic signal $\mathbf{x}$ of length N which can be expressed as a linear combination of Fourier basis vectors, $\mathbf{g}_m[n] = \frac{1}{\sqrt{N}} e^{i2\pi mn/N}, n \in \mathcal{N}$,

$$\mathbf{x} = \sum_{m \in \mathcal{N}} < \mathbf{x}, \mathbf{g}_m > \mathbf{g}_m. \tag{6.8}$$

Note that (6.8) is equal to the inverse discrete-time Fourier series coefficients defined in (1.14) where the expansion coefficients are equal to the discrete-time Fourier series coefficients, that is, $< \mathbf{x}, \mathbf{g}_m >= \frac{1}{\sqrt{N}} X[m]$. For example, if $N = 8$, (6.8) in matrix/vector form is equivalent to

$$\begin{pmatrix} x[0] \\ x[1] \\ x[2] \\ x[3] \\ x[4] \\ x[5] \\ x[6] \\ x[7] \end{pmatrix} = \frac{1}{8} \begin{bmatrix} 1 & 1 & 1 & 1 & 1 & 1 & 1 & 1 \\ 1 & W_8^{-1} & W_8^{-2} & W_8^{-3} & W_8^{-4} & W_8^{-5} & W_8^{-6} & W_8^{-7} \\ 1 & W_8^{-2} & W_8^{-4} & W_8^{-6} & 1 & W_8^{-2} & W_8^{-4} & W_8^{-6} \\ 1 & W_8^{-3} & W_8^{-6} & W_8^{-1} & W_8^{-4} & W_8^{-7} & W_8^{-2} & W_8^{-5} \\ 1 & W_8^{-4} & 1 & W_8^{-4} & 1 & W_8^{-4} & 1 & W_8^{-4} \\ 1 & W_8^{-5} & W_8^{-2} & W_8^{-7} & W_8^{-4} & W_8^{-1} & W_8^{-6} & W_8^{-3} \\ 1 & W_8^{-6} & W_8^{-4} & W_8^{-2} & 1 & W_8^{-6} & W_8^{-4} & W_8^{-2} \\ 1 & W_8^{-7} & W_8^{-6} & W_8^{-5} & W_8^{-4} & W_8^{-3} & W_8^{-2} & W_8^{-1} \end{bmatrix} \cdot \begin{pmatrix} X[0] \\ X[1] \\ X[2] \\ X[3] \\ X[4] \\ X[5] \\ X[6] \\ X[7] \end{pmatrix}$$

$$\mathbf{x}(\mathcal{N}) = \mathbf{G}(\mathcal{N}, \mathcal{N}) \cdot \mathbf{X}(\mathcal{N}) \tag{6.9}$$

where $\mathbf{G} = \mathbf{DFT}_N^{-1}$.

Fourier-based linearly approximated signals

A Fourier-based linear approximation $\tilde{\mathbf{x}}_{LF}$ of a signal $\mathbf{x}$ is obtained by keeping the first M, with $M < N$, discrete-time Fourier series coefficients and by putting

the last $N - M$ to zero. This is equivalent to lowpass filtering the signal or bandlimiting the signal to M, that is,

$$\tilde{\mathbf{x}}_{LF}(\mathcal{N}) = \mathbf{G}(\mathcal{N}, \mathcal{N}_M) \cdot \mathbf{X}(\mathcal{N}_M) \tag{6.10}$$

where $\mathcal{N}_M = \{0, \ldots, M-1\}$.
Consider an irregular set of samples $\mathbf{x}_{LF}(\mathcal{N}_K)$ then the Fourier-based linear approximation $\tilde{\mathbf{x}}_{LF}$ can be reconstructed using a direct method such as finding a least squares solution or using an iterative method such as the Papoulis Gerchberg algorithm described in Section 6.1.2. The submatrix $\mathbf{G}(\mathcal{N}_K, \mathcal{N}_M)$ associated to the system of equations is a Vandermonde matrix. Since all of the columns of the Vandermonde matrix are linearly independent and the rank of $\mathbf{G}(\mathcal{N}_K, \mathcal{N}_M)$ is equal to M, this guarantees the convergence of the PG algorithm.

Fourier-based nonlinearly approximated signals

A Fourier-based nonlinear approximation $\tilde{\mathbf{x}}_{NLF}$ of a signal $\mathbf{x}$ is obtained by keeping the M largest discrete-time Fourier series coefficients $X[m]$ and putting the least $N - M$ to zero. This corresponds to

$$\tilde{\mathbf{x}}_{NLF}(\mathcal{N}) = \mathbf{G}\big(\mathcal{N}, \mathcal{N}_M(\mathbf{x})\big) \cdot \mathbf{X}\big(\mathcal{N}_M(\mathbf{x})\big) \tag{6.11}$$

where

$$\mathcal{N}_M(\mathbf{x}) = \{m_i \in \mathcal{N}, i = 0, \ldots, M-1 : |X[m_0]| \geq \cdots \geq |X[m_{M-1}]|\}.$$

The set $\mathcal{N}_M(\mathbf{x})$ is different for each signal and therefore the submatrix $\mathbf{G}\big(\mathcal{N}_K, \mathcal{N}_M(\mathbf{x})\big)$ is not necessarily a Vandermonde matrix. For example if $\mathcal{N}_K = \{0, 1, 4, 5\}$ and $\mathcal{N}_M(\mathbf{x}) = \{0, 2, 4\}$ then the matrix involved in the system is

$$\mathbf{G}(\mathcal{N}_K, \mathcal{N}_M(\mathbf{x})) = \frac{1}{8} \begin{bmatrix} 1 & 1 & 1 \\ 1 & W_8^{-2} & W_8^{-4} \\ 1 & 1 & 1 \\ 1 & W_8^{-2} & W_8^{-4} \end{bmatrix}. \tag{6.12}$$

It is evident that the matrix $\mathbf{G}\big(\mathcal{N}_K, \mathcal{N}_M(\mathbf{x})\big)$ is rank deficient which implies that the system is not consistent and the PG algorithm will not converge to desired signal.

6.2.2 Wavelet bases

Similarly to the Fourier basis, a signal can be linearly and nonlinearly approximated using an orthogonal wavelet basis. For signals belonging to wavelet subspaces, the transform matrix becomes the discrete wavelet transform, **DWT**. The **DWT** depends on the quadrature mirror filters (qmf) used in the decomposition and the number of decomposition levels J [50, 71, 79]. Consider for simplicity the Haar wavelet basis, the qmf's are the lowpass $\frac{1}{\sqrt{2}}[1, 1]$ and the highpass $\frac{1}{\sqrt{2}}[1, -1]$. Then a signal of length $N = 8$ in matrix/vector form is

defined by

$$\begin{pmatrix} x[0] \\ x[1] \\ x[2] \\ x[3] \\ x[4] \\ x[5] \\ x[6] \\ x[7] \end{pmatrix} = \frac{1}{2\sqrt{2}} \begin{bmatrix} 1 & -1 & -\sqrt{2} & 0 & -2 & 0 & 0 & 0 \\ 1 & -1 & -\sqrt{2} & 0 & 2 & 0 & 0 & 0 \\ 1 & -1 & \sqrt{2} & 0 & 0 & -2 & 0 & 0 \\ 1 & -1 & \sqrt{2} & 0 & 0 & 2 & 0 & 0 \\ 1 & 1 & 0 & -\sqrt{2} & 0 & 0 & -2 & 0 \\ 1 & 1 & 0 & -\sqrt{2} & 0 & 0 & 2 & 0 \\ 1 & 1 & 0 & \sqrt{2} & 0 & 0 & 0 & -2 \\ 1 & 1 & 0 & \sqrt{2} & 0 & 0 & 0 & 2 \end{bmatrix} \begin{pmatrix} s_{30} \\ w_{30} \\ w_{20} \\ w_{21} \\ w_{10} \\ w_{11} \\ w_{12} \\ w_{13} \end{pmatrix}$$

$$\mathbf{x}(\mathcal{N}) = \mathbf{G}(\mathcal{N}, \mathcal{N}) \cdot \mathbf{s}(\mathcal{N}) \tag{6.13}$$

where $\mathbf{G} = \mathbf{DWT}^{-1}$ and s_{30} is the scaling coefficient at level $J = 3$ and w_{mn} are the wavelet coefficients at level m, $m = J, \ldots, 1, n = 0, \ldots, 2^{J-m} - 1$.

Wavelet-based linearly approximated signals

In [84] the Papoulis Gerchberg algorithm is generalized to signals lying in wavelet subspaces. Scale-time limited signals are considered which corresponds to saying that the M first coefficients of the wavelet transform are nonzero. The PG reconstruction algorithm for wavelet-based linearly approximated signals is similar to Algorithm 6.1 except that the transform matrix is the **DWT**. Since the **DWT** matrix depends on the quadrature mirror filters the convergence of the PG algorithm is not as straightforward as in the linear approximation Fourier case where the submatrix was Vandermonde. This is perfectly shown by a simple example with samples whose indices are $\mathcal{N}_K = \{0, 1, 2, 3\}$ and scalelimited to $M = 3, \mathcal{N}_M = \{0, 1, 2\}$, or,

$$\begin{pmatrix} x[0] \\ x[1] \\ x[2] \\ x[3] \end{pmatrix} = \frac{1}{2\sqrt{2}} \begin{bmatrix} 1 & -1 & -\sqrt{2} \\ 1 & -1 & -\sqrt{2} \\ 1 & -1 & \sqrt{2} \\ 1 & -1 & \sqrt{2} \end{bmatrix} \begin{pmatrix} s_{30} \\ w_{30} \\ w_{20} \end{pmatrix} \tag{6.14}$$

The rank of the matrix in (6.14) is equal to two which is less than $M = 3$. Therefore the system will not admit a unique solution and the PG algorithm will not converge to the desired signal. The convergence of the algorithm depends on the rank of the associated submatrix which depends on the locations at which the samples are taken as illustrated in the example.

Wavelet-based nonlinearly approximated signals

The reconstruction of a wavelet-based nonlinearly approximated signal is done by taking the index set corresponding to the M largest scaling and wavelet coefficients, $\mathcal{N}_M(\mathbf{x}) = arg \max_{m,n}\{|s_{mn}|, |w_{mn}|\}$. Hence the submatrix associated to the problem depends not only on the locations of the irregular set of samples but also on the set $\mathcal{N}_M(\mathbf{x})$ which varies from one signal to another.

The variants of the PG algorithm are summarized in Table 6.1.

PG variants	Linear approximation	Nonlinear approximation
Fourier-based	$\mathcal{N}_M = \{0, 1, \ldots, M-1\}$ $Proj_1 \longleftarrow \mathbf{DFT}^{-1}\mathcal{P}_{\mathcal{N}_M}\mathbf{DFT}\,\mathbf{x}^{(i)}$	$\mathcal{N}_M(\mathbf{x}) = \max$(Fourier coefficients) $Proj_1 \longleftarrow \mathbf{DFT}^{-1}\mathcal{P}_{\mathcal{N}_M(\mathbf{x})}\mathbf{DFT}\,\mathbf{x}^{(i)}$
Wavelet-based	$\mathcal{N}_M = \{0, 1, \ldots, M-1\}$ $Proj_1 \longleftarrow \mathbf{DWT}^{-1}\mathcal{P}_{\mathcal{N}_M}\mathbf{DWT}\,\mathbf{x}^{(i)}$	$\mathcal{N}_M(\mathbf{x}) = \max$(wavelet coefficients) $Proj_1 \longleftarrow \mathbf{DWT}^{-1}\mathcal{P}_{\mathcal{N}_M(\mathbf{x})}\mathbf{DWT}\,\mathbf{x}^{(i)}$

Table 6.1: Variants of the Papoulis Gerchberg algorithm

6.3 Numerical experiments

Consider the problem of sending a signal or an image through a binary erasure channel (BEC) with a probability of erasure equal to p. Figure 6.2 illustrates the result of sending a 1D signal (upper left) and a 2D signal (lower left) through a binary erasure channel (in the middle). The 1D signal received has two missing segments (upper right) and the 2D signal has missing packets of size 2×2 (lower right). In the following sections numerical experiments are effectuated on these two signals and he sets $\mathcal{N}_M$ and $\mathcal{N}_M(\mathbf{x})$ are supposedly known.

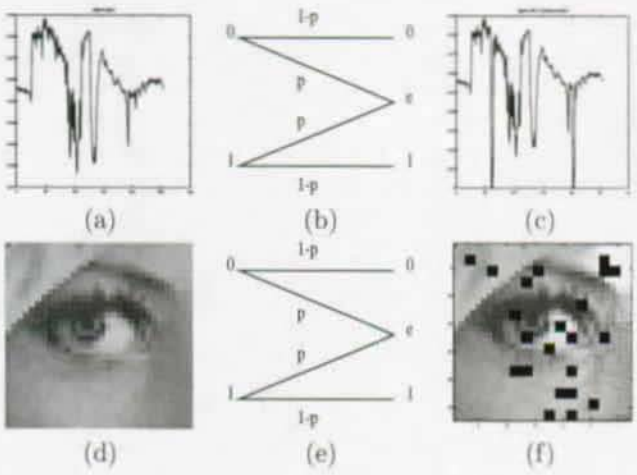

Figure 6.2: (a) A 1D signal of length $N = 256$ (column 128 of Lena image); (b) Binary erasure channel (BEC) with probability of erasure p; (c) Received signal with 2 lost segments of size 4; (d) An image of size $N \times N$ with $N = 32$ (portion of Lena's eye) (e) BEC (f) Received image with 10% packet loss.

6.3.1 Erasure correction in 1D

Suppose the Fourier and wavelet-based linearly and nonlinearly approximated 1D signal illustrated in Figure 6.2(a) is sent through a binary channel. We then apply the PG variants on the received signal which contains missing segments. The difference between the reconstruction and the approximation is illustrated in Figure 6.3

Figure 6.4 shows the convergence of the diverse reconstructions in the numerical experiment shown in Figure 6.3. The speed of reconstruction between linear and non-linear approximations in both Fourier and wavelet subspaces are compared and it is noticed that after the 15th iteration the reconstruction error of the Fourier-based nonlinearly approximated signal is not less than the linearly approximated signal which contradicts (6.7). This hints that the associated system of equations is rank deficient and the PG algorithm will not converge to the desired signal. The wavelet case agrees with the theory. Hence if the system is not rank deficient then recovering the signal using the information in the nonlinear approximation gives a better reconstruction than in the linear one.

6.3.2 Erasure correction in 2D

We do the same experiment on an image, that is, we apply the respective PG variants on the four approximations illustrated in the left column of Figure 6.5. The respective reconstructions are illustrated in the middle column and the difference between the approximation and the reconstruction obtained with the PG variant in the right column. Which approximation gives the best reconstruction? The convergence of the PG variants is compared in Figure 6.6. It shows that PG reconstruction error for the nonlinearly approximated image in each Fourier and wavelet subspace is less than the linear approximation which agrees with (6.7). It also shows that in this particular case the Fourier basis is better than the wavelet basis. The advantage of recovering signals in Fourier subspaces is that the information about the signal is spread throughout the whole of the Fourier spectrum. Wavelets are well-known for their localization property which in this case is a drawback if the signal has contiguous missing samples or lost packets.

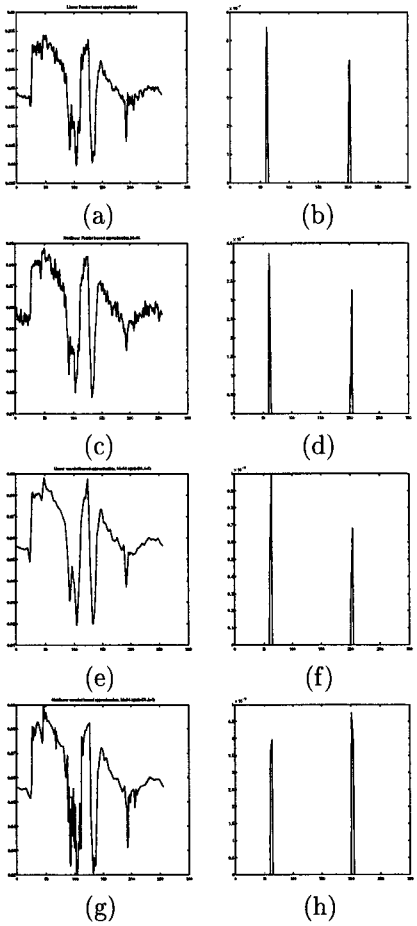

Figure 6.3: (a) Fourier-based linear approximation; (b) Difference between approximation and reconstruction MSE=10^{-7}; (c) Fourier-based nonlinear approximation; (d) Difference between approximation and reconstruction MSE=10^{-4} ; (e) Wavelet-based linear approximation of signal; (f) Difference between approximation and reconstruction MSE=10^{-10}; (g) Wavelet-based nonlinear approximation of signal; (h) Difference between approximation and reconstruction MSE=10^{-12}. In all of the approximations $M = 64$. The quadrature mirror filter used in the wavelet-based approximation is the Daubechies length 6 filter and J=3 levels of decomposition.

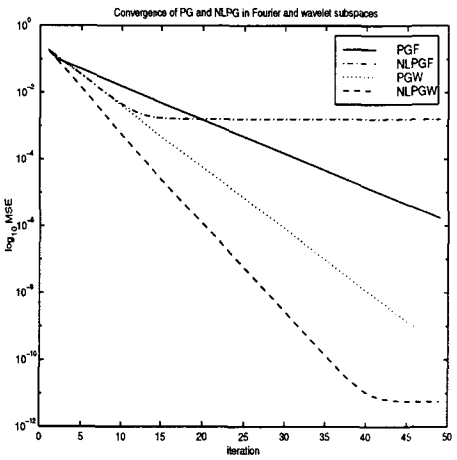

Figure 6.4: Convergence of Papoulis Gerchberg (PG) variants for Fourier (F) and wavelet (W) based linear (L) and nonlinear (NL) approximation on the previous 1D signal of length $N = 256$ with two missing segments of length 4.

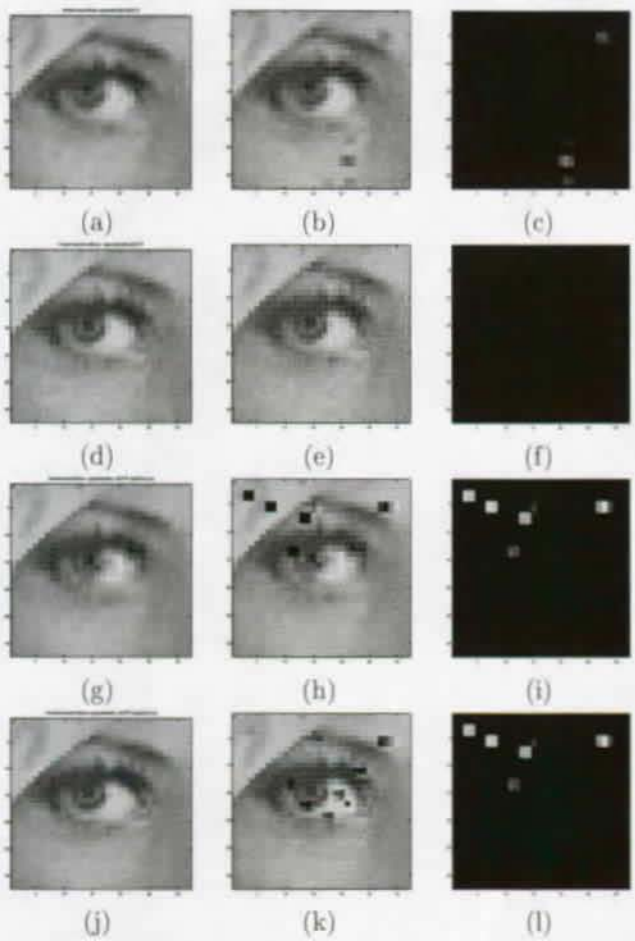

Figure 6.5: Erasure correction for 2D signals. (a) Fourier-based linear (FL) approximation; (b) Reconstruction using the FL PG variant; (c) Difference between the FL approximation and the FL PG reconstruction; (d) Fourier-based nonlinear (FNL) approximation; (e) Reconstruction using the FNL PG variant; (f) Difference between the FNL approximation and the FNL PG reconstruction; (g) Wavelet-based linear (WL) approximation; (h) Reconstruction using the WL PG variant; (i) Difference between the WL approximation and the WL PG reconstruction; (j) Wavelet-based nonlinear (WNL) approximation; (k) Reconstruction using the WNL PG variant. (l) Difference between the WNL approximation and the WNL PG reconstruction; Approximated images with lost packets of size 2×2, $M = 24 \times 24$, qmf=Daubechies length 4, J=4 levels of decomposition.

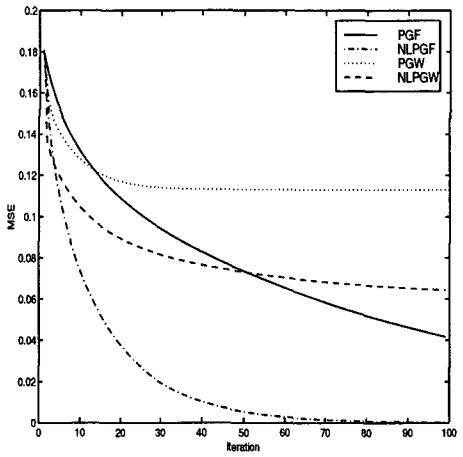

Figure 6.6: Convergence of Papoulis Gerchberg (PG) variants for Fourier (F) and wavelet (W) based linear (L) and nonlinear (NL) approximation on a portion of Lena's eye.

6.4 Summary

- Extension of PG algorithm to linearly and nonlinearly approximated signals in Fourier and wavelet subspaces.
- The existence of a solution depends on the rank of the submatrix with rows $\mathcal{N}_K$ and columns $\mathcal{N}_M(\mathbf{x})$ of the **DFT** or **DWT**. When the submatrix is rank deficient then the PG variants do not converge to the approximated signal.
- Upon convergence of the PG variant the reconstruction error of the nonlinearly approximated signal is less than the linear one.
- In the wavelet subspace the length and type of filter used in the decomposition plays an important role due to the localization property of wavelets.

Bibliography

[1] J. H. Ahlberg, E. N. Nilson, and J. L. Walsh. *The Theory of Splines and their Applications.* Academic Press, New York, 1967.

[2] A.V. Balakrishnan. On the problem of time jitter in sampling. *IRE. Trans. Info. Theory*, IT-8:226–236, April 1962.

[3] M. S. Bazaraa, H. D. Sherali, and C. M. Shetty. *Nonlinear Programming Theory and Algorithms.* John Wiley and Sons, New York, 1993.

[4] J. J. Benedetto. Irregular sampling and frames. In C. K. Chui, editor, *Wavelets: A Tutorial in Theory and Applications.* Academic Press, New York, 1992.

[5] J. J. Benedetto and P. J. S. G. Ferreira, editors. *Modern Sampling Theory: Mathematics and Applications.* Birkhäuser, Boston, 2000.

[6] J. J. Benedetto and M. W. Frazier, editors. *Wavelets: Mathematics and Applications.* CRC Press, Boca Raton, 1994.

[7] F. J. Beutler. Recovery of randomly sampled signals by simple interpolators. *Info. Contr.*, 26:312–340, 1974.

[8] R .E. Blahut. *Theory and Practice of Error Control Codes.* Addison-Wesley, Reading, MA, 1983.

[9] R. N. Bracewell. *The Fourier Transform and its Applications.* McGraw-Hill, New York, NY, Second edition, 1986.

[10] W. L. Briggs and Van Emden Hensen. *The DFT An Owner's Manual for the Discrete Fourier Transform.* SIAM, Philadelphia, 1995.

[11] W. M. Brown. Sampling with random jitter. *J. Soc. Indust. Appl. Math.*, 11 no.2:460–473, 1963.

[12] P. L. Butzer and R. L. Stens. Sampling theory for not-necessarily band-limited functions; a historical overview. *SIAM Rev.*, 34:40–53, 1992.

[13] D. C. Champeney. *A Handbook of Fourier Theorems.* Cambridge University Press, Cambridge, UK, 1987.

[14] W. Chen, S. Itoh, and J. Shiki. Irregular sampling theorems for wavelet subspaces. *IEEE Trans. Inform. Th.*, 44 3:1131–1142, May 1998.

[15] C. K. Chui. *An Introduction to Wavelets.* Academic Press, New York, 1992.

[16] I. Daubechies. *Ten Lectures on Wavelets.* SIAM, Philadelphia, PA, 1992.

[17] P. J. Davis. *Interpolation and Approximation.* Blaisdell, New York, 1965.

[18] R. J. Duffin and A. C. Schaeffer. A class of nonharmonic Fourier series. *Trans. Amer. Math. Soc.*, 72:341–366, 1952.

[19] H. G. Feichtinger and K. Gröchenig. Theory and practice of irregular sampling. In J. J. Benedetto and M. W. Frazier, editors, *Wavelets: Mathematics and Applications*, pages 305–363. CRC Press, Boca Raton, Florida, 1994.

[20] H. G. Feichtinger, K. Gröchenig, and T. Strohmer. Efficient numerical methods in non-uniform sampling theory. *Numerische Mathematik*, 69:423–440, 1995.

[21] H. G. Feichtinger and T. Strohmer. Recovery of missing segments and lines in images. In P.S. Idell, editor, *Digital Image Recovery and Synthesis*, volume 33:10 of *Optical Engineering*, pages 3283–3289. SPIE, 1994.

[22] P. Feng and Y. Bresler. Spectrum-blind minimum-rate sampling and reconstruction of multi-band signals. *IEEE Int. Conf. Acoust., Speech, and Signal Proc.*, 3:1689–1692, May 1996.

[23] P. J. S. G. Ferreira. Stability issues in error control coding in the complex field, interpolation, and frame bounds. *IEEE Signal Processing Letters*, 7(3):57–59, 2000.

[24] P. J. S. G. Ferreira and J. M. N. Vieira. Detection and correction of missing samples. In *Proceedings of the 1997 Workshop on Sampling Theory and Applications, SampTA'97*, pages 169–174, Aveiro, Portugal, 1997.

[25] P. J. S. G. Ferreira and J. M. N. Vieira. Locating and correcting errors in images. In *Proc. IEEE Int. Conf. on Image Proc.*, volume I, pages 691–694, Santa Barbara, CA, U.S.A., October 1997.

[26] P. J. S. G. Ferreira and J. M. N. Vieira. Designing fast interpolation and extrapolation algorithms. In *IEEE Int. Conf. Acoust., Speech, and Signal Proc.*, Istanbul, Turkey, June 2000.

[27] B. Foster and C. Herley. Exact reconstruction from periodic nonuniform samples. In *IEEE Int. Conf. Acoust., Speech, and Signal Proc.*, pages 1452–1455, Detroit, USA, May 1995.

[28] M. Gastpar and Y. Bresler. On the necessary density for spectrum-blind nonuniform sampling subject to quantization. *IEEE Int. Conf. Acoust., Speech, and Signal Proc.*, June 2000.

[29] Fred Glover. Tabu search-part I. *ORSA Journal on Computing*, 1, No. 3:190–206, Summer 1989.

[30] G. H. Golub and C. F. Van Loan. *Matrix Computations.* John Hopkins University Press, London, 1996.

[31] K. Gröchenig. A discrete theory of irregular sampling. *Linear Algebra and its applications*, 193:129–150, 1993.

[32] S. Haykin. *Communication Systems.* John Wiley and Sons, McMaster University, Canada, 1994.

[33] C. Herley and P. W. Wong. Minimum rate sampling of signals with arbitrary frequency support. *Proc. IEEE Int. Conf. on Image Proc.*, September 1996.

[34] J. R. Higgins. *Sampling Theory in Fourier and Signal Analysis: Foundations.* Oxford University Press, New York, 1996.

[35] J. R. Higgins and R. L. Stens, editors. *Sampling Theory in Fourier and Signal Analysis: Advanced Topics.* Oxford University Press, New York, 1999.

[36] R. A. Horn and C. R. Johnson. *Matrix Analysis.* Cambridge University Press, New York, 1985.

[37] Robert J. Marks II. *Introduction to Shannon Sampling Theory.* Springer-Verlag, New York, USA, 1991.

[38] Robert J. Marks II, editor. *Advanced Topics in Shannon Sampling and Interpolation Theory.* Springer-Verlag, Seattle, USA, 1992.

[39] A. K. Jain. *Fundamentals of Digital Image Processing.* Prentice-Hall, Englewood Cliffs, NJ, 1989.

[40] A. J. Jerri. The Shannon sampling theorem-its various extensions and applications: A tutorial review. *Proceedings of the IEEE*, 65:1565–1597, 1977.

[41] M. I. Kadec. The exact value of the Paley-Wiener constant. *Soviet Math. Dokl.*, 5:559–561, 1964.

[42] D. Klamer and E. Masry. Polynomial interpolation of randomly sampled BL functions and processes. *SIAM Journ. Appl. Math.*, 42:1004–1019, 1982.

[43] V. A. Kotel'nikov. On the transmission capacity of "ether" and wire in electrocommunications. In *Izd. Red. Upr. Svyazzi*, RKKA (Moscou), 1933.

[44] V. A. Kotel'nikov. Reprint: On the transmission capacity of "ether" and wire in electrocommunications. In J.J. Benedetto and P.J.S.G. Ferreira, editors, *Modern Sampling Theory: Mathematics and Applications.* Birkhauser, Boston, MA, 2000.

[45] H.J. Landau. Necessary density conditions for sampling and interpolation of certain entire functions. *Acta Math.*, 117:37–52, 1967.

[46] O. Leneman. Random sampling of random processes: Optimum linear interpolation. *J. Franklin Inst.*, 281:302–314, 1966.

[47] O. Leneman and J. Lewis. Random sampling of random processes: Mean-square comparison of various interpolators. *IEEE Trans. Automat. Contr.*, AC-10:396–403, July 1965.

[48] N. Levinson. Gap and density theorems. *Amer. Math. Soc.*, Colloquium Publication 26, 1940.

[49] B. Liu and T. Stanley. Error bounds for jittered sampling. *IEEE Trans. Automat. Contr.*, AC-10:449–454, 1965.

[50] S. Mallat. *A Wavelet Tour of Signal Processing.* Academic Press, San Diego, Ca, 1998.

[51] J. E. Marsden. *Elementary Classical Analysis.* W. H. Freeman and Company Springer-Verlag, New York, USA, 1974.

[52] F. A. Marvasti. *A Unified Approach to Zero-Crossings and Nonuniform Sampling of Single and Multidimensional Signals and Systems.* Nonuniform, P. O. Box 1505, Oak Park, Illinois 60304, 1987.

[53] P. Marziliano and M. Vetterli. Irregular sampling in approximation subspaces. In *Sampling Theory and Applications Workshop Proc.*, pages 58–63, Loen, Norway, August 1999.

[54] P. Marziliano and M. Vetterli. Irregular sampling with unknown locations. In *IEEE Int. Conf. Acoust., Speech, and Signal Proc.*, volume 3, pages 1657–1660, Phoenix,USA, March 1999.

[55] P. Marziliano and M. Vetterli. Fast reconstruction in periodic nonuniform sampling of discrete-time bandlimited signals. In *IEEE Int. Conf. Acoust., Speech, and Signal Proc.*, pages 317–320, Istanbul, Turkey, June 2000.

[56] P. Marziliano and M. Vetterli. Reconstruction of irregularly sampled discrete-time bandlimited signals with unknown sampling locations. *IEEE Trans. Signal Processing*, 12:3462–3471, Dec. 2000.

[57] A. Mertins. *Signal Analysis.* Wiley, England, 1999.

[58] A. Netravali and B. Haskell. *Digital Pictures.* Plenum Press, New York, 1988.

[59] A. V. Oppenheim and R. W. Schafer. *Discrete-Time Signal Processing.* Prentice-Hall, Englewood Cliffs, NJ, 1989.

[60] R. E. A. C. Paley and N. Weiner. Fourier transforms in the complex domain. *Providence: Amer. Math. Soc.*, Coll. Publ. 19, 1934.

[61] A. Papoulis. *Signal Analysis.* McGraw-Hill, New York, NY, 1977.

[62] A. Papoulis. *Probability, Random Variables and Stochastic Processes, Second Edition.* McGraw-Hill, New York, NY, 1984.

[63] M. B. Ruskai, G. Beylkin, R. Coifman, I. Daubechies, S. Mallat, Y. Meyer, and L. Raphael, editors. *Wavelets and their Applications.* Jones and Bartlett, Boston, 1992.

[64] W. Schmidt. On reconstruction of images from structured sampling sets: classification, morphology, TILS, POCS, and applications. Master's thesis, University of Vienna, 1997.

[65] S. C. Scoular and W. J. Fitzgerald. Periodic nonuniform sampling of multiband signals. *Signal Processing*, 28:195–200, 1992.

[66] C. E. Shannon. Communications in the presence of noise. *Proc. of the IRE*, 37:10–21, January 1949.

[67] H. Stark, editor. *Image Recovery: Theory and Application.* Academic Press, San Diego, 1987.

[68] J. F. Steffensen. *Interpolation.* Chelsea, New York, 1950.

[69] P. Stoica and R. Moses. *Introduction to Spectral Analysis.* Prentice Hall, 2000.

[70] G. Strang. *Linear Algebra and Its Applications, Third Edition.* Harcourt Brace Jovanovich, San Diego, CA, 1988.

[71] G. Strang and T. Nguyen. *Wavelets and Filter Banks.* Wellesley Cambridge Press, Boston, 1996.

[72] T. Strohmer. *Efficient Methods for Digital Signal and Image Reconstruction from Nonuniform Samples.* PhD thesis, University of Vienna, 1994.

[73] T. Strohmer. Computationally attractive reconstruction of band-limited images from irregular samples. *IEEE Trans. Image Processing*, 6:540–548, 1997.

[74] T. Strohmer. On the estimation of the bandwidth of nonuniformly sampled signals. In *IEEE Int. Conf. Acoust., Speech, and Signal Proc.*, volume 4, pages 2047–2050, Phoenix, USA, March 1999.

[75] M. Unser. Splines: A perfect fit for signal and image processing. *IEEE Signal Processing Magazine*, 16 no. 6:22–38, November 1999.

[76] M. Unser. Sampling–50 years after Shannon. *Proceedings of the IEEE*, 88 4:569–587, April 2000.

[77] P. P. Vaidyanathan. *Multirate Systems and Filter Banks.* Prentice-Hall, Englewood Cliffs, NJ, 1993.

[78] M. Vetterli. Sampling of piecewise polynomial signals. In *LCAV technical report*, EPFL, Switzerland, Dec. 1999.

[79] M. Vetterli and J. Kovačević. *Wavelets and Subband Coding.* Prentice-Hall, Englewood Cliffs, NJ, 1995.

[80] M. Vetterli, P. Marziliano, and T. Blu. Sampling signals with finite rate of innovation. Submitted to IEEE Trans. Signal Processing May 2001. Also technical report DSC-017, EPFL, Switzerland, April 2001.

[81] M. Vetterli, P. Marziliano, and T. Blu. Sampling piecewise bandlimited signals. In *Sampling Theory and Applications Workshop Proc.*, pages 97–102, Orlando, USA, May 2001.

[82] M. Vetterli, P. Marziliano, and T. Blu. A sampling theorem for periodic piecewise polynomial signals. In *IEEE Int. Conf. Acoust., Speech, and Signal Proc.*, Salt Lake City, USA, May 2001.

[83] J.M. Whittaker. The Fourier theory of the cardinal functions. *Proc. Math. Soc. Edinburgh*, 1:169–176, 1929.

[84] X. Xia, C.-C. J. Kuo, and Z. Zhang. Signal extrapolation in wavelet subspaces. *SIAM Journ. Sci. Comput.*, 16 1:50–73, January 1995.

[85] X. Xia and Z. Zhang. On sampling theorem, wavelets, and wavelet transforms. *IEEE Transactions on Signal Processing, Special Issue on Wavelets and Signal Processing*, 41(12):3524–3535, December 1993.

[86] D. C. Youla. Mathematical theory of image restoration by the method of convex projections. In H. Stark, editor, *Image Recovery: theory and Application*, pages 29–77. Academic Press, Florida, 1987.

[87] Robert M. Young. *An Introduction to Nonharmonic Fourier Series.* Academic Press, 1980.

Pina Marziliano

Born in Montreal, May 12 1971
Canadian and Italian citizenship

Ave. Tivoli 4,
1007 Lausanne, Switzerland
http://lcavwww.epfl.ch/~marzilia

Education

Sept. '97 – April 2001	Ph. D. student in the Audio Visual Communications Laboratory (LCAV), Communication Systems Department (DSC), EPFL. Research Topic : *Sampling theory and applications in communications and signal processing.* Applications : recovering signals with jitter, super resolution, erasure and error correction, compression and reconstruction of woodcut pictures.
Oct. '96 – July '97	Certificate, Doctoral School in Communication Systems, DSC, EPFL. Research Topic: *Long-range dependence in Internet network traffic.*
Sept. '94 – Nov. '96	M. Sc. Computer Science, Université de Montréal, Canada. Research Topic: Multi-objective assignment problem. Applications : scheduling, timetables .
Jan. '91 – May '94 **Oct. '93 – March '94**	B. Sc. Applied Mathematics, Université de Montréal, Canada. GPA : 4.1/4.3 Exchange student, Mathematics Department, EPFL.

Languages

English, French, Italian	Fluent, written and oral.
German, Arabic	Beginner

Computer Skills

Languages	LaTeX, Matlab, Maple, Splus, Mathematica, Pascal, C.
Operating Systems	UNIX, Linux, Windows.

Experience

Sept. '97 – April 2001	**Audio Visual Communications Laboratory, EPFL, Switzerland** Research assistant • Supervising students, semester projects. • Initiated and organized a monthly seminar on wavelet theory and applications in Nov. '98 - July '99. Teaching assistant • "Signal Processing for Communications", undergraduate level. • "Information and Communication Theory", graduate level.
Sept. '95 – May '96	**Operations Research Laboratory, Université de Montréal, Canada** Teaching assistant • "Introduction to Operations Research" , undergraduate level.

Scholarships

Oct. '96 – July '97	Communication Systems Department, EPFL for Doctoral school in communication systems .
Sept. '94- Sept. '96	Natural Sciences and Engineering Research Council of Canada (NSERC) for the M. Sc. Degree.
May- Aug. '92 and '93	NSERC summer internship research scholarships in the Mathematics and Statistics Department, Université de Montréal, Canada.

Personal interests

Sports	Skiing, hiking, tennis, dancing.
Favorite activities	Cooking, piano, traveling, organizing social events (e.g. school visits, seminars).

Publications

Journal papers	• M. Vetterli, P. Marziliano, T. Blu, ***Sampling Signals with Finite Rate of Innovation***, submitted to IEEE Trans. Signal Processing. • P. Marziliano, M. Vetterli, ***Reconstruction of Irregularly Sampled Discrete-Time Bandlimited Signals with Unknown Sampling Locations***, IEEE Transactions on Signal Processing, vol. 48, pp. 3462 - 3471, Dec. 2000.
Conference papers	• M. Vetterli, P. Marziliano, T. Blu, ***A Sampling Theorem for Periodic Piecewise Polynomial Signals***, International Conference on Acoustics, Speech and Signal Processing (ICASSP), Salt Lake City, USA, May 2001. • M. Vetterli, P. Marziliano, T. Blu, ***Sampling Discrete-time Piecewise Bandlimited Signals***, Sampling Theory and Applications (SampTA) Workshop, Orlando, Florida, USA, May 2001. • P. Marziliano, M. Vetterli, ***Fast Reconstruction in Periodic Nonuniform Sampling of Discrete-time Band-limited Signals*** , IEEE Proc. ICASSP, Istanbul, Turkey, June 2000. • P. Marziliano, M. Vetterli, ***Irregular Sampling in Approximation Subspaces*** , Proc. SampTA, Loen, Norway, August 11-14, 1999. • P. Marziliano, M. Vetterli, ***Irregular Sampling with Unknown Locations*** , IEEE Proc. ICASSP, Phoenix, USA, March 1999.
Miscellaneous	• P. Marziliano, ***First Steps in Forecasting Long Range Dependent Traffic on the Internet***, Internal Report, Communication Systems Doctoral School, EPFL, Switzerland, July 1997. • P. Marziliano, ***Problèmes multicritère avec contraintes d'affectation*** , M. Sc. Thèse, Département d'Informatique et de Recherche Operationelle, Université de Montréal, Canada, novembre 1996.